PB82-256876

Energy Model of a Cadmium Stream with Correlation of Embodied Energy and Toxicity

Florida Univ.
Gainesville

Prepared for

Environmental Research Lab.
Athens, GA

Apr 82

EPA 600/3-82-048
April 1982

PB82-256876

ENERGY MODEL OF A CADMIUM STREAM WITH CORRELATION OF EMBODIED ENERGY AND TOXICITY

by

Robert L. Knight

Systems Ecology-Energy Analysis Program
Department of Environmental Engineering Sciences
and
Center for Wetlands
University of Florida
Gainesville, Florida 32601

Principal Investigator: Howard T. Odum

Grant.No. R-806080

Project Officer

Lawrence A. Burns
Environmental Systems Branch
Environmental Research Laboratory
Athens, Georgia 30613

ENVIRONMENTAL RESEARCH LABORATORY
OFFICE OF RESEARCH AND DEVELOPMENT
U.S. ENVIRONMENTAL PROTECTION AGENCY
ATHENS, GEORGIA 30613

TECHNICAL REPORT DATA
(Please read Instructions on the reverse before completing)

1. REPORT NO.	2.	3. RECIPIENT'S ACCESSION NO.
EPA-600/3-82-048	ORD Report	PB82 256876

4. TITLE AND SUBTITLE	5. REPORT DATE
Energy Model of a Cadmium Stream with Correlation of Embodied Energy and Toxicity	April 1982
	6. PERFORMING ORGANIZATION CODE

7. AUTHOR(S)	8. PERFORMING ORGANIZATION REPORT NO.
Robert L. Knight	

9. PERFORMING ORGANIZATION NAME AND ADDRESS	10. PROGRAM ELEMENT NO.
Department of Environmental Engineering Sciences University of Florida Gainesville FL 32601	CCULIA
	11. CONTRACT/GRANT NO.
	R-806080

12. SPONSORING AGENCY NAME AND ADDRESS	13. TYPE OF REPORT AND PERIOD COVERED
Environmental Research Laboratory--Athens GA Office of Research and Development U.S. Environmental Protection Agency Athens GA 30613	Final, 9/78 -3/81
	14. SPONSORING AGENCY CODE EPA/600/01

15. SUPPLEMENTARY NOTES

16. ABSTRACT

In surviving systems that have evolved designs for maximizing power, ability to amplify and control may be in proportion to embodied energy. The evaluation of control effect and energy required in equivalent embodied energy units allows the direct correlation of these two properties of a controller such as a toxic chemical. The heavy metal cadmium (Cd) was used to analyze this toxin control hypothesis. A literature review indicated a stimulatory (Arndt-Schulz) effect of Cd at low concentrations in many growth studies. Most data sets were found to be described by a general subsidy-stress curve. The bioconcentration of Cd as a mechanism in natural systems for controlling free Cd concentration and its toxic effect is discussed. Information collected during previous research on Cd effect in experimental streams was summarized and used to calibrate an energy and material model of the Cd streams. Several mechanisms of Cd toxicity were examined and the model includes a simulation of system components at low Cd levels. The results of this study with Cd are predicted to be general to most other toxic substances and may allow synthesis of the burgeoning quantity of information concerning chemicals in the environment.

17. KEY WORDS AND DOCUMENT ANALYSIS

a. DESCRIPTORS	b. IDENTIFIERS/OPEN ENDED TERMS	c. COSATI Field/Group

18. DISTRIBUTION STATEMENT	19. SECURITY CLASS *(This Report)*	21. NO. OF PAGES
RELEASE TO PUBLIC	UNCLASSIFIED	127
	20. SECURITY CLASS *(This page)*	22. PRICE
	UNCLASSIFIED	

EPA Form 2220-1 (9-73)

NOTICE

Mention of trade names or commercial products does not consititute endorsement or recommendation for use.

FOREWORD

Environmental protection efforts are increasingly directed towards preventing adverse health and ecological effects associated with specific compounds of natural or human origin. As part of this Laboratory's research on the occurrence, movement, transformation, impact, and control of environmental contaminants, the Environmental Systems Branch studies complexes of environmental processes that control the transport, transformation, degradation, and impact of pollutants or other materials in soil and water and assesses environmental factors that affect water quality.

Essential to the rational management of ecosystems is an understanding of the mechanisms that control environmental systems. In this report, the theory that aquatic ecosystems may be controlled by toxic substances that can affect energy flows that are greater than their own energy flows is examined using the heavy metal cadmium. Using a model of energy and material flows in streams with and without cadmium, embodied energy of this toxic metal is correlated with the embodied energy of producers and consumers and with amplification effect on primary production. With additional development, the ecosystem control theory could provide a quantitative means of evaluating, comparing, and using controlling agents in environmental management.

David W. Duttweiler
Director
Environmental Research Laboratory
Athens, Georgia

ABSTRACT

In surviving systems that have evolved designs for maximizing power, ability to amplify and control may be in proportion to embodied energy. The evaluation of control effect and energy required in equivalent embodied energy units allows the direct correlation of these two properties of a controller such as a toxic chemical.

The heavy metal, cadmium (Cd), was used to analyze this toxin control hypothesis. A literature review indicated a stimulatory (Arndt-Schulz) effect of Cd at low concentrations in many growth studies. Most data sets were found to be described by a general subsidy-stress curve. The bioconcentration of Cd as a mechanism in natural systems for controlling free Cd concentration and its toxic effect is discussed.

The energy embodied in Cd storages by three different systems was evaluated. Calculations suggest that the world geological cycle is producing economically recoverable Cd at a very slow pace, only 53 $kg \cdot yr^{-1}$. The energy transformation ratio of this Cd is 2.5×10^{16} Solar Equivalent Calories (S.E. Cal)$\cdot g\ Cd^{-1}$. The industrial concentration of Cd adds an additional 4.6×10^{7} S.E. Cal$\cdot g\ Cd^{-1}$ in the synthesis of the pure metal. A calculation of the biological concentration in experimental stream systems indicated a cost of 1.3×10^{9} S.E. Cal$\cdot g\ Cd^{-1}$ at a concentration of only 0.8 ppm on a live-weight basis.

Information collected during previous research of Cd effect in experimental streams (Giesy et al. 1979) was summarized and used to calibrate an energy and material model of the Cd streams. Several mechanisms of Cd toxicity were examined and the model includes a stimulation of system components at low Cd levels. Simulation results allowed a detailed correlation of the relationship between embodied energy in Cd and the Cd effect in equal units (S.E. Cal$\cdot g\ Cd^{-1}$). This correlation was found to be first positive, then negative, and eventually approached zero at higher Cd concentrations. The results of this study with Cd are predicted to be general to most other toxic substances and may allow synthesis of the burgeoning quantity of information concerning chemicals in the environment.

This Report was submitted in fulfillment of Grant No. R806080 by the University of Florida under the sponsorship of the U.S. Environmental Protection Agency. The report covers the period September 1978 to March 1981, and work was completed as of March 1981.

CONTENTS

FIGURES

Figures, continued.

Figures, continued.

Number Page

Figures, continued.

Number Page

Figures, continued.

TABLES

SECTION 1

INTRODUCTION

The study of mechanisms controlling environmental systems is essential for understanding ecosystems and for their rational management. Toxic substances may control ecosystems and cause new ecosystems to emerge that can directly utilize the substances to aid their competitive roles. Substances may directly aid positive physiological mechanisms, stress a system that is not adapted, or subsidize an adapted system. The aim of the present study is to develop a theoretical and quantitative means to evaluate, compare, and utilize controllers in environmental management and to illustrate the approach with one substance—the heavy metal cadmium (Cd).

By "controller," we mean an agent, a chemical substance or biological component, that has the ability to divert, enhance, or stop energy flows that are greater than its own energy flow. A chemical substance may control biological controllers. Small quantities of Cd are toxic to individual organisms and have sharp effects on biological systems.

A theory proposed by Odum (1979) and the author is that control action or "amplification" ability may be a function of the energy embodied in the controlling agent. Embodied energy is defined as the total energy flow of a system necessary to form the agent through convergence of webs or concentrating factors. In systems selected for maximum energy flow, controlling agents may be used to manipulate productive processes through positive amplification. The theory suggests that controllers will have an energy consumption from the system that may not exceed their value as a stimulant to productivity and that natural selective processes will eliminate items that use more energy than they stimulate. In an immature system, two values of a controller, i.e., the embodied energy and the amplifier effect, might be widely different, but in an adapted system they must balance or a more productive system will take over. Thus, an adapted system may be able to use toxins.

In this study, we apply these theories on toxins as controllers to Cd. Embodied energy of Cd in various forms has been calculated for geological, biological, and technological processes. Using a model of energy and material flows in streams with and without Cd, embodied energy of this toxic metal is correlated with the embodied energy of producers and consumers and with amplification effect on primary production. The controlling roles of Cd and animals and their interactions were related using simulations that were able to generate observable patterns. It is hoped that the research and ideas reported here may be a catalyst for further development of ecosystem-control theory.

SECTION 2

CONCLUSIONS

Cadmium consistently stimulates growth parameters of biological systems at concentrations slightly above ambient levels. This stimulatory role of Cd may be useful in maximizing the productivity of human-perturbed ecosystems. Cadmium-adapted systems may be useful in the recovery of Cd wastes by bioconcentration.

At higher concentrations, Cd is extremely toxic to biological systems. A continuous input of only 5 ppb Cd lowered average gross production and respiration by 40% in soft-water stream systems over a 1-yr period. Thus, intermediate levels of Cd may be useful as a toxic control of biological systems.

Cadmium is an easily depleted resource because of its extremely low natural production rates. The embodied energy of Cd storages is high, making the conservation and recovery of Cd important for long-term survival of human systems.

An energy analysis of the data from a calibrated Cd-stream model indicated a positive-negative correlation between the energy cost of Cd and its energy effect. The model data indicated a possible equivalence between the stimulatory and toxic actions of Cd and its energy cost of concentration at naturally occurring concentrations.

SECTION 3

RECOMMENDATIONS

Tables of embodied energy should be calculated for all chemical substances of potential environmental impact as a way to organize the understanding of which wastes are important.

Toxicity studies of chemicals should include careful examination of effects at low, stimulatory levels as well as at higher toxic levels. More studies concerned with the stimulatory and toxic effects of chemicals on ecosystem parameters are needed. Large-scale microcosms may provide the best means to study hierarchical effects of chemicals.

Additional data concerning energy inputs to toxicity research should be routinely reported. These inputs include: energy (illumination, stirring, heating, etc.); materials (nutrients, gases, inocula, etc.); structure (cost); and human services. In addition, ambient concentrations of toxins should be monitored and reported in batch studies.

Results of all toxicity studies should be organized under one general system such as the energy quality—energy effect curves presented in this report.

SECTION 4

BACKGROUND AND CONCEPTS

INTRODUCTION

The controlling action of toxic substances seems to be as variable a subject as the number of toxic chemicals and affected organisms that exists. In order to discuss those principles that are general to toxicity, we must first consider those principles that are general to all real systems. The ways a toxic chemical may participate in an ecosystem are examined with models and the simulations are compared with data on Cd toxicity.

MAXIMUM POWER THEORY

The designs of systems and their ways of processing toxins are related to energy. Lotka (1922) proposed a principle of thermodynamics for open systems which states that selection in the struggle for existence is based on maximum energy flow (power). Later, Odum and Pinkerton (1955) and Odum (1968, 1971, 1979) suggested ways control actions generate more power and thus tend to persist in real, competing systems.

Power has been defined as the rate of useful energy transformation. The concept of useful power is important in the maximum power theory. Useful power is a measure of the energy flows and transformations that result in structures or processes feeding back to help maintain themselves or to increase their power. Thus, useful power differs from dissipation of energy that is not part of a self-maintaining system. The conceptual idea of maximum power is illustrated by an autocatalytic unit (Fig. 4.1). In this simple model, a nonlinear interaction acts to accelerate energy flow to the maximum sustainable level. The generality of autocatalysis (i.e., chemical reaction theory, Malthusian growth in biology, growth of physical systems such as storms or fires, etc.) is some measure of support for the theory that systems are selected for maximum power.

Observation indicates that there is more to the maximization of power of natural systems than just rapid growth, depletion, and loss of a storage. The systems that are surviving have mechanisms to sustain the cycling of materials to facilitate the overall energy being processed by the system (system power). Tuned complexity is a criterion for maximum power in competing systems, and the diversity of natural systems is further circumstantial evidence in support of this theory.

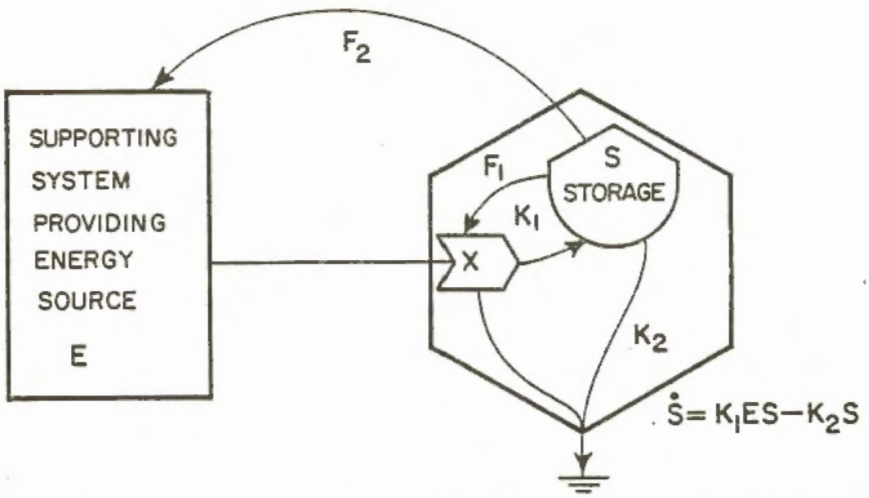

Figure 4.1. Model of autocatalysis. The feedback interaction between a storage (S) and an energy source (E) develops rapid growth as long as source can supply increased flow. Feedbacks include those to maximize the system directly (F_1) and those to maximize the larger system (F_2).

The power of a system may be limited by the quantity of usable energy, temporal pattern of energy inputs, and by the constraints of energy transformation. These limits to the growth of power of a system are not reached immediately, but are approached in time after succession and evolution.

Few environmental systems have just one energy source; most have several types of energy inputs. If untapped energy sources exist, some of the existing energy flow is routed to help use new sources through exchange or pumping. The system that effectively increases its power by using additional energies has a competitive advantage over other systems. Energy may be used to meet all contingencies.

Given a finite available energy source, a system is further limited in its power level by the energy required for each transformation. This observed energy for transformation is described by the second law of thermodynamics as a necessary decrease of available work energy in most energy-transforming processes. In other words, much energy is converted to a lower quality state when a transformation to another type occurs. This phenomenon has been quantified in various branches of science and was summarized by Odum and Pinkerton (1955). Their review of physical and biological systems concluded that maximum power level is possible only at lower-than-maximum efficiency for competing systems and may be at 50% transformation efficiency for a single storing process. The necessary loss to unusable heat limits the total number of tranformations possible for any energy entering a system and results in a predictable spectrum of energy transformers in all adapted systems (Odum 1979).

All systems are but subsystems within larger competing systems and thus are exposed to control by the next system's behavior. Therefore, biological systems such as mature forests or ancient lakes may be greatly simplified by volcanic eruptions or human toxic wastes, resulting in a decreased local power level but an increased power at the next larger scale. Circumstantial evidence is available to show that many systems are on a successional and evolutionary course towards the maximum power level within the boundaries of their exogenous controls.

Biological food chains represent concentrations of energy, with each level requiring energy diverted from the machinery of primary production. This diverted energy must be compensated for by energies fed back from storages to capture greater free energy for the system. Thus, a control hypothesis follows directly from the maximum power theory. In adapted systems, components must have controlling actions that are equal to their energy of transformation.

Since powerful poisons may be powerful controllers of ecosystems, knowledge of stimulative and toxic roles of poisons may be used to enhance productivity and manage systems. More control may be achieved by using toxins to control consumer organisms that, in turn, have controlling roles. If a toxin occurs at low concentration, biological energies may be used to concentrate it to a stimulatory level; or, if the natural concentration of a toxin is high, biological energy may be used to detoxify the substance by reducing its effective concentration in the environment.

EMBODIED ENERGY

In the previous section it was stated that the degraded energy resulting as a by-product of any energy transformation may be considered as "low quality" in that it is no longer capable of performing work in the system. On the other hand, we may consider the remainder of the transformed energy as being of higher quality than both the original input energy to the transformation process and the dispersed low-quality energy that was a necessary by-product of the transformation. As a logical convention, we can assume that the total energy of one type necessary to make another type is embodied in the energy of the second type.

If we divide the energy of one type necessary to produce another by the energy of the second type, we have the ratio of "energy transformation." This dimensionless parameter has been called the "energy quality factor" or the "energy transformation ratio" by Odum (1978) and may be assumed to have some theoretically minimum value in competing systems. When transformation ratios for various processes are related to energy of one type (e.g., S.E. Cal or Coal Equivalent Calories), we have a parameter to compare quality of all types of energy or matter.

In order to evaluate the primary energy necessary to produce an energy flow after several transformations, we must recognize that the energy necessary to produce the intermediaries is necessary to the production of the final product. Thus, if a food-chain system were relying on a single input source, the embodied energy for all energy flows and storages would be evaluated in terms of the single incoming energy flow.

If a production process has more than one major energy input, then the embodied energies of all inputs must be summed to evaluate the energy quality of the resulting products. In most systems, some of the auxillary energies of the process are fed back from the products and therefore must not be added to avoid double counting. Examples of energy transformation ratio calculations for Cd are included below, or, for a more detailed discussion of this concept, see Odum (1978).

Embodied Energy of Cadmium

The atoms of an element such as Cd have been in a continuous turnover as long as the solar system has been in existence, with dispersion of atoms followed by concentration and repeated dispersion. Energy is required for concentration of any substance, and the total energy degraded to heat in the coupled process of Cd concentration is the "embodied energy."

The embodied energy of Cd must be calculated at various concentrations and in different systems to evaluate its role as a toxin or stimulator of metabolism. Calculated values of embodied energy are based on global averages or specific production cases, so the numbers resulting are subject to considerable variability and revision. Of most importance in this report are comparisons of energy costs to Cd concentration in different systems and the relationship of these costs to the feedback effect.

Earth Production—

The concentration of Cd in the solar system on a weight to weight basis is roughly 3 ppb (calculated from elemental abundances given by Abell [1964]) as compared to an average value of 110 ppb in the earth's crust (Vlasov 1966). Thus the crustal Cd has embodied energy from the earth's formation process. Since this energy is the result of concentration in the next larger system (i.e., the solar system), the crustal Cd embodied energy is assumed to be equal to zero in order to set a baseline for the calculation of energy embodied by the earth's production process of Cd ore.

Figure 4.2 illustrates the energies used to estimate the Cd concentration in the earth process. Cadmium ores are very rare in nature so the much more abundant Cd-bearing zinc (Zn) ores are considered. Although Cd concentrations as high as 8000 ppm are found in some Zn ores (Wedepohl 1970), the world average for minable ores is 4% Zn (Cammarota 1978), and with an average Zn:Cd ratio of 200 in sedimentary ores (Lucas 1979), this is equal to 200 ppm Cd. Solar energy or solar-produced hydrologic energy (Flow B) was used as the major input to this concentration process, although traditional view regards residual deep heat (Flow A) as a separate input to ore production processes.

As mentioned above, the earth's average crustal concentration of Zn and Cd was taken as zero-embodied energy because these elements cannot be used in work processes at such low densities. Therefore, Flow C in Fig. 4.2 is equal to zero.

Flow B is the rate of energy absorption from the sun by the entire earth system, and was taken as 13.4×10^{20} Cal·yr^{-1} (Sellars 1965).

Flow D is the production rate of Zn and Cd ore in the world system. Of interest is the production of recoverable ore that may be mined and has enough purity to warrant extraction. Estimates for the world resources of Zn and Cd are 1.8×10^{9} tonnes (t) and 9×10^{6} t, respectively (Bureau of Mines 1980). Since this ore is largely contained in sedimentary-derived deposits (Lucas 1979) and an approximate turnover time is known for the world sedimentary cycle (1.7×10^{8} yr; from Judson 1968), we can calculate the formation rate of new ores if we assume a steady state of production:

Production rate of recoverable Zn in ore =
$(1.8 \times 10^{9}$ t Zn$)/(1.7 \times 10^{8}$ yr$) = 10.6$ t Zn·yr^{-1}
Production rate of recoverable Cd in ore =
$(9 \times 10^{6}$ t Cd$)/(1.7 \times 10^{8}$ yr$) = 53$ kg Cd·yr^{-1}

Thus, Flow D in Fig. 4.2 is 265 t of recoverable Zn ore per year for the whole world, or 10.6 t Zn and 53 kg Cd in ore produced each year. At a world mining rate of about 5.4×10^{6} t Zn and 17×10^{3} t Cd in 1978, the depletable nature of these resources is obvious.

The transformation ratios (TR) for Zn and Cd in ore may now be calculated if we assume that the production of ore is a by-product of the whole earth sedimentary system driven by solar energy:

$$TR_{Zn\ ore} = (13.4 \times 10^{20}\ \text{S.E. Cal·yr}^{-1})/(265\ \text{t Zn ore·yr}^{-1}) = 5.1 \times 10^{18}\ \text{S.E. Cal·t Zn ore}^{-1}$$

$$TR_{Zn\ in\ ore} = (13.4 \times 10^{20}\ \text{S.E. Cal·yr}^{-1})/(10{,}600\ \text{kg Zn·yr}^{-1}) = 12.6 \times 10^{16}\ \text{S.E. Cal·kg Zn}^{-1}\ \text{in ore}$$

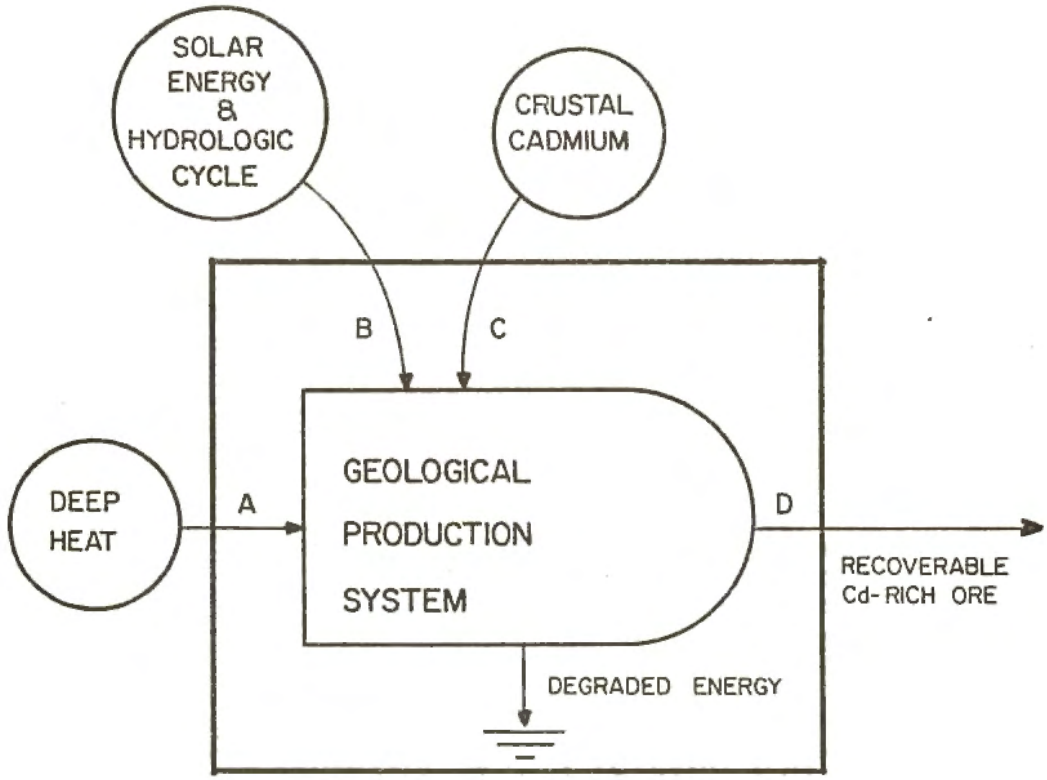

Figure 4.2. Model of geological production process for Cd-rich sulfide ores. Flow B is assumed to be more important than Flow A, and Flow C is assumed to have zero embodied energy as discussed in the text. Calculations indicate that Flow D, the rate of production of recoverable, Cd-rich ore may contain only 53 kg $Cd \cdot yr^{-1}$ for the entire earth.

$$TR_{Cd \text{ in ore}} = (13.4 \times 10^{20} \text{ S.E. Cal} \cdot \text{yr}^{-1})/(53 \text{ kg Cd} \cdot \text{yr}^{-1})$$
$$= 2.5 \times 10^{19} \text{ S.E. Cal} \cdot \text{kg Cd}^{-1} \text{ in ore}$$

Industrial Concentration—

Cadmium metal is produced commercially from by-products of Zn production; therefore, in order to evaluate the embodied energy for Zn and the resulting flue dust with Cd content, it is necessary to evaluate the Cd case. Figure 4.3 presents a simplified model of this process showing the evaluated actual energy and material flows. Table 4.1 lists the flows and their equivalent values in embodied energy of solar equivalent kilocalories. Figure 4.4 presents an aggregated model of this purification process with embodied energy flows of one type. These calculations indicate that the human costs of extracting and purifying these metals greatly underevaluate their overall embodied energy in the world system. Using the input flows alone and the percent recovery of each metal, we calculate the transformation ratios as:

$$TR_{\text{pure Zn}} = 1.6 \times 10^{17} \text{ S.E. Cal} \cdot \text{kg pure Zn}^{-1}$$
$$TR_{\text{pure Cd}} = 4.2 \times 10^{19} \text{ S.E. Cal} \cdot \text{kg pure Cd}^{-1}$$

Although the industrial embodied energy inputs in the Cd purification process are much smaller than the environmental energies, they represent the minimum amplification ability that the Cd must have in the human system. Thus, metals such as these may be used very inefficiently compared to their actual embodied energy because of their cheapness of extraction from world storages. If we evaluate the embodied energy in pure Cd only from the industrial energy inputs, we calculate 4.6×10^{10} S.E. Cal·kg pure Cd^{-1}.

Biological Concentration—

As discussed earlier in this section, most biological components have the ability to concentrate Cd to elevated levels over water concentrations. This concentration represents an embodiment of solar energy into upgraded Cd storage. Several calculations of biological Cd processing are made in this section.

Figure 4.5a illustrates the inputs evaluated in these calculations. Primary energy inputs are the embodied energy in the dissolved Cd and solar energy being processed by the biological system. Cadmium uptake is generalized in Fig. 4.5b as a simple charge-up model. The inputs of solar, water potential, structural, and Cd embodied energies are integrated over the time indicated on the graph.

Data for the entire biological communities of the Cd streams of Giesy et al. (1979) were used for analysis. Using the figure of 50 days for saturation of the periphyton Cd levels and embodied energy flows for solar, water, and structure reported in the results section of this report, we calculate 1.6×10^{6} S.E. Cal·m^{-2} of stream to attain equilibrium Cd concentrations in the biological components.

For the control channels this energy input resulted in 1256 µg Cd·m^{-2} stored in the biological community. If we follow the convention of not including the energy embodied in the Cd by the next larger system, we calculate 1.3×10^{9} S.E. Cal·g Cd^{-1} at a concentration of 0.8 ppm on a live-weight basis.

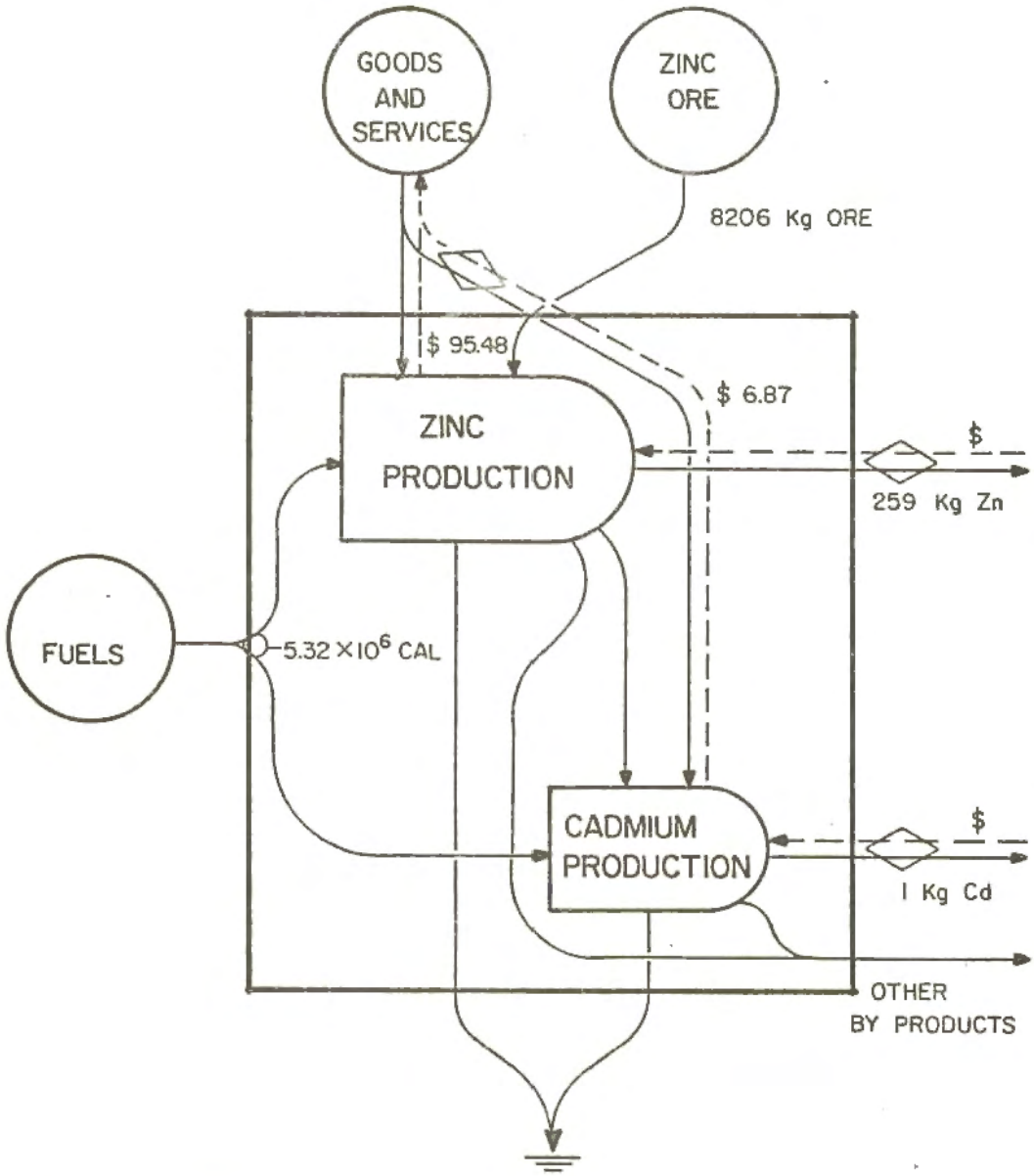

Figure 4.3. Model of Zn and Cd production by the electrolytic process with actual energy and dollar flows evaluated. Cadmium production is entirely a by-product recovery of Zn purification.

TABLE 4.1. ACTUAL AND EMBODIED ENERGY FLOWS IN THE INDUSTRIAL PURIFICATION OF ZN AND CD FROM ZN ORE RESULTING IN 1 KG OF PURE CD AS ILLUSTRATED IN FIGS. 4.3–4.4

Type	Actual Energy	Energy Transformation Ratio	Embodied Energy
Zn ore	8206 kg Zn ore[a]	5.1×10^{15} S.E. Cal/kg[b]	4.19×10^{19} S.E. Cal
Fuels	5.31×10^{6} Elec. Cal[c]	8000 S.E. Cal/Elec. Cal[d]	4.25×10^{10} S.E. Cal
Goods and services	\$95.48[e]	37×10^{6} S.E. Cal/\$[f]	3.53×10^{9} S.E. Cal
Fuels	2597 Elec. Cal[g]	8000 S.E. Cal/Elec. Cal	2.08×10^{7} S.E. Cal
Goods and services	\$ 6.87[h]	37×10^{6} S.E. Cal/\$	2.54×10^{8} S.E. Cal
Purified Zn	259 kg[i]	1.62×10^{17} S.E. Cal/kg	4.19×10^{19} S.E. Cal
Purified Cd	1 kg	4.19×10^{19} S.E. Cal/kg	4.19×10^{19} S.E. Cal

[a]From Petrick et al. (1979), 492 kg Zn concentrate with 60% Zn; 90% recovery from ore with 4% Zn content.
[b]From this report, page 8.
[c]Battelle Columbus Laboratories (BCL) (1975) total energy costs in Zn production converted to electrical Btu.
[d]From Odum and Odum (1980).
[e]From BCL (1975), \$36.34 materials and reagents; from Cammarota (1978), \$36.34 labor and \$22.80 capital assuming 20-yr life for plant.
[f]Odum et al. (1980).
[g]Petrick et al. (1979).
[h]Ibid.
[i]79% efficiency of recovery from ore (Cammarota and Lucas 1977).

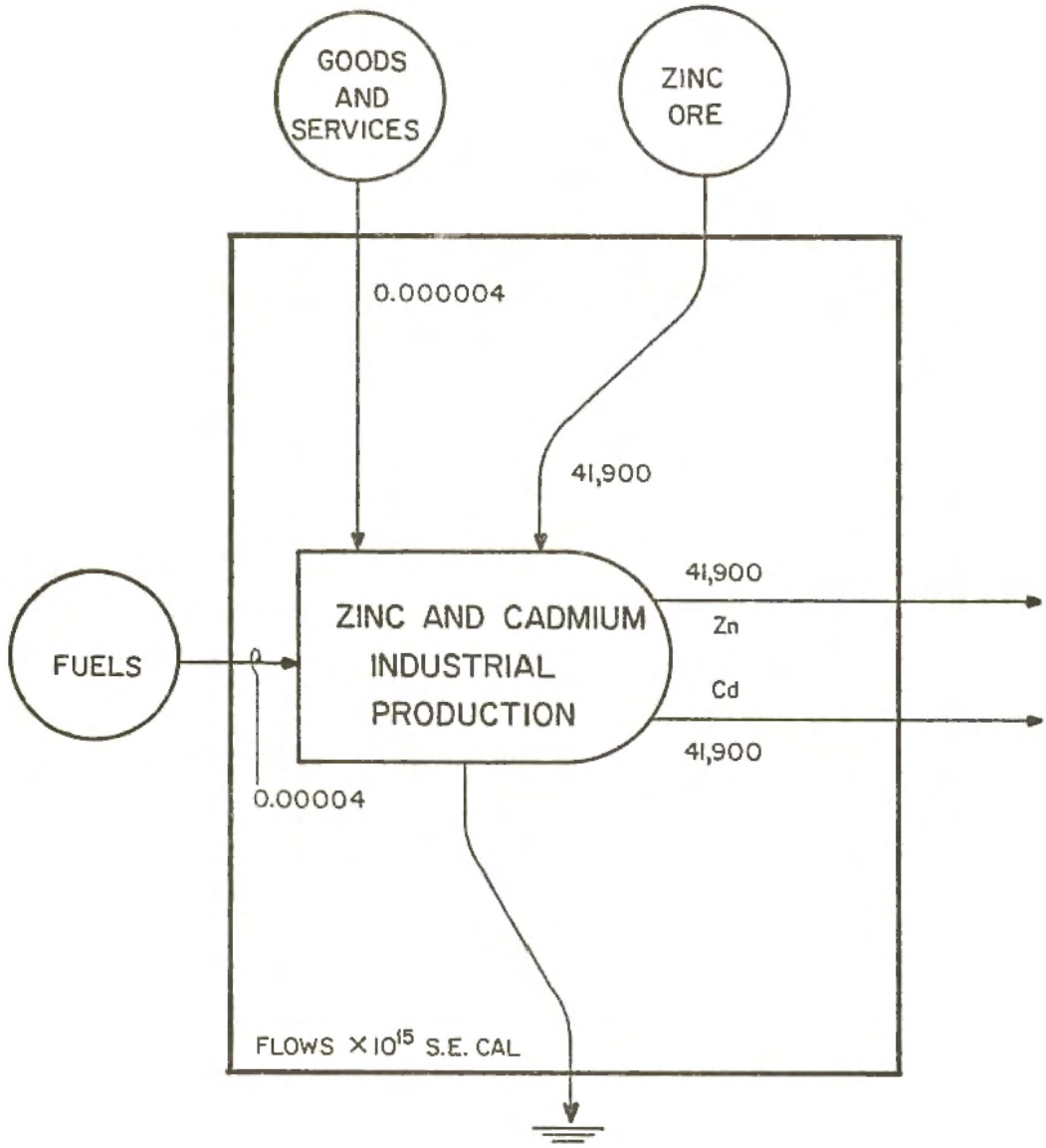

Figure 4.4. Aggregated model of Zn and Cd production with flows evaluated in terms of S.E. Cal.

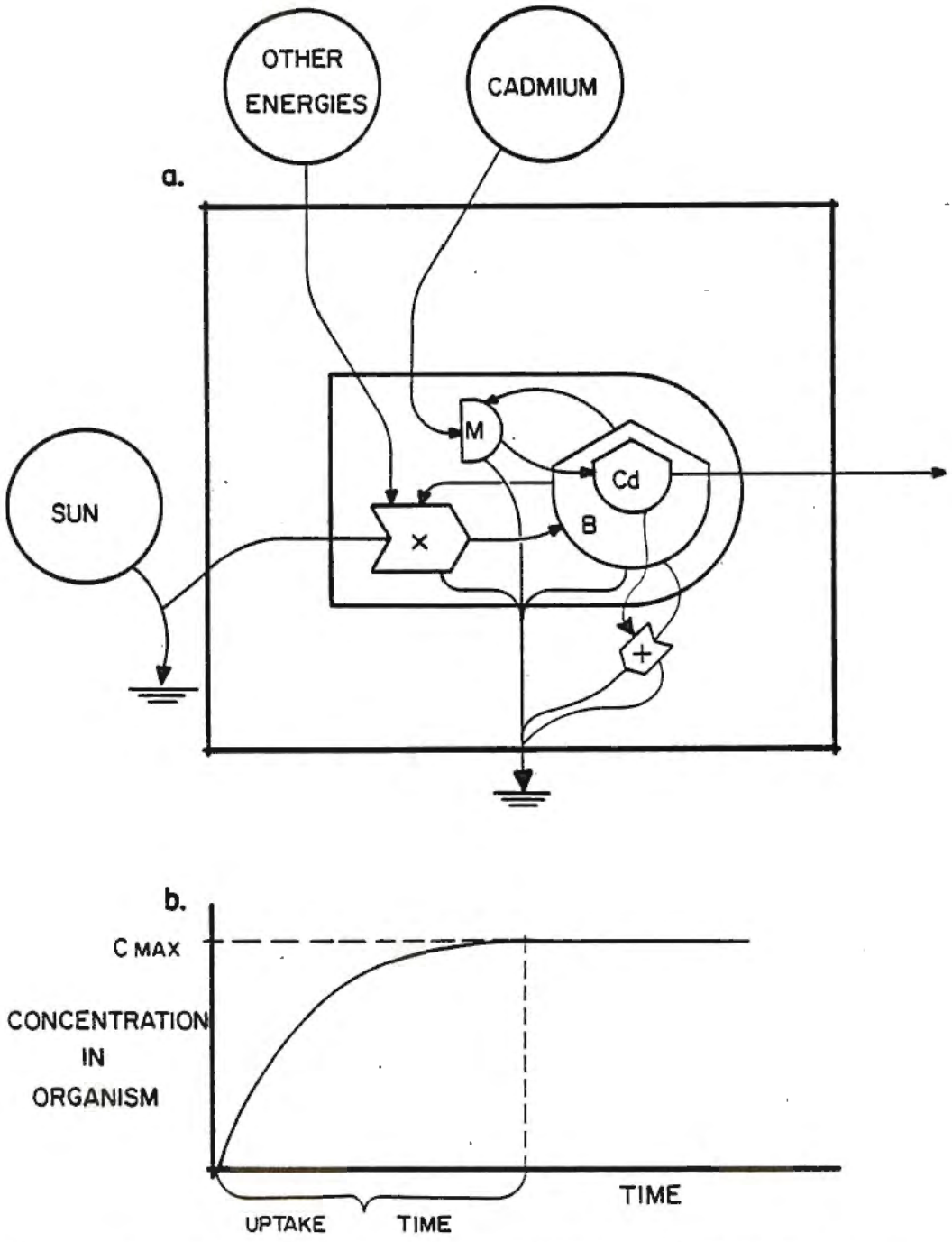

Figure 4.5. Evaluation of Cd embodied energy in biological systems. (a) Model of Cd and energy inputs to concentration process; (b) Idealized uptake curve for Cd in biomass with uptake time used to evaluate embodied energy. B is biomass; M is a Michaelis-Menton accumulation process.

For the Cd-treated streams we must add the embodied energy of the Cd inputs by the human controllers to the other energy inputs to the streams. This embodied energy was taken as the industrial cost of the Cd (4.6×10^{10} S.E. Cal·kg Cd^{-1}) rather than the much greater world system cost. At 136,800 $L \cdot d^{-1}$ flow rate, 55.8 m^2 surface area, and 50 days charge-up time, we calculate inputs of 0.615 g $Cd \cdot m^{-2}$ for the 5 ppb treatment, and 1.23 g $Cd \cdot m^{-2}$ for the 10 ppb treatment, resulting in storages of 0.013 g $Cd \cdot m^{-2}$ and 0.020 g $Cd \cdot m^{-2}$, respectively. Adding the input energies and dividing by the Cd storages gives 2.3×10^9 S.E. Cal·g Cd^{-1} at a biological concentration of 7.5 ppm, and 2.9×10^9 S.E. Cal·g Cd^{-1} at 11.6 ppm.

TOXICITY EFFECT

As a natural part of organic evolution, some biological systems have developed toxic substances, which may control energy flows and perhaps maximize power. Thus, plants have allelopathic chemicals and insects have venom. These substances represent a concentration of energies and have a high embodied energy.

Human technological systems may be similar in this respect. Toxins are collected from nature or synthesized in laboratories for the purpose of controlling environmental energy flows. In addition, toxic substances often result as by-products of industrial processes. These substances also represent large energy flows and have high embodied energy.

On the other hand, toxicity is a drag on the energy flow in a system if it is not a part of material cycles and regenerative processes. If the system's goal is maximum power, the ideal use for a controlling substance is to enhance the capture and use of energy sources. Consequently, toxins that decrease a system's power must be detoxified by surviving systems or be adapted to through species selection and evolution. If possible, powerful controlling agents may be incorporated into productive processes within an organism as part of enzyme systems or respiratory and photosynthetic pathways. Thus, copper and zinc are recognized essential nutrients for many plants at low concentrations, but are toxic at higher levels. We propose that this subsidy-stress gradient (see Odum et al. 1979) is the general case for any substance that has been a part of natural systems for evolutionary time, and quantification of this effect is possible through embodied energy calculations.

Arndt-Schulz Law

In the fields of medicine and bacteriology there has long been a recognition of stimulation by a variety of normally toxic substances at low levels. This phenomenon is known as the "Arndt-Schulz Law" after two German physicians working on the effects of drugs in the late 19th century. Lamanna and Mallette (1953) discuss this effect in their treatise on bacteriology. "Growth rates, crop yields, and specific metabolic activities of all bacterial species studied have been found to be stimulated by low concentrations of

a diversity of inorganic and organic poisons" (p. 598). This phenomenon has been recognized in the effects of ionizing radiation on plants (Gloyna and Ledbetter 1969) and on whole forest communites (Woodwell [1967]; Odum and Pigeon [1970]). Atlan (1968) has discussed this phenomenon with particular reference to the information content of organisms. He provides a general theory of organization where optimum doses of any normal environmental factor (ionizing radiation, heat, oxygen tension, etc.) tend to reduce noise and maximize information content and flow. Of particular interest to this report are the observations of stimulatory effect for heavy metals with no known biological role such as mercury (Rzewuska and Wernikowska-Ukleja 1974) and Cd (Doyle et al. 1975).

In their summary of the Arndt-Schulz effect for bacteria, Lamanna and Mallette (1953) continue: "While the universal occurrence of stimulation by poisons suggests the possibility for the existence of a single basic mechanism, the very diversity of chemical compounds and biological processes involved presents enormous difficulties to the imagination in conceiving of such a mechanism" (p. 599). They present several plausible mechanisms for this effect in biology, but in their attention to detail, these authors seem to miss another important possibility; perhaps the mechanisms of the response vary, but the cause of these adaptations is consistent—namely, the criterion of maximum power. Thus, all biological organisms have evolved under selection pressure to maximize their life processes and have been continually exposed to minute concentrations of toxic metals, free radicals, and ionizing radiation. Given evolutionary time, mechanisms that utilize these "poisons" in stimulatory ways would be selected. In experimental toxicity studies, these low stimulatory levels are often below the range of the lowest concentration studied and when stimulation is measured, the data are often ignored. Stimulatory effects are evidences of organization for maximum power. Adaptive systems can gain by using substances with large effects.

Just as there is a range of concentration effects by a chemical, there is also a range of reactions by different organisms to a single concentration. Due to the tremendous diversity of adaptation, some species may thrive at extreme chemical concentrations and flourish because of reduced competition from other organisms. Species with short generation times may quickly recover from a chronic toxin level through intensive selection pressure. By the same manner, ecosystems may adapt to continuous toxin inputs through redesigning of food webs with resistent organisms. A look at some specific reactions to varying Cd concentrations will allow the formulation of some general toxicity models.

Review of Cd Toxicity and Proposed Models

Data from the literature are examined for the effect of Cd concentrations on growth in order to determine a general organism response to this toxin. Parameters of the storages examined were net yield, cell density, and chlorophyll content; and, the parameters of energy flow examined were growth rate, oxygen evolution for algae, and oxygen uptake by animals.

Microbes—

Hammons et al. (1978) reviewed the literature on Cd toxicity to microorganisms and determined that, in general, levels above 0.2 ppm were neces-

sary to show a toxic effect on bacteria. Doyle et al. (1975) published data for several bacteria and one yeast in which toxicity effects were generally observed above 10–20 ppm (Fig. 4.6). A whole range of toxic responses is seen in this figure, several of which show some stimulation at the lower Cd concentrations studied (Escherichia coli, Streptococcus faecalis, and Lactobacillus acidophilus).

Plants—

In most aquatic systems there are generally two distinct groups of primary producers—the algae (attached and planktonic) and the macrophytes, or vascular plants. Due to their difference in size, microscopic algae may have generation times of a few days while aquatic macrophytes generally have one generation per year. Although laboratory studies show similar sensitivities for these two groups, species replacement and redesign by plant communities are much faster in the algae.

Most laboratory studies of algal toxicity have been made with the "laboratory weed" algae, which are easy to culture in artificial conditions. Sensitivity of these species to a chemical may not be typical of all algae just as their ease of culture is not typical of all algae. Nevertheless, the replicability of laboratory studies is useful in a comparison over a large range of concentrations of Cd.

Figure 4.7 shows the effect of Cd up to 1 ppm on oxygen evolution in a blue-green algae, Anacystis nidulans, reported by Katagiri (1975). A concentration of 100 ppb was found to be inhibitory while 50 ppb gave a slight stimulation over controls. A small amount of photosynthesis was reported at 1 ppm Cd.

In a study of Cd effect on growth of Scenedesmus quadricauda (Fig. 4.8), Klass et al. (1974) reported reduced cell densities at 6.1 ppb with some cell growth still observed at 610 ppb. Once again a small stimulation of maximum cell numbers was reported at a concentration of 0.6 ppb Cd.

Studying another green alga, Chlamydomonas reinhardii, Kneip et al. (1974) reported reduced growth at a Cd concentration of 10 ppb (Fig. 4.9) and almost total inhibition at 1 ppm Cd. Once again at the lowest levels tested, 0.01 ppb, a slight stimulation of net growth was observed.

No controlled experiments of Cd's effect on aquatic macrophytes at a series of different concentrations were found; however, a large number of experiments have been reported from crop species of terrestrial plants. In hydroponic culture, Turner (1973) found the yield of garden vegetables (radishes, lettuce, beets, tomatoes, carrots, and swiss chard) to be lowered by 100 ppb Cd; yet tomatoes, lettuce, and radishes were all stimulated at 10 ppb Cd. Hydroponic culture of bush beans (Wallace et al. 1977) and beans, beets, turnips, and corn (Page et al. 1972) also showed yield reduction at 100 ppb Cd in solution, but no lower experimental levels were tested.

Vascular plants, when grown in soil, show sensitivity only at much higher Cd concentrations. John and van Laerhoven (1976) found growth reduction of nine lettuce varieties at 1 ppm Cd and slight stimulation at 0.5 ppm. Wallace et al. (1977) found yield reductions of 60%–80% at Cd concentrations of 200 ppm in soil. Bingham et al. (1976) found slight reduction in growth of several pasture species at soil Cd concentration of 5 ppm.

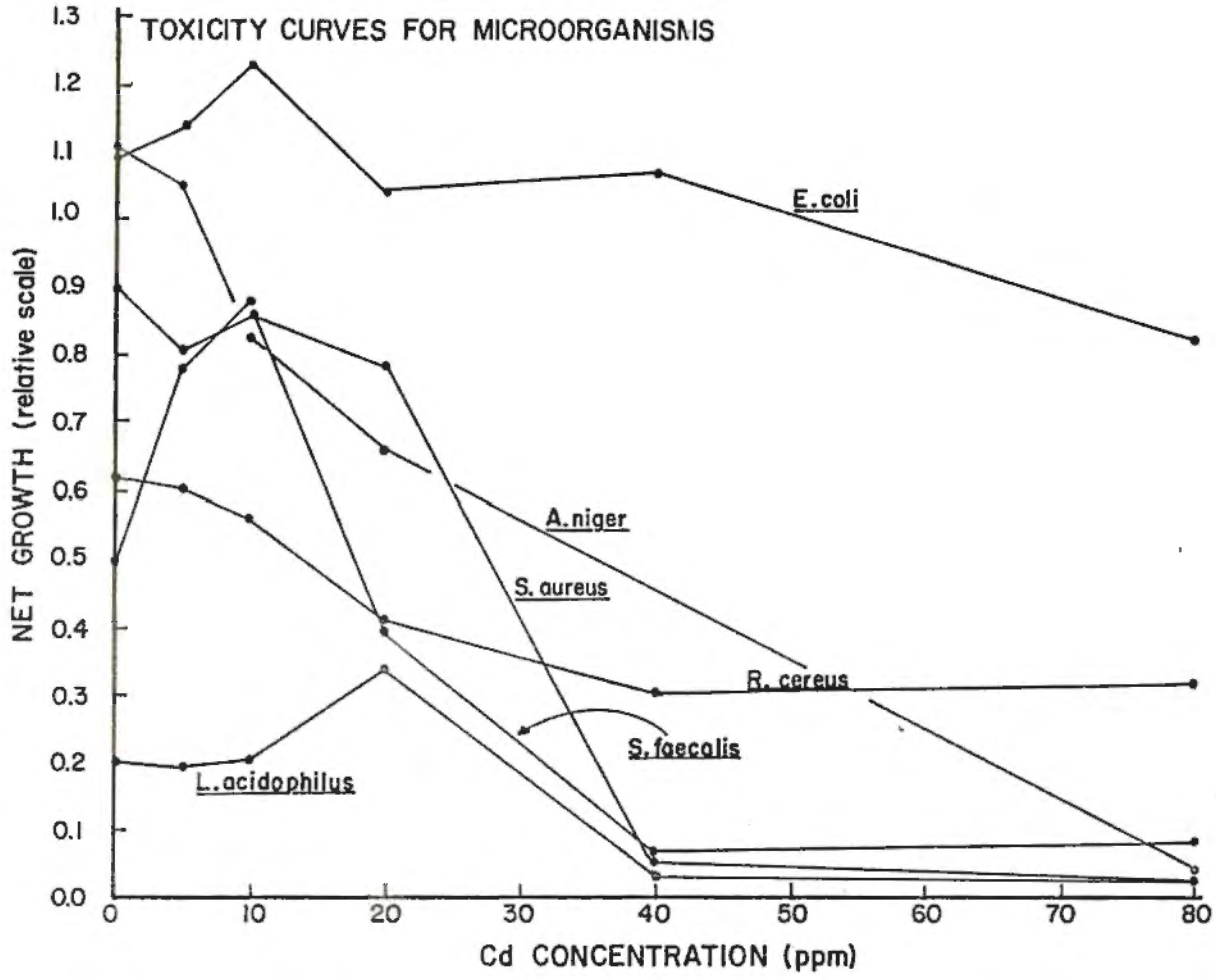

Figure 4.6. Effect of Cd on net growth of six microorganisms in batch culture (from Doyle et al. 1975).

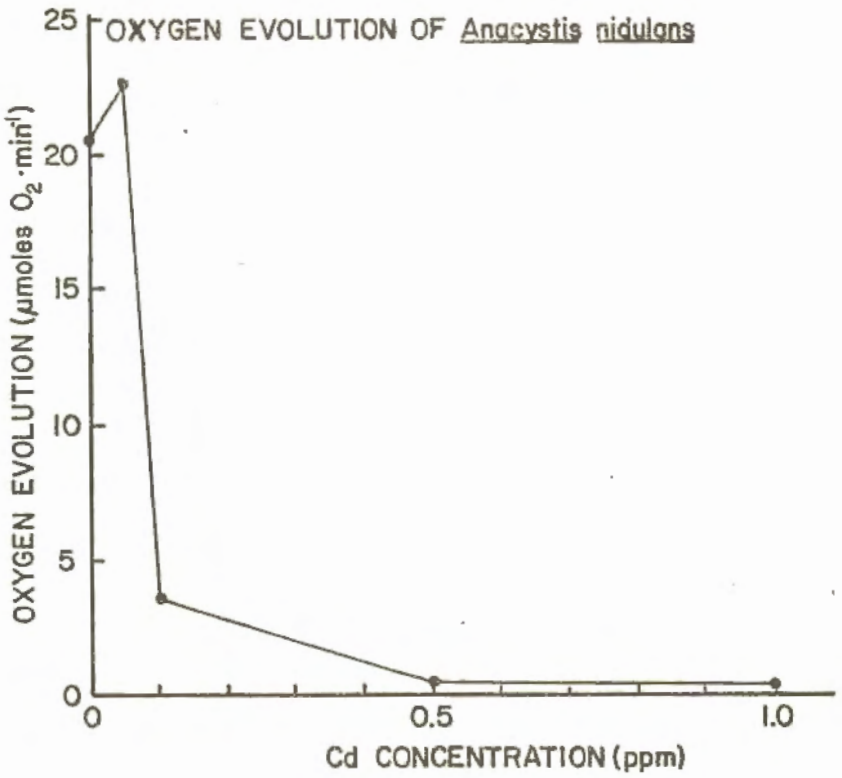

Figure 4.7. Effect of Cd on oxygen evolution by the blue-green alga Anacystis nidulans in batch culture (from Katagiri 1975).

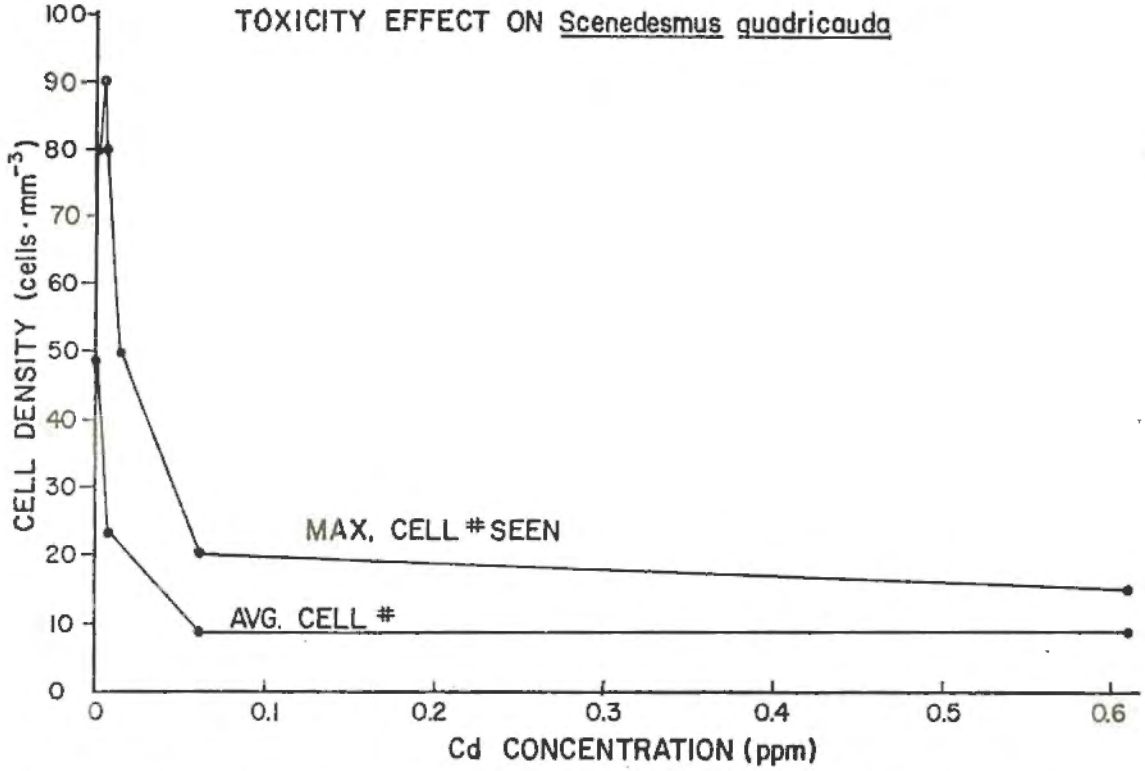

Figure 4.8. Effect of Cd on cell numbers of the green alga Scenedesmus quadricauda in batch culture (from Klass et al. 1974).

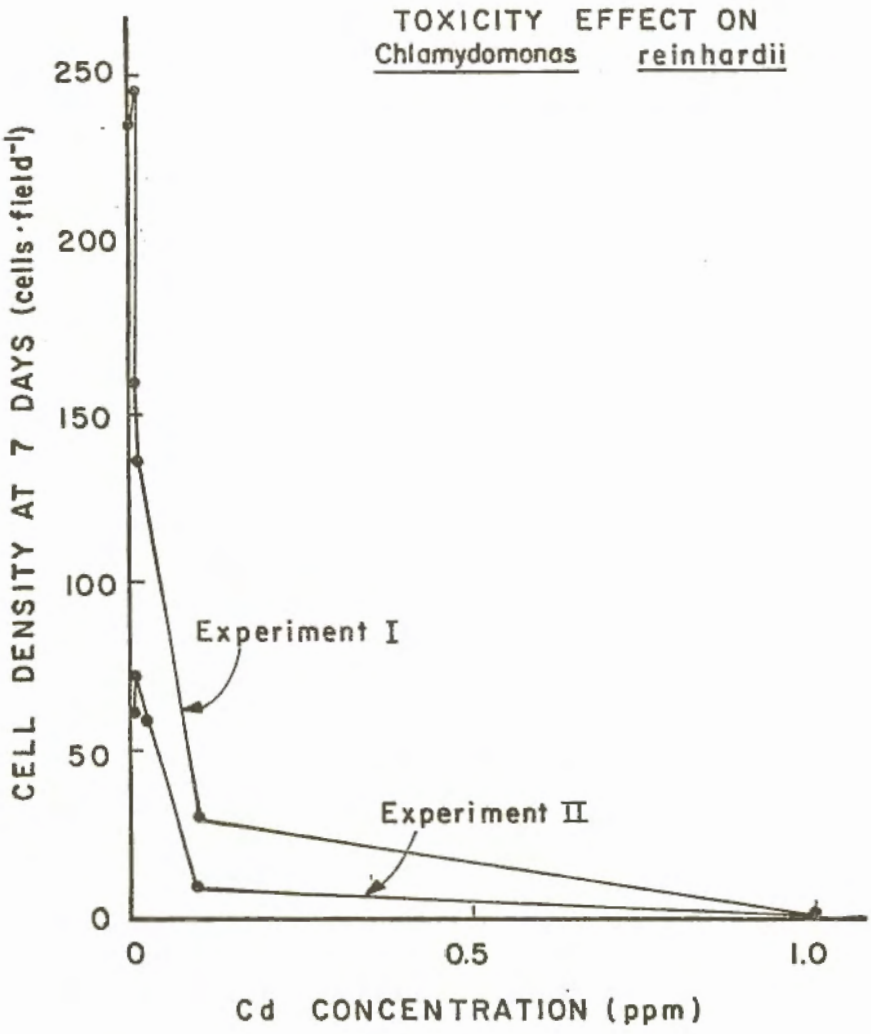

Figure 4.9. Effect of Cd on net growth of the green alga Chlamydomonas reinhardii in batch culture (from Kneip et al. 1974).

Animals—

Many species of aquatic animals have been tested for sensitivity to Cd exposure. The most useful experiments to this report are those where some functional property such as metabolism, net growth, or reproductive capacity is determined for a series of Cd concentrations from just above background to severely toxic. LC-50 (the lethal concentration for 50% of the test organisms in a stated time period) values or survivorship curves may also be useful if they are determined for several Cd concentrations over the life span of the test organisms.

Spehar et al. (1978) found that 27.5 ppb Cd severely reduced the survivorship of a freshwater snail, Physa integra, at 28 days, while concentrations of 3 and 8.3 ppb increased survivorship. Working with another freshwater snail, Biompharia glabrata, Ravera et al. (1974) observed severe Cd toxicity at 100 ppb.

Respiration in tubificid worms was found to be enhanced by 10 ppb Cd by Brkovic-Popovic and Popovic (1977) and decreased with respect to controls at 60 ppb (see Fig. 4.10). The percent survival of a mayfly, Ephemerella sp., was considerably reduced at the lowest concentration tested (3 ppb Cd) by Spehar et al. (1978).

The effect of Cd on egg production and percent survival at 30 days on fathead minnows, Pimephales promelas, was reported by Pickering and Gast (1972). As may be seen in Fig. 4.11, both parameters were reduced compared to controls at 30 ppb, but egg production was greatly stimulated at 15 ppb Cd. Benoit et al. (1976) found embryo viability in brook trout to be inhibited at less than 1 ppb Cd (Fig. 4.12). Survivorship in two other fish species, bluegill sunfish and largemouth bass, was lowered at 8 ppb in laboratory tests reported by Cearley and Coleman (1974).

Summarizing the review of Cd toxicity, animals have sensitivity similar to that of plant and algal species. Concentrations of Cd as low as 30 ppb are toxic to many aquatic animals, and some sensitive organisms or life-history stages are sensitive to less than 10 ppb. Cadmium at low levels may enhance functional parameters in aquatic animal species, but toxicity is highly dependent on hydrogen ion, ligand concentrations, salinity, and temperature. All curves of toxicity were similar to one of the three graph forms in Fig. 4.13. Figure 4.13a represents an accelerating effect of Cd concentration on growth reduction presumably resulting from a drain on the structure remaining. Figure 4.13b illustrates a decreasing effect with concentration indicating a saturation of the toxic action at elevated concentrations. Figure 4.13c may be the most general in that the other two are special cases. This is the typical Arndt-Schulz effect curve described for all poisons by Lamanna and Mallette (1953). Although some toxicity data reviewed did not show a region of stimulatory Cd concentration, low concentrations were not always tested.

Models—

If general models of Cd effect are recognized, data from diverse experiments may be organized in terms of model parameters and more precise comparisons can be made. Although only species-effect data have been reviewed for Cd toxicity, models presented are descriptive of trophic levels, also. In Section 6 these trophic-level models are combined in an ecosystem model calibrated with data from the Cd streams study of Giesy et al. (1979).

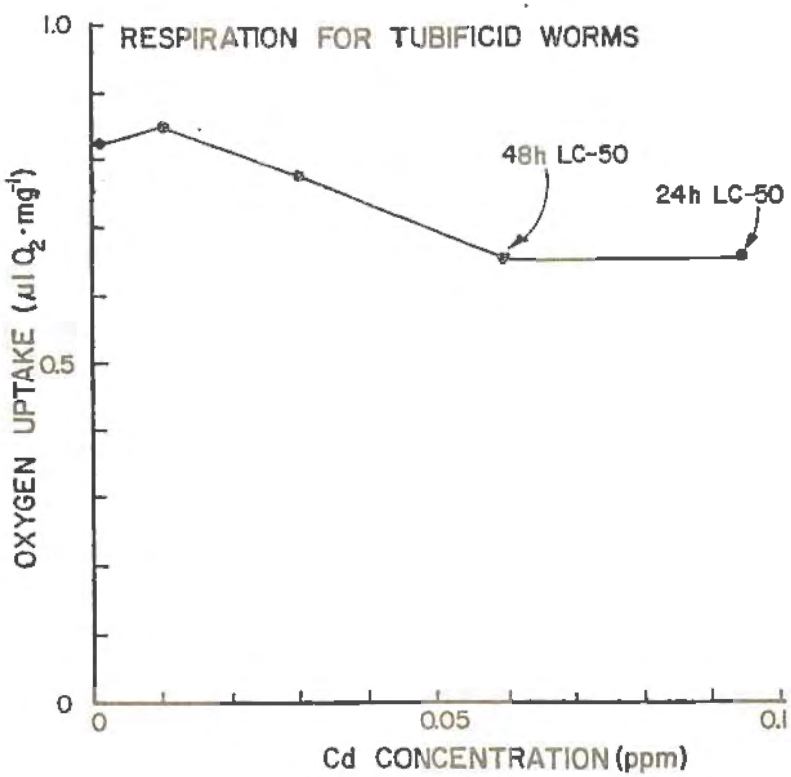

Figure 4.10. Effect of Cd on respiration of tubificid worms in static culture (from Brkovic-Popovic and Popovic 1977).

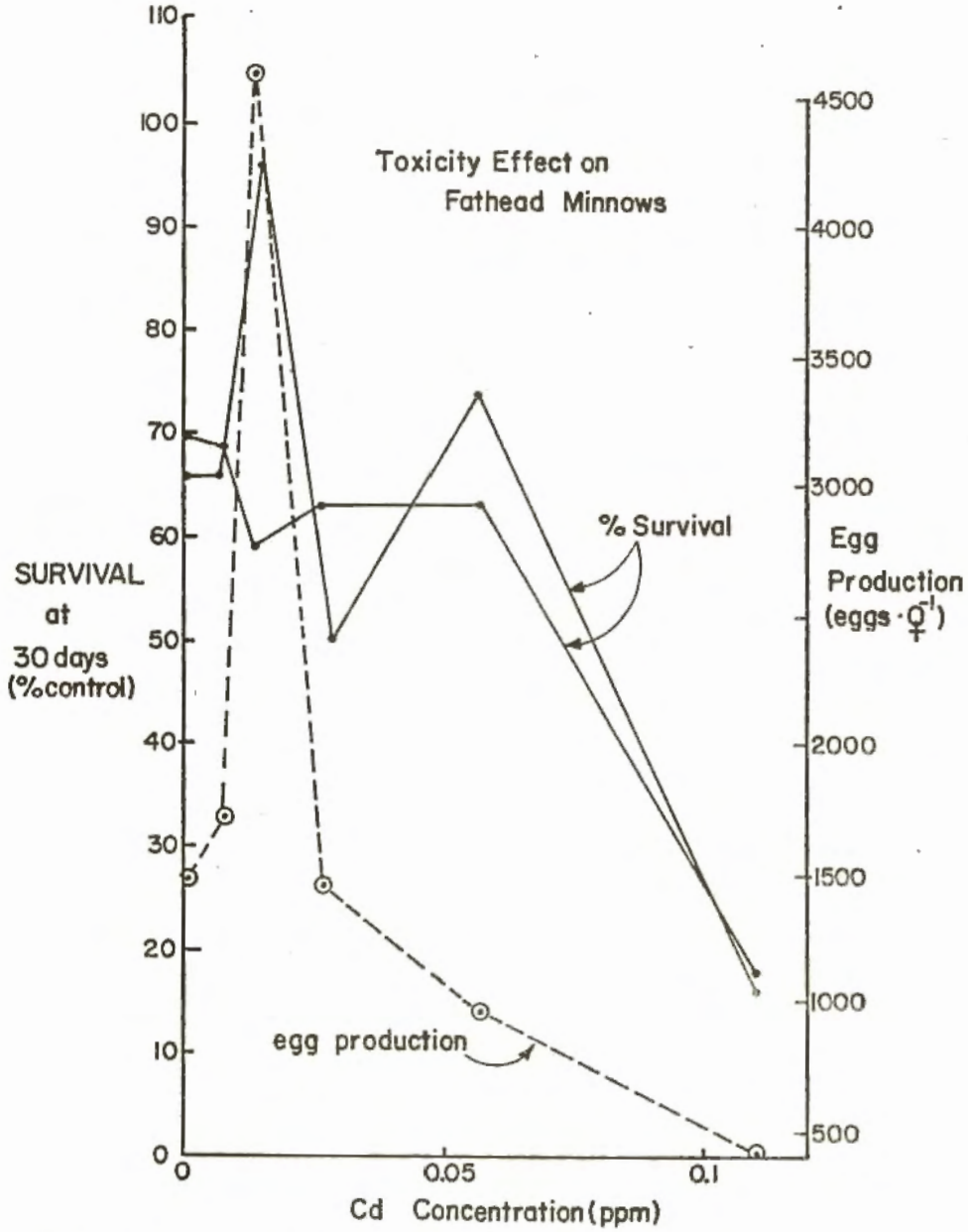

Figure 4.11. Effect of Cd on egg production and survival of fathead minnows in flow-through culture (from Pickering and Gast 1972).

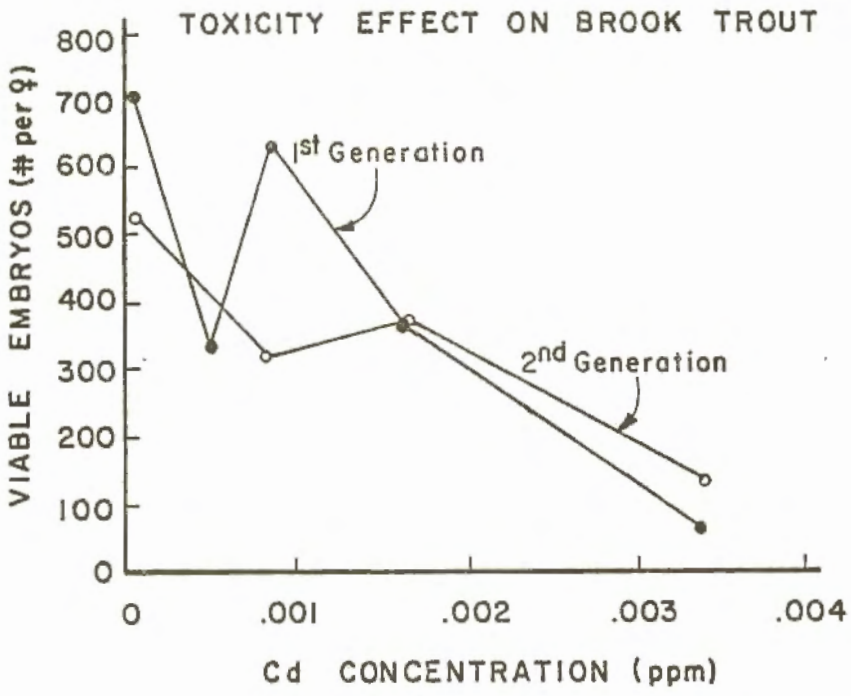

Figure 4.12. Effect of Cd on brook trout in flow-through systems (from Benoit et al. 1976).

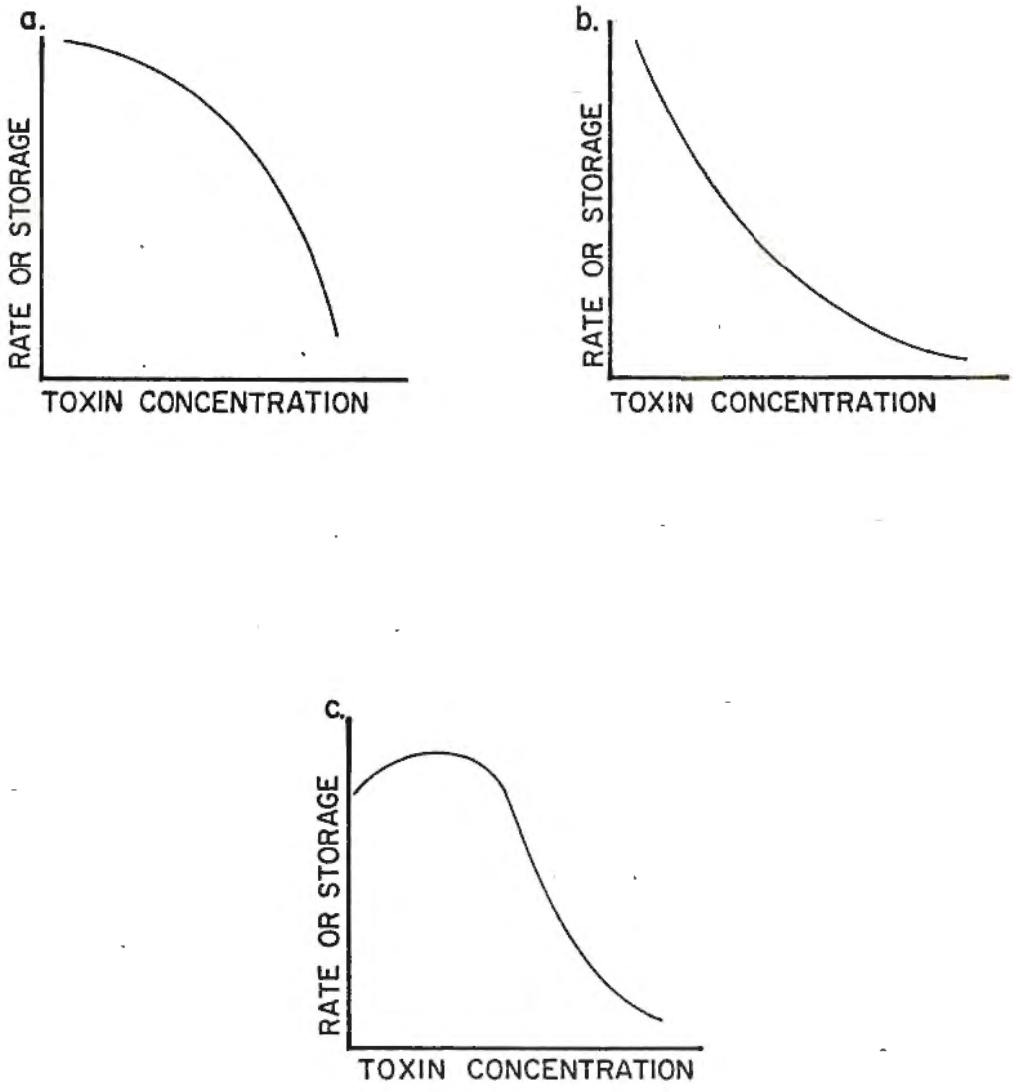

Figure 4.13. General curves relating toxin concentration to toxin effect. (a) accelerating effect; (b) exponential effect; and (c) general curve with optimum concentration.

Numerous mechanisms of Cd toxicity have been suggested for particular organisms and groups of species. As reviewed by Hammons et al. (1978), most of these mechanisms result from inactivation of enzymes by binding of Cd with sulfhydral groups of proteins interfering with photosynthetic and respiratory pathways of energy transformation. Although no known requirement for Cd exists in living systems (Hiatt and Huff 1975), the stimulatory responses measured at low Cd concentrations must result from some beneficial mechanisms. Three models of Cd action are presented to generalize these experimental results.

Figure 4.14 illustrates a model of the overall effect of a toxicant (T) on a storage (Q). The storage is modeled using the logistic growth equation (squared respiratory drain [R]) and the toxicant reduces structure (J) as a product of storage and toxin concentration (Fig. 4.14a). A BASIC computer program of this model is given in Table B.1. The curves generated by this simplified model (Fig. 4.14b) are typical of the results seen for many studies in the literature (see Figs. 4.6–4.12).

Figure 4.15 summarizes the effect of the toxicant in a more mechanistic manner. In this model, Cd is represented both as a required nutrient for organic synthesis and as an inhibitor on metabolic feedback processes such as enzyme reactions. The computer program for this model is given in Table B.2. Figure 4.15b presents representative output for this model at two toxicities for several toxin concentrations. These curves show a stimulatory region for the metal as well as the stress region more generally considered.

In Fig. 4.16a toxic action is combined with nutrient recycle. The computer program is given in Table B.3. A wide range of toxicities and nutrient uptake rates were examined and stimulation of production was found at some combinations even though biomass was simultaneously reduced (Fig. 4.16b). The optimum effect was the result of an increase in available nutrients and would not be found in systems with nutrient excess.

In summary, we conclude that observed Cd toxicity data may be generated from simple models of toxin interaction for organisms or trophic levels. Models of toxicity must include more than just negative interactions such as those in Fig. 4.14 to be inclusive of the Arndt-Schulz phenomenon; however, for producers, stimulation is possible indirectly through nutrient recycling (Fig. 4.16).

Cadmium Bioconcentration

Through passive and active concentrating mechanisms, biological systems can have a large impact on cycling of minerals in nature. When absorbed or adsorbed by a motile organism, elements may be transported and relocated in a system. Through uptake and death, an animal or plant may store toxicants for varying time spans, effectively removing them from biological circulation. If inputs of a metal such as Cd are low, biological uptake may greatly lower effective toxin concentration. Mechanisms of storage are systems of detoxification. However, when systems receive chronic elevated inputs, detoxifying systems may be overloaded.

Different species have variable abilities to remove Cd. Through system selection, species with high resistence to Cd and detoxifying mechanisms may be selected at elevated Cd concentrations.

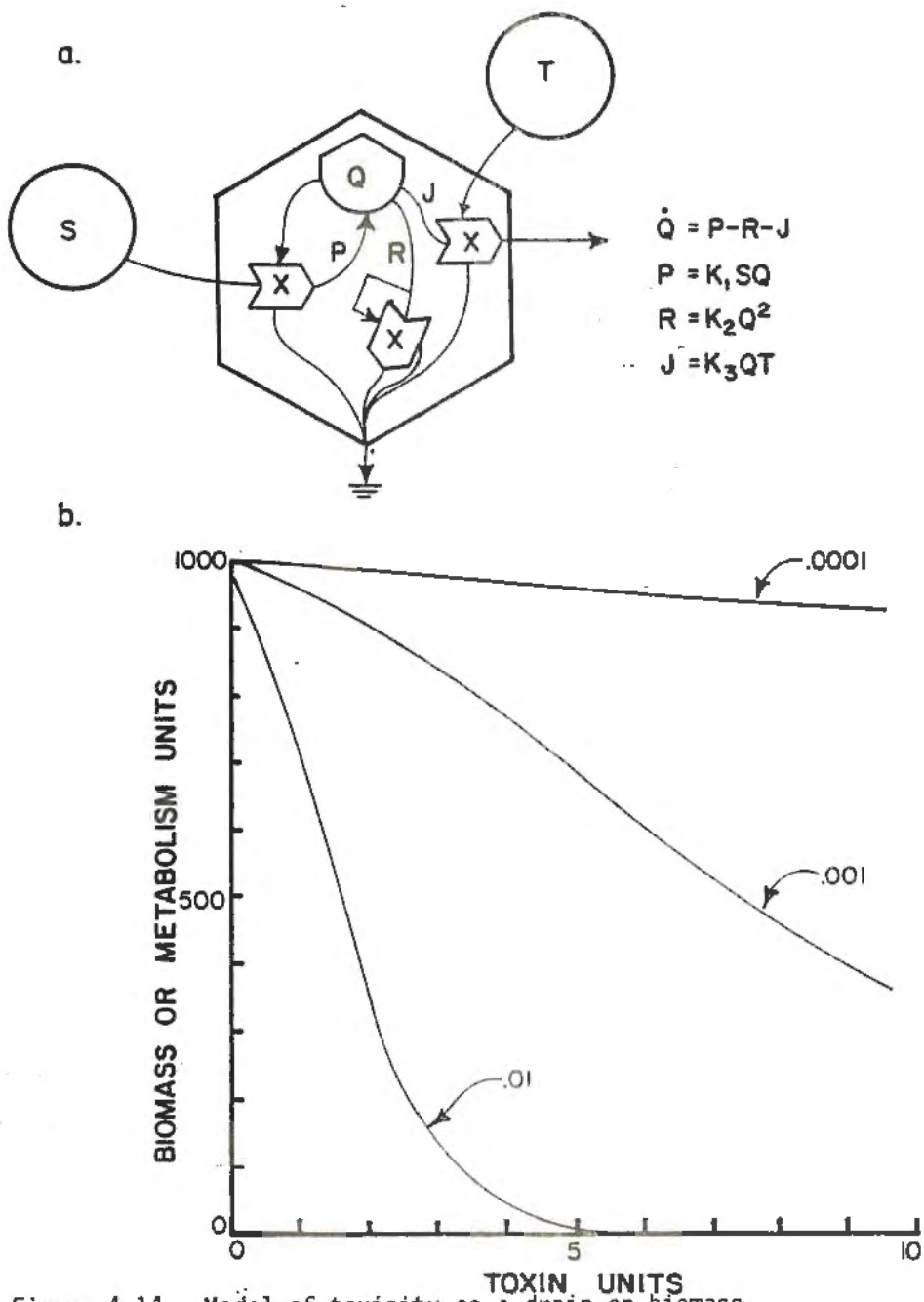

Figure 4.14. Model of toxicity as a drain on biomass. (a) model; (b) representative output for three values of K_3.

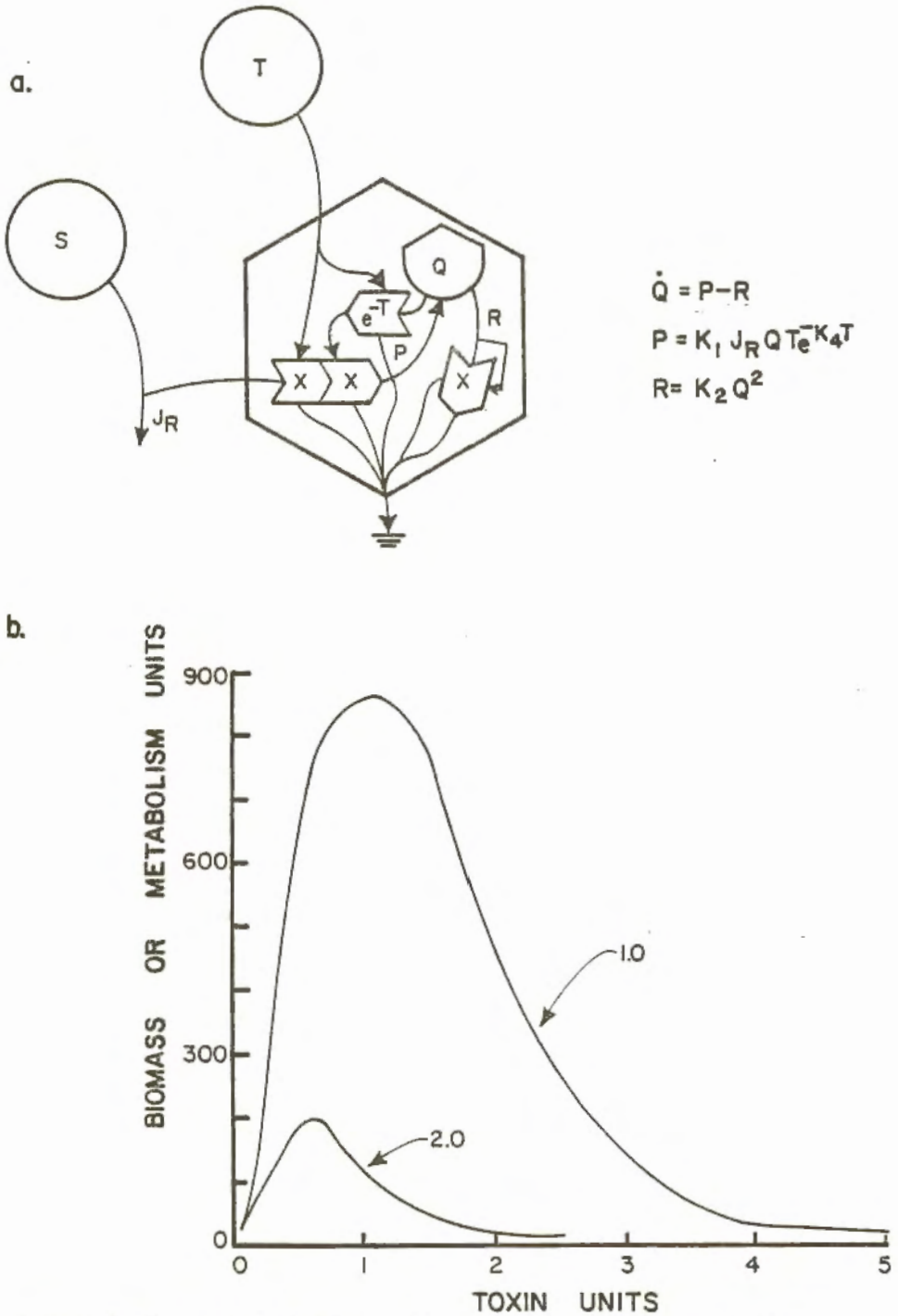

Figure 4.15. Model of toxin effect on an organism including a stimulatory function and an exponential toxic function. (a) model; (b) representative output for two toxicity levels.

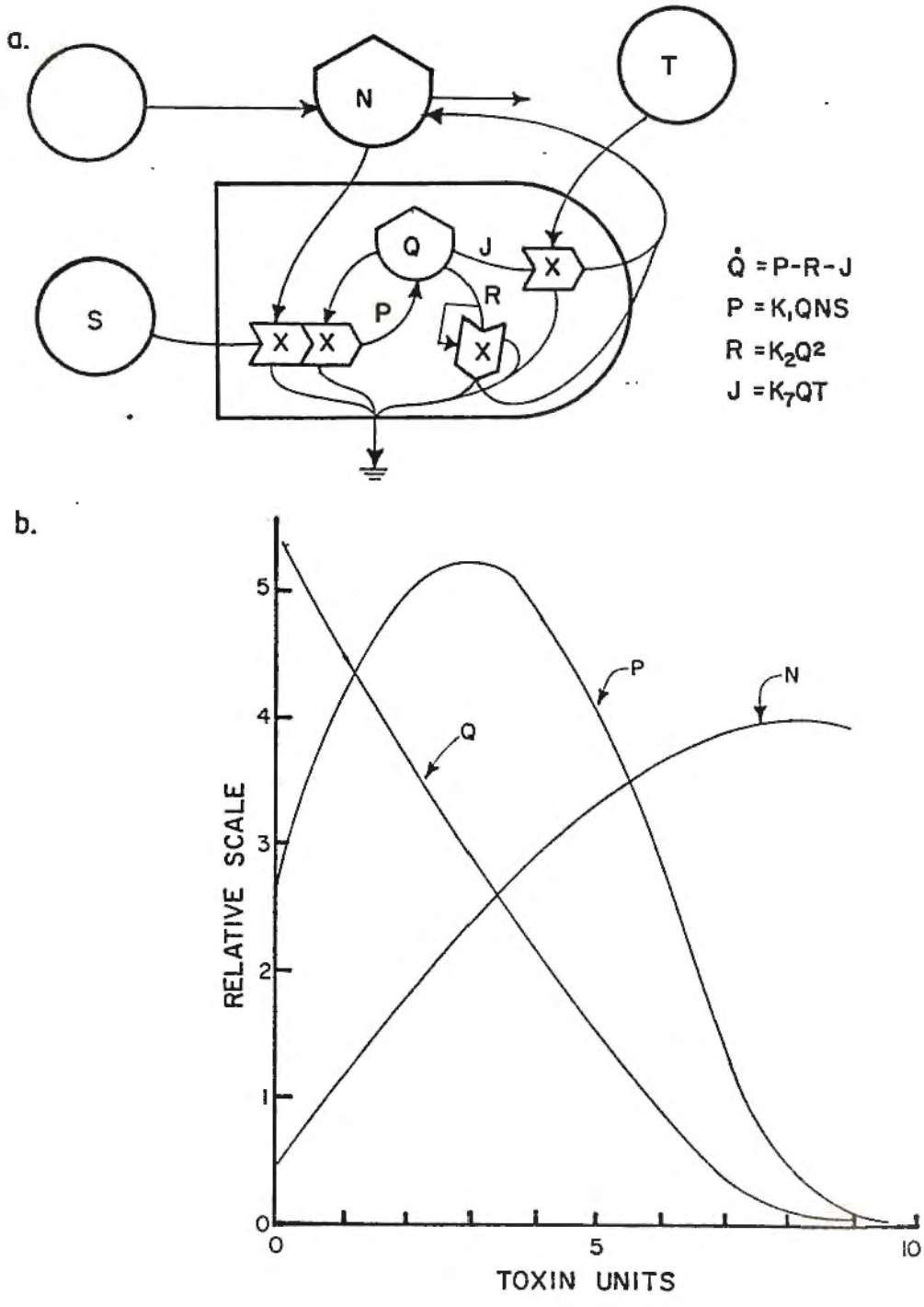

Figure 4.16. Model of toxicity effect on recycle showing stimulation of production (P) because of storage (Q) decay and nutrient (N) recycle. (a) model; (b) representative output.

In order to generalize on Cd uptake ability, a short review is made of curves of Cd uptake as a function of Cd concentration for various groups of organisms. A simple computer model is presented that generates similar results.

Microbes—

Research reported by Doyle et al. (1975) for various microbial species shows the variability of uptake by different species (Fig. 4.17). However, concentration factors (defined as ratio of concentration in cell to concentration in solution) generally decline as high solution concentrations are tested and curves are possibly hyperbolic for some organisms. The one fungal species, Aspergillus niger, did not demonstrate this effect and was able to concentrate Cd from solution by a factor of 2000X. Of the microbial organisms tested, Bacillus cereus had the greatest concentration factor with a value of 3870X at 10 ppm Cd in solution.

Plants—

A great number of Cd uptake studies have been made for plants and algae. Two representative curves are shown in Figs. 4.18 and 4.19. The uptake of Cd was studied by Hart and Cook (1975) for Chlorella pyrenoidosa at a series of Cd concentrations (Fig. 4.18). As Cd concentration in solution was increased, concentration factor in the algae declined with the highest concentration factor reported as 4500X (assuming protein represents 50% of total algal mass) at a solution concentration of 0.25 ppm Cd. Other workers have found Cd concentration by algae of 2000X for Anacystis nidulans (Katagiri 1975); 4000X–6700X for marine diatoms (Kerfoot and Jacobs 1976); 80,000X for mixed algae (Kumada et al. 1973); and 10,000X for marine phytoplankton (Knauer and Martin 1973). Although these concentration factors are dependent on water chemistry as well as reaction time (e.g., see Fig. 4.18), they may represent significant immobilization of Cd in biological systems.

Figure 4.19 presents an uptake curve for the aquatic macrophyte Najas guadalupensis reported by Cearley and Coleman (1973), which is representative of Cd uptake by plants at increasing metal concentrations. At a Cd concentration of 100 ppb in solution, a concentration factor of 40,000X was measured. Giesy et al. (1979) reported Cd concentrations >40,000X for roots of Juncus diffusissimus and 10,000X for leaves in stream microcosms.

Animals—

As with microbes and plants, Cd uptake by animals is a hyperbolic function of Cd in solution. Figure 4.20 illustrates steady state Cd levels reported by Spehar et al. (1978) for larval stages of Hydropsyche betteni, a caddisfly, and Pteronarcys dorsata, a stonefly. Once again we see the general hyperbolic relationship between Cd in solution and Cd concentrated by the organisms. A concentration factor for Cd >30,000X was seen at low solution concentration for the caddisfly and 2300X for the stonefly.

Model—

A model of Cd uptake and concentration by organisms must generate asymptotic charge-up curves and a hyperbolic relationship between steady state concentration in the organism and in its growth medium. Models used previously for adsorption of metals by solids include the Fruendlich isotherm (Gardiner 1974) and the Langmiur isotherm (Castellan 1964). These models of

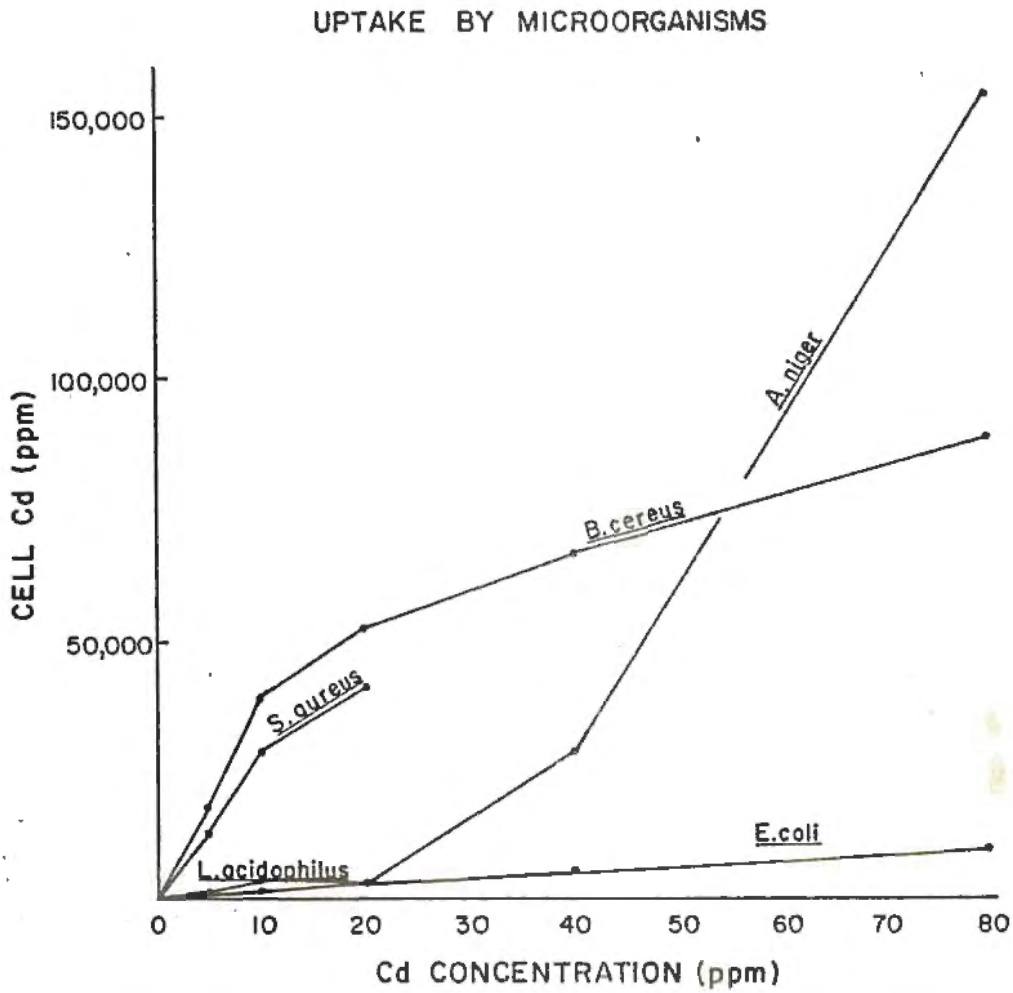

Figure 4.17. Uptake of Cd by five microorganisms in static culture (from Doyle et al. 1975).

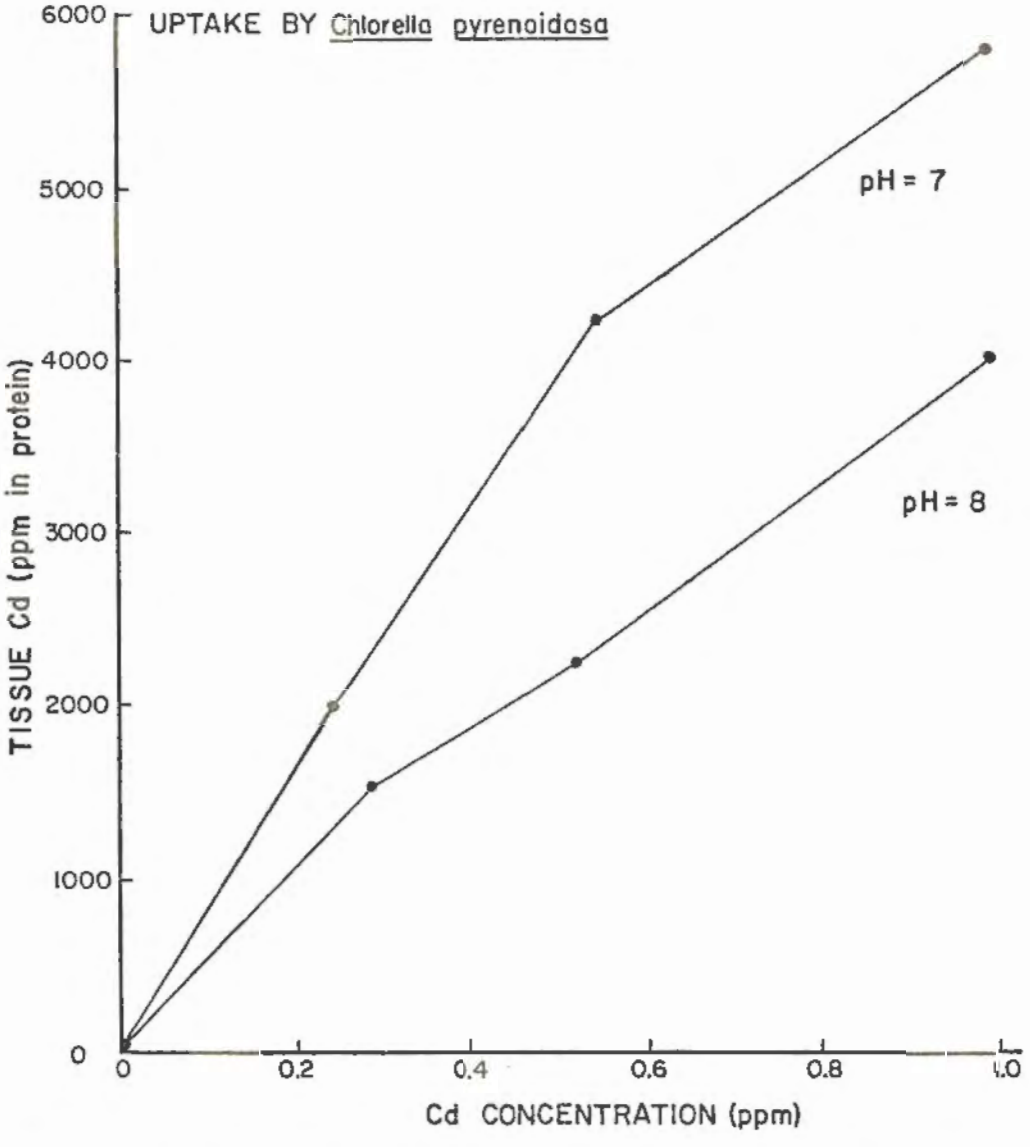

Figure 4.18. Uptake of Cd by Chlorella pyrenoidosa at two pH values in static culture (from Hart and Cook 1975).

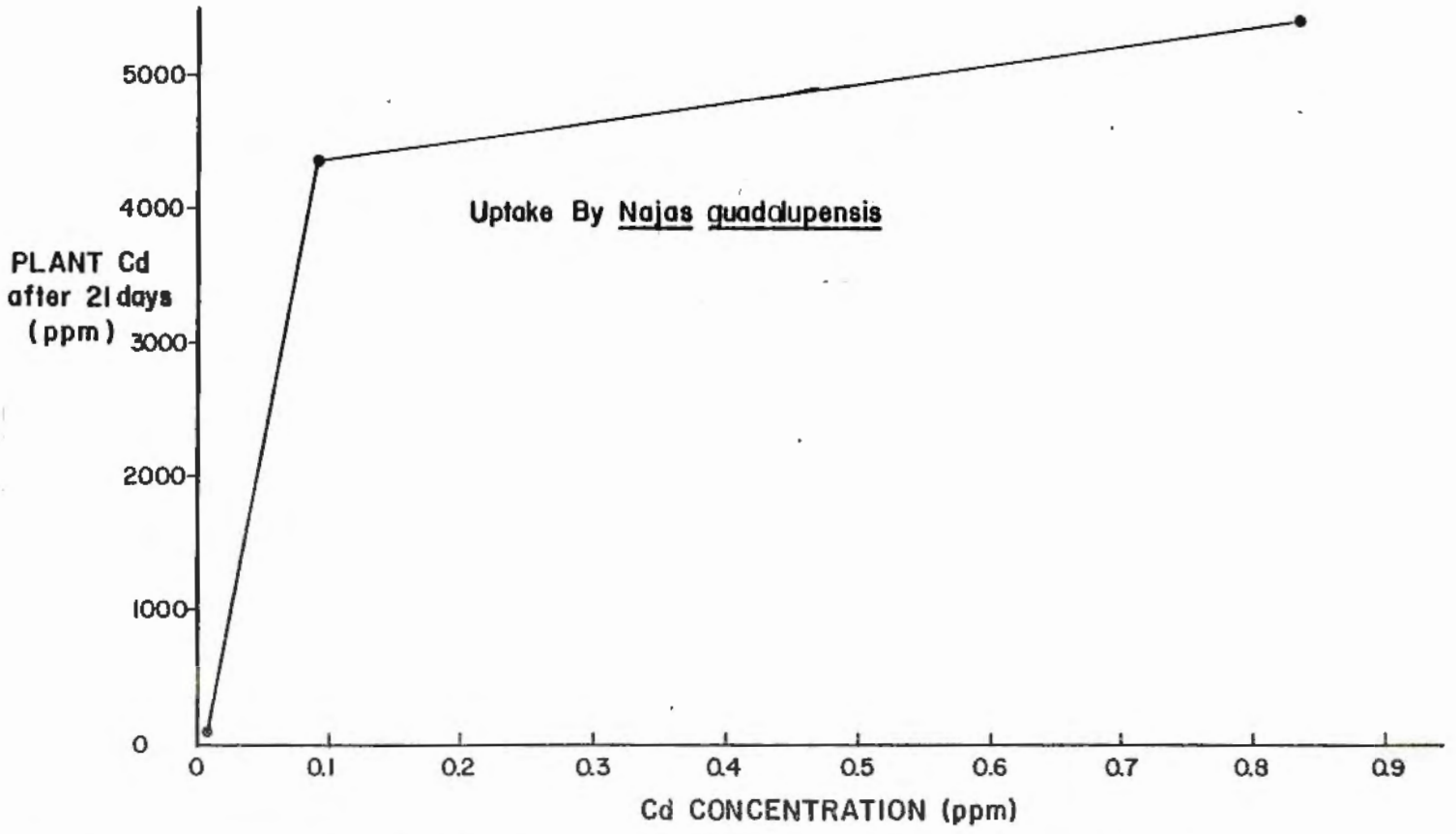

Figure 4.19. Uptake by Cd by the submerged macrophyte Najas quadalupensis in flow-through systems (from Cearley and Coleman 1973).

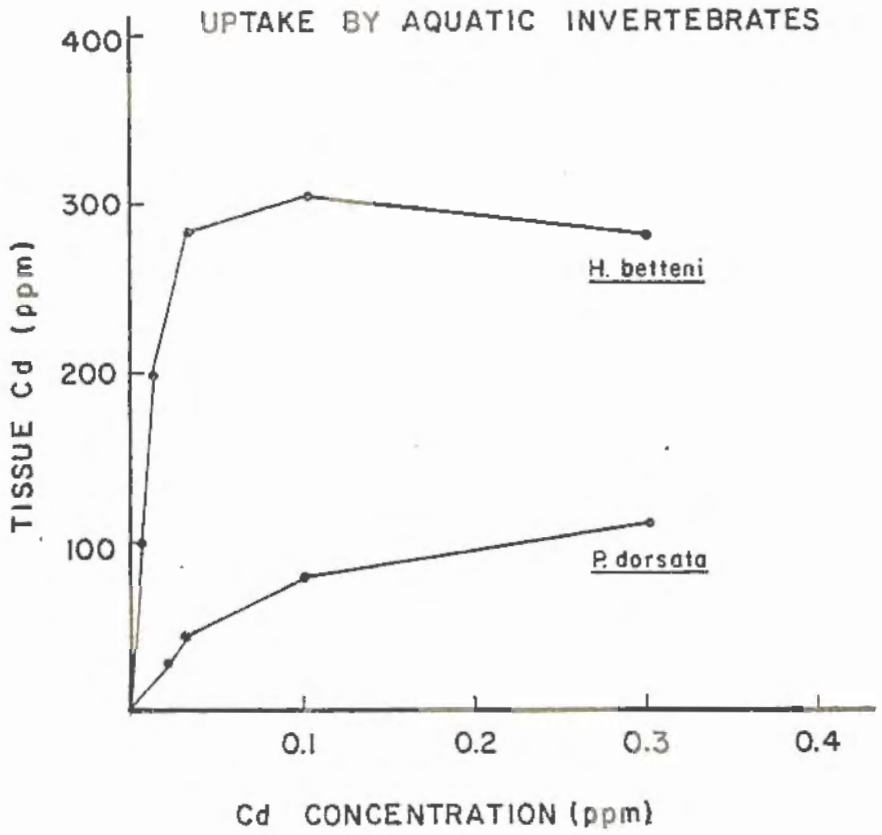

Figure 4.20. Uptake of Cd by two aquatic invertebrates in batch cultures (from Spehar et al. 1978).

Cd uptake by adsorption include a cycling-receptor of surface area for collection of Cd. The model diagramed in Fig. 4.21a showing Cd accumulation as regulated by biomass includes the adsorption loop. The BASIC computer program used for simulations of this uptake model is listed in Table B.4.

Figure 4.21b presents results of a simulation of this model in which the surface area/absorbed Cd ratio was varied from 10 to 300 $cm^2 \cdot \mu g\ Cd^{-1}$. Where fewer Cd adsorption sites are present, a lower total Cd concentration is possible. Smaller sizes have a greater surface area per biomass and may collect more but store it for shorter times. Figure 4.21c illustrates the effect of increasing the average radius from 0.1 mm to 1.0 mm in this model. Thus, there are two mechanisms available to reduce the effective concentration of a toxin in solution: increasing number of surface binding sites and developing small size.

Embodied Energy–Toxicity Correlation

As discussed earlier in this report, we expect a consistent relationship between the controlling effect of a toxin such as Cd and its embodied energy. The nature of this correlation may now be hypothesized. Given the generalized toxicity curve in Fig. 4.22a, we expect major changes in the correlation between these parameters for any given system, tending to give zero control effect at very low and very high toxin concentrations (Fig. 4.22b). A positive correlation is expected at low concentration and a negative effect at higher toxic concentrations. The segment of the curve where there is no correlation between embodied energy of the ocntroller and its control effect represents massive toxicity by the controller and may correspond the concentrations of the toxin that the living system has not been exposed to long enough for adaptations to occur. We hypothesize that the segment of the curve showing a positive correlation corresponds to toxin levels naturally occurring in the environment.

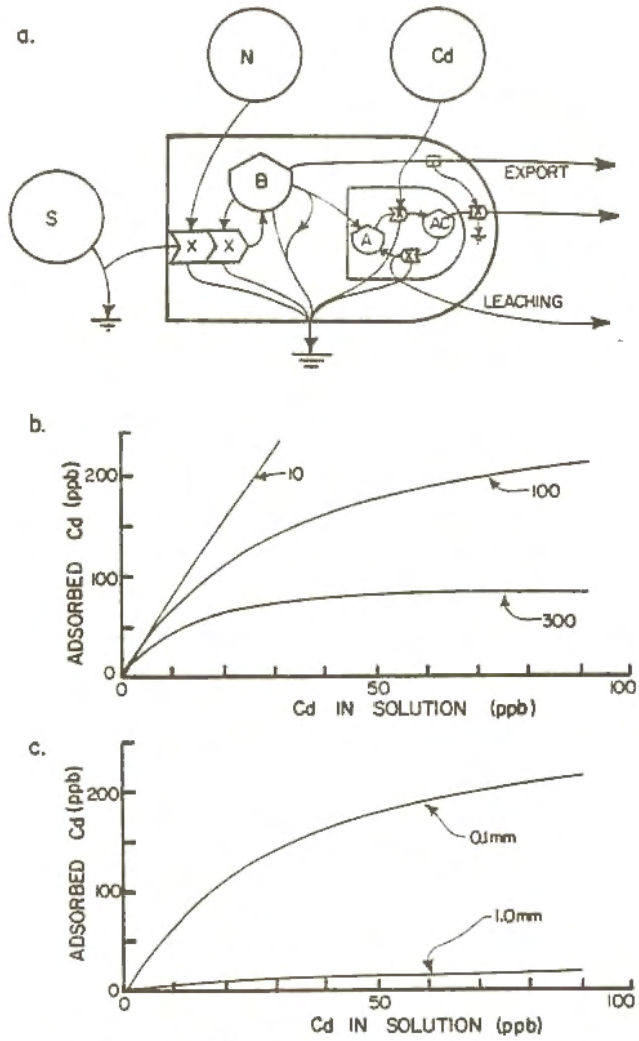

Figure 4.21. Model of Cd adsorption in periphyton. Growth of biomass (B) is dependent on sunlight (S) and nutrients (N). Cadmium is adsorbed by surface area (A) resulting in Cd-saturated surface area (AC). (a) model; (b) effect of increasing surface area/Cd ratio; (c) effect of increased cell radius.

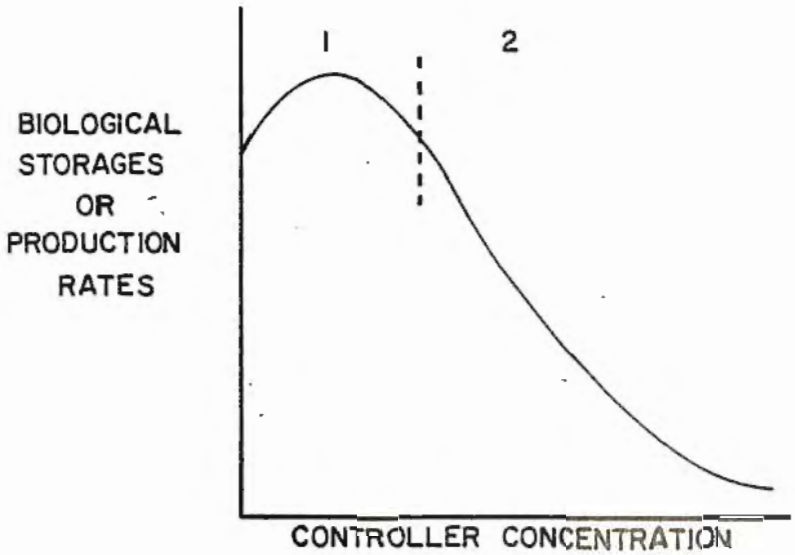

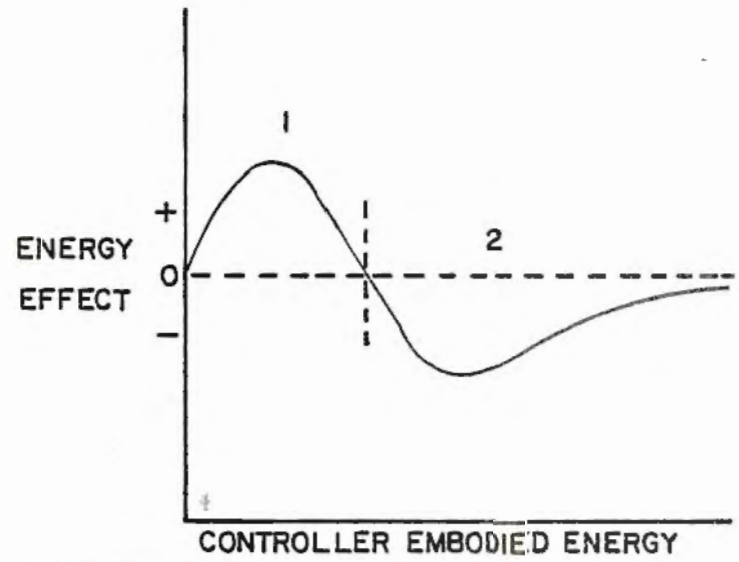

Figure 4.22. Toxicity curve (a) and corresponding energy effect—energy quality correlation curve (b). Region 1 represents a positive amplifier action and region 2 indicates a negative action.

SECTION 5

METHODS

CADMIUM STREAMS

Six experimental streams were operated as microcosms receiving two different Cd treatments. Detailed descriptions of the methods used in the Cd streams study are presented by Giesy et al. (1979).

Site Description

The artificial streams used to study Cd fate and effects are located in Aiken County, South Carolina, on the Savannah River Plant, which is operated by the United States Department of Energy. The streams were built with funds provided by the Environmental Protection Agency to study the fate of pollutants in natural water systems. Previous work at this site has included studies of the fate of NTA and mercury in stream ecosystems (Kania and Beyers 1974; Kania et al. 1976).

The six channels used for the Cd study measured 92 m long, 0.61 m wide, and 0.31 m deep, with head and tail pools 1.5 m long, 3 m wide, and 0.9 m deep. The pools and channels were lined with 0.05-cm-thick black polyvinyl chloride film. Washed quartz sand was distributed in the channels to a uniform depth of 5 cm, and a 10-cm layer of natural streambed sediment was distributed in the pools.

Water for the channels was taken from a deep well and mixed with a hydrated lime slurry before being added to the systems. Major parameters of input water quality are listed in Table 5.1 and indicate the soft, low organic carbon nature of the stream water. Flows were maintained continuously at 95 $L \cdot min^{-1}$ and resulted in a water depth of 20 cm in the channels. The mean water retention time and current were 2 hr and 1.3 $cm \cdot s^{-1}$, respectively.

Water flow was started on November 1, 1975, and the systems were seeded from the control channels of a previous study (Kania et al. 1976) to rapidly establish biological communities known to be well adapted to channel conditions. Two macrophytes, Juncus diffusissimus and Gratiola virginiana, which had naturally colonized the channels during previous studies, were transplanted into the systems. Consumer organisms consisting of clams, crayfish, and two species of fish (mosquito fish and bluegill) were added to the systems after some plant growth had occurred.

Cadmium inputs into four of the six channels were started on March 18, 1976. Cadmium (as $CdCl_2$) was metered into the turbulent region of the head

TABLE 5.1. AVERAGE ANALYSIS OF MAJOR WATER QUALITY PARAMETERS IN CD STREAMS INPUT WATER AFTER TREATMENT WITH HYDRATED LIME

Parameter	Average value
Total dissolved solids	20.5 $mg \cdot L^{-1}$
Total alkalinity	9.14 $mg \cdot L^{-1}$ as $CaCO_3$
Hardness (EDTA)	11.08 $mg \cdot L^{-1}$ as $CaCO_3$
Specific conductance	31 $\mu mho \cdot cm^{-1}$
Ionic strength	2.5×10^{-4}
Calcium	3.17 $mg \cdot L^{-1}$
Sulfate	1.9 $mg \cdot L^{-1}$
Magnesium	0.24 $mg \cdot L^{-1}$
Nitrogen (NO_2 and NO_3)	15.8 $\mu g \cdot L^{-1}$
Phosphorus (total)	2.9 $\mu g \cdot L^{-1}$
Cd	0.023 $\mu g \cdot L^{-1}$

pools with a 4-channel peristaltic tubing pump. The Cd levels established were 5 $\mu g \cdot L^{-1}$ in two channels and 10 $\mu g \cdot L^{-1}$ in another two, with the remaining two channels serving as controls. Cadmium inputs were discontinued on March 18, 1977, a full year after they were started, and data were collected for 5 mo after that date.

Community Structure

Periphyton biomass, pigment levels, species composition (algal only), and algal volume were determined monthly on vertical glass microscope slides oriented parallel to the current flow in the channels. The same parameters were also measured bimonthly on clean glass slides that were allowed to colonize for 30 days, as well as from the channel walls on four occasions, and twice as complete cores through the water column, macrophytes, benthic mat, and sand substrate. Samples were also analyzed for total Cd content from all of these substrates.

On two occasions after Cd inputs were terminated, population densities of naturally colonizing macrophytes were high enough that plant biomass sampling by quadrat analysis was feasible. Ten 0.25-m^2 sections of sediment and associated plants were removed from each channel and plant biomass per unit area by species was calculated.

Quantitative samples for macroinvertebrates and microinvertebrates were taken on a routine basis from plate samplers and polyurethane sponges. Most organisms were identified as to species, and biomass and Cd concentrations were measured when practical.

System Responses

Measurements of total community primary production and respiration were made over 24-hr periods by measuring upstream-downstream change in oxygen by a method adapted from Odum (1956). Water samples were removed from the streams by siphon at 2-hr intervals and dissolved oxygen (DO) content was determined using a YSI model 54 DO meter calibrated using the azide modification of the Winkler method (APHA 1975).

In the spring of 1977 a semiautomatic method of collecting oxygen diurnal data was put into service. This system utilized 12 solenoid valves (one at the head and one at the tail of each channel), two YSI oxygen probes and meters, two timer boxes, and a chart recorder with another timer attached. At each end all six gravity-fed lines passed through solenoid valves into a single common line feeding the water over the end of the probe. Dissolved oxygen was monitored for 10 min each hour. Signals from the corresponding meters were fed into a timer that switched input to the recorder at 5-min intervals. In this manner, 5-min recordings of DO concentrations at each location were recorded for each hour during day and night. Probes were calibrated several times during each 24-hr period.

The hourly rate of change of DO was calculated for a given water mass using the flow time between stations of 2 hr. These values were corrected for diffusion by calculating percent saturation and using equation 5.1:

$$D = kS \qquad (5.1)$$

where D = diffusion rate (g $O_2 \cdot m^{-2} \cdot hr^{-1}$)
k = diffusion coefficient (g $O_2 \cdot m^{-2} \cdot hr^{-1}$ at 100% saturation deficit)
S = saturation deficit, calculated as S = (100 - % saturation)/100.

A positive diffusion value indicates oxygen diffusion into the water and therefore changes in DO are corrected by subtracting D. Values of k between 0.04 and 0.8 g $O_2 \cdot m^{-2} \cdot hr^{-1}$ were measured in the streams using the floating-dome method of Copeland and Duffer (1964) modified by McKellar (1975). Values of k between 0.1 and 1.0 were used in the productivity calculations depending on weather conditions, with the highest value used for windy and rainy days. In no case did the diffusion correction alter metabolism values by more than 10% of their uncorrected values.

Corrected rate-of-change data was plotted and areas integrated by counting squares. Nighttime respiration values were averaged and 24-hr respiration (R_{24}) was assumed to be equal to the average nighttime hourly rate times 24 hr. Gross photosynthesis (P_G) was the area above this average R line and net photosynthesis (P_{net}) equals P_G-R_{24}. P/R ratios were calculated as P_G/R_{24}.

Exported organic material and associated Cd were quantified from October 1976 until August 1977. All effluent water from each channel was passed through a 4-in. plastic pipe that contained a motor-driven, stainless-steel mixer blade. Material collected on the end screens was washed into the sampling system daily. Mixed effluent was subsampled from each channel at a rate of 4 $L \cdot d^{-1}$ with a peristaltic pump. These subsamples were filtered onto prefired, Gelman A-E glass-fiber filters, dried, weighed, ashed at 450°C, and reweighed to obtain ash-free dry weight of exported material. From the length of sampling, the volume of water exported, and the volume of the collected subsample, channel export was calculated as grams per square meter of channel bottom per day.

Cadmium Analysis

For Cd analysis, dried biological samples were wet-ashed in 30-ml porcelain crucibles with 2 ml of concentrated nitric acid at 80°C for 1–3 hr or until all solid material had dissolved and NO_2 evolution ceased. The samples were cooled, 2 ml of 30% hydrogen peroxide added, and reheated until gas evolution ceased. Samples were cooled to room temperature, diluted volumetrically using deionized water, and stored in acid-washed polyethylene bottles.

Total Cd was determined using flameless atomic absorption spectrophotometry. For 10 µL samples, sensitivity was approximately 0.2 µg $Cd \cdot L^{-1}$ in solution. All determinations were corrected for reagent blanks and compared to commercially prepared certified standards. Standard addition curves had the same slope as curves constructed from standards in distilled water, indicating the selected charring and atomization time and temperature regime removed most matrix interferences.

Other Studies

Concurrent studies of Cd toxicity were run using the stream water with crayfish (Thorp et al. 1979), mosquito fish (Giesy et al. 1977; Williams and Giesy 1978), and leaf decomposition (Giesy 1978).

STREAM MODEL

An energy and matter flow model of the artificial streams was constructed first as a diagram using the energy circuit language of Odum (1971). The model is of intermediate complexity, combining storages of nutrients, algae, macrophytes, consumers, and detritus and their uptake of and response to Cd at different concentrations. Further details of the model are described in the results section of this report.

The major biomass storages and their Cd content were monitored throughout the 2-yr study and have been used directly to calibrate the model when possible. However, few of the data are for average levels throughout the microcosms, but rather are for concentrations on replicable substrates. Thus, to calibrate the model to whole-system averages, assumptions and extrapolations from a few measurements were made to other data.

Also, few of the rates were actually measured during the project other than Cd uptake and release, system production and respiration, and export; and therefore, a considerable amount of parameterization was done by simulating the model and comparing results to the actual measured storages over time. Specific rates from the literature were used when available.

Computer simulations were made in FORTRAN computer language during the early stages and finished using BASIC language with an Intercolor desk top microcomputer. Integration was by means of simple difference equations with variable time steps.

The model evolved considerably during the 12-mo period of simulations as mechanisms were seen to be inconsistent with actual data or other mechanisms necessary to generate the observed results became clear.

ENERGY RELATIONSHIPS

Calculations of embodied energy have been made according to the conventions set forth by Odum (1978). Basically, embodied energy is the energy of one type necessary to produce an energy flow or storage of another type. The units of embodied energy are reported in terms of some reference energy type chosen for convenience in a given situation. For the comparisons made in this report, average insolation has been chosen as the reference energy (S.E. Cal).

In order to calculate the energy embodied in a particular energy flow or storage, a model was prepared showing all of the major energy flows responsible for generating the flow of interest. Figure 5.1 presents such a model for a simplified production process. Production (C) produces biomass (Q)

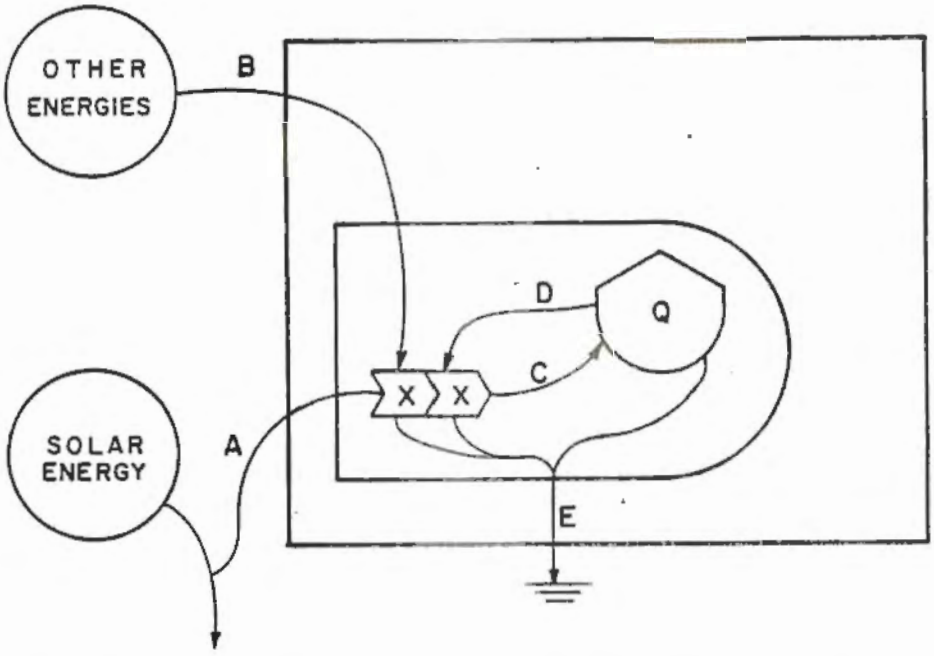

Figure 5.1. Aggregated model of a production process with two energy inputs (A and B), gross production (C) of a stored product (Q) with feedback maintenance (D) and maintenance energy loss from the system (E). The embodied energies of flows C, D, and E are equivalent and are equal to the sum of input embodied energies (A + B). The embodied energy in Q is equal to the total embodied energy input (A + B) multiplied by the turnover time of Q.

with maintenance energy loss (E) and feedback maintenance (D). For example, this model could represent production in a pond where A represents direct solar energy and B represents the energy associated with all other inputs such as nutrients in rain and runoff from the land . These other energy flows must also be calculated in terms of S.E. Cal. This calculation may be made with the use of estimates of energy content (free energy of chemicals, kinetic energy of rain, etc.) and values for energy transformation ratios (quality factors) published by Odum and Odum (1980), Odum et al. (1980), Wang et al. (1980), and others.

As defined by Odum (1978) each energy flow within the system boundary has equal embodied energy flow. Thus the embodied energy in flows C, D, and E are equal although their heat equivalent energies may be very different. The embodied energy of a storage is equal to the integrated input energy flows during one turnover time of the storage.

If the actual energies in C, D, and E (Calories) are known, then transformation ratios (TR) may be calculated from this model by dividing the total input energy (A + B) by the actual energy in each resulting flow. Thus (A + B)/C represents the TR for gross productivity in Fig. 5.1, with units of S.E. $Cal \cdot Cal^{-1}$. These TR values may then be used to evaluate some other situation.

Values for TR for a particular energy flow may be calculated from several different models and compared. There may be a theoretical minimum value for each TR that represents the optimal efficiency for the given energy transformation. Precise TR values of many energy types and flows are not yet known, so all calculations are assumed to be preliminary.

Toxicity Effect

The energy effect of a toxin or controller is measured as an amplification (either positive or negative) of an energy flow or storage expressed in embodied energy units. This amplification or perturbation may be measured relative to a control with zero concentration of the toxin or other controller.

For example, assume that a Cd input of 1 $\mu g\ Cd \cdot m^{-2} \cdot d^{-1}$ to a steady state microcosm is found to decrease primary productivity relative to a control by 10 $Cal \cdot m^{-2} \cdot d^{-1}$. From other estimates we find that the TR for primary productivity is 100 S.E. $Cal \cdot Cal^{-1}$ and thus the energy effect of the given Cd input is -1000 S.E. $Cal \cdot m^{-2} \cdot d^{-1}$. This toxin effect may be divided by the Cd input to give -1000 S.E. $Cal \cdot \mu g\ Cd^{-1}$ as the normalized effect. The energy effect of a controlling substance may be a function of its concentration and therefore the concentration must be specified for comparisons. As with embodied energy calculations, energy effect calculations are in a preliminary stage and subject to revision. The importance of the energy calculations made in this report is as much in presenting new, untested but promising methods as in the actual comparisons of embodied energy and toxicity effect.

SECTION 6

RESULTS

CADMIUM STREAMS

The Cd-stream study lasted 2 yr with five persons actively sampling various components of the biota for toxicity effects and measurement of Cd concentration. The final report for the project (Giesy et al. 1979) summarized the major findings but did not include a summary model of how the overall system was reacting to Cd dosing. In this section we integrate the data that are necessary to calibrate a simulation model of the streams.

Unfortunately, only a small part of the data was collected in convenient form for a system model; therefore, it has been necessary to extrapolate from artificial samplers to the whole stream community and to prepare new graphs on a square-meter basis. All of the data presented here are averaged over the entire stream area of 56 m^2, but in fact, the communities observed were quite variable depending on their location in the streams. Thus, colonization by algae and macrophytes was most rapid at the upstream end of the channels while a few species were always most abundant at the downstream end. Data from all samplers showed position effects; however, a zonation model of the channels was not attempted.

Biological Effects

The biological effects of Cd input to the artificial streams were affected by season, successional state, and taxonomic affinity. Prior to the addition of Cd the streams were all similar in composition of periphyton, populations of invertebrates, and plant growth. After Cd inputs of 5 or 10 ppb began, the streams demonstrated significant changes in response to the low Cd levels tested.

Algal populations in the treated channels were never as high as those in control channels (Fig. 6.1). Significant treatment as well as seasonal effects on algal pigment ratios were observed throughout the Cd input, and, on a macroscopic basis, the different treatments were visibly different in color. At least two algal species common in the control channels were never found in the treated channels during Cd input while other species formed luxurient filamentous blooms in the Cd streams.

The nonalgal portion of the periphyton was considered collectively as detritus and microbes. The biomass of this community was significantly lower in the treated channels than in controls within 2 mo of initial Cd input, but within 6 mo significant differences in this assemblage between treatments had

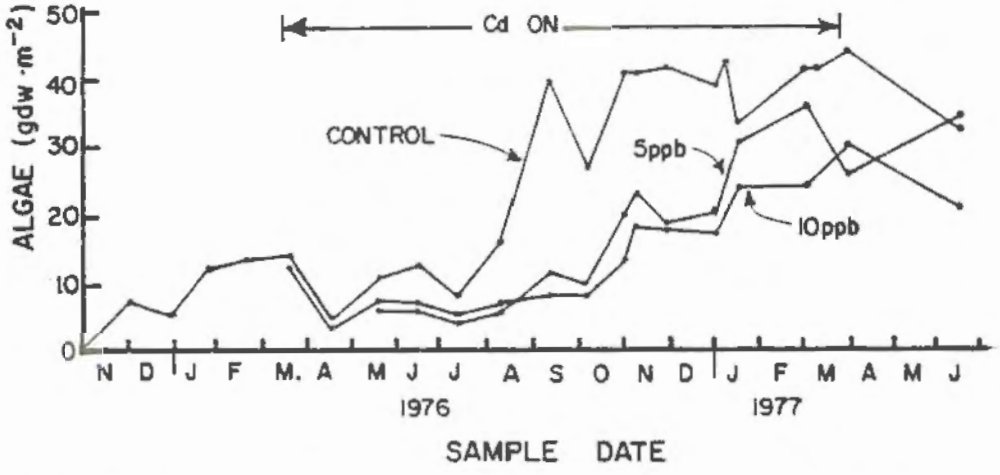

Figure 6.1. Live algal biomass during the 22-mo Cd-stream study. Values are stream averages extrapolated from glass slide and wall data for control, 5 ppb Cd, and 10 ppb Cd.

disappeared (Fig. 6.2). At all times during the study, the detrital biomass was about 5X as great as the algal component individually.

At the end of 1 yr of continuous Cd dosing, macrophyte populations were greatly reduced with respect to control populations. In March 1977, average dry matter densities were: control, 39; 5 ppb Cd, 5; and 10 ppb Cd, 6 $g \cdot m^{-2}$. Cadmium input was suspended in the spring and by the end of that summer the macrophyte populations had increased greatly, resulting in a substantial change of habitat in the channels.

An initial sensitivity of some groups such as protozoans, ostracods, cladocerans, and copepods to Cd input was demonstrated in microinvertebrate studies. Cadmium severely reduced copepods, ostracods, and testate amoebe; however, overall populations of microinvertebrates were increased because of stimulation of protozoans and rotifers.

Macroinvertebrate data indicated variable population responses in the different Cd treatments. At some sampling times, chironomid larvae were more abundant in the Cd streams than in controls; but, during most of the study, total macroinvertebrate biomass was reduced in the treated channels (Fig. 6.3).

Initially, 200 mosquito fish, Gambusia affinis, were released into each channel. Recovery of dead fish indicated increased mortality in the 10 ppb Cd treatment (55%) compared to the 5 ppb Cd treatment (23%) and controls (21%) within 3 mo of the beginning of Cd inputs. No further attempt was made to quantify the fish populations during this study.

Overall community metabolism was significantly lower in Cd-treated streams throughout the period of Cd input, and showed quick recovery soon after Cd input was stopped (Figs. 6.4a, b, and 6.5). The complete diurnal oxygen change curves from the Cd streams are given in Appendix A. All streams were autotrophic (P/R > 1), although the treated streams were less so. Cadmium treatment also significantly lowered community export of organic matter during this study with rapid recovery after treatments stopped (Figs. 6.4c and 6.5). Nutrient regeneration by microbial communities was significantly reduced by Cd treatment as indicated by weight loss in leaf litter packs.

In summary, Cd input at concentrations of 5 and 10 ppb demonstrated inhibitory effects in every trophic level examined, and yet was not completely inhibitory to any biological parameter.

Bioconcentration

Cadmium uptake by the stream periphyton communities was rapid with steady state levels reached within 50 days. Steady state levels were 3, 36, and 58 µg Cd·g dry weight^{-1} for control, 5, and 10 ppb Cd treatments. When Cd inputs were turned off, periphyton Cd concentrations dropped to control levels within 50 days.

Macrophyte uptake of Cd in the treated channels was much slower than for the periphyton, with steady state concentration attained after 5 mo of continuous input. Root Cd concentrations were 3–4X as high as leaf concentration in the two macrophytes examined. Whole plant averages were approximately 2, 75, and 150 µg Cd·g dry weight^{-1} for control, 5, and 10 ppb Cd treatments.

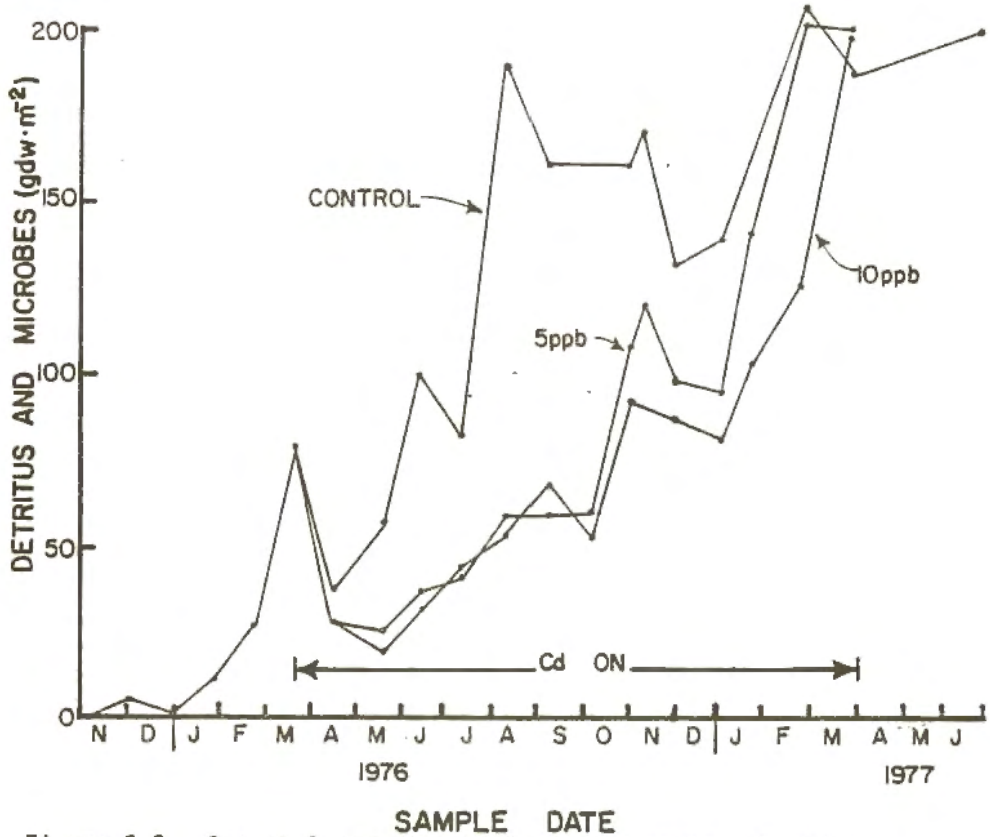

Figure 6.2. Detrital and microbial biomass during the 22-mo Cd-stream study. Values are extrapolated from glass slides, wall, and core samples for control, 5 ppb Cd, and 10 ppb Cd.

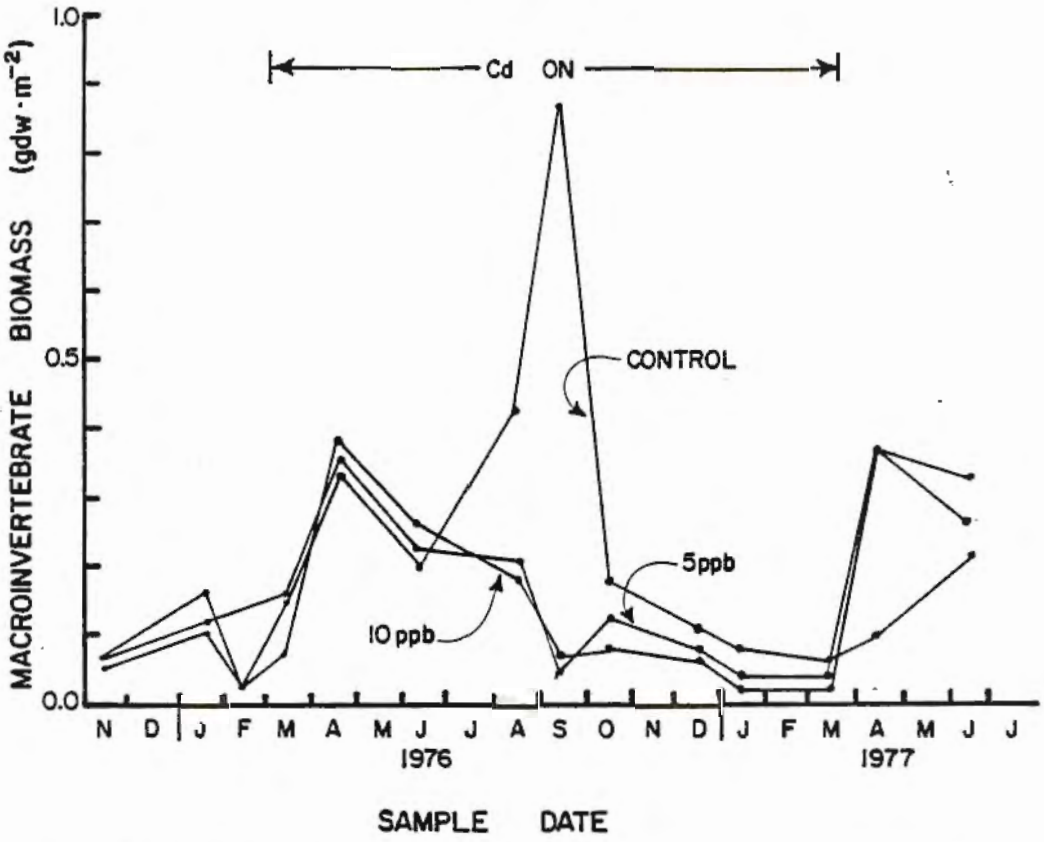

Figure 6.3. Biomass of macroinvertebrates during the Cd--stream study. Data are extrapolated from plate samples for control, 5 ppb Cd, and 10 ppb Cd.

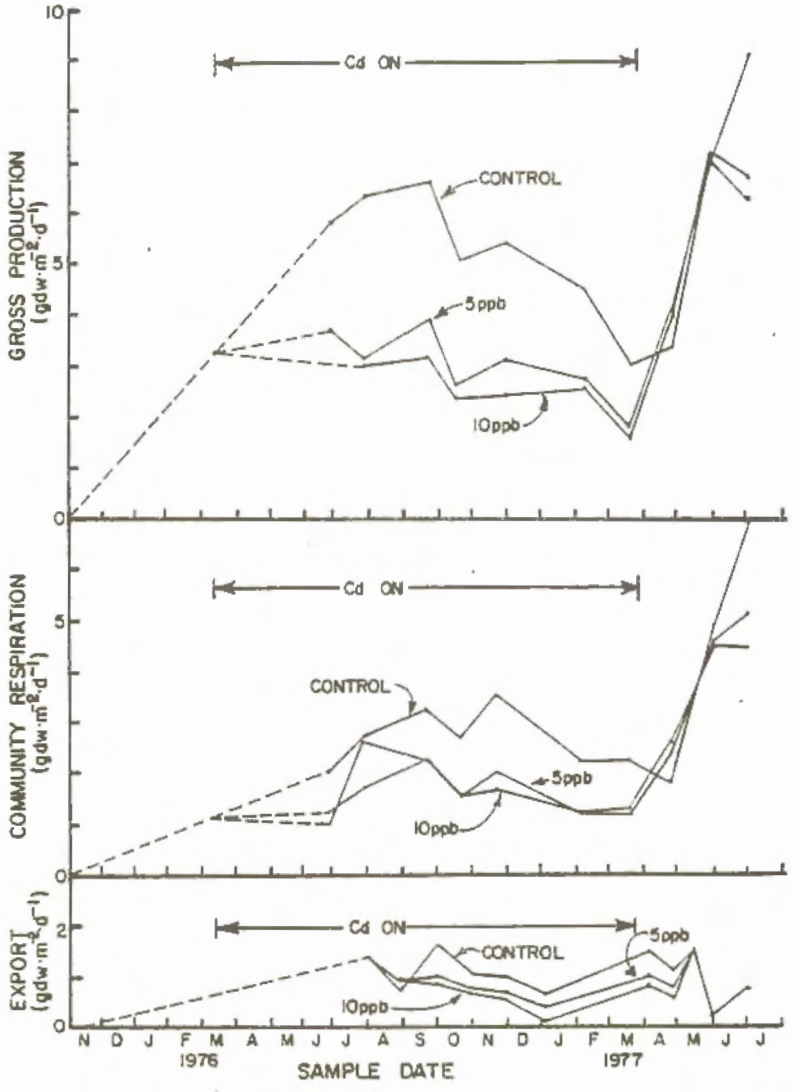

Figure 6.4. Summary of system-level data during the Cd-stream study for control, 5 ppb Cd, and 10 ppb Cd treatments. (a) gross production; (b) community respiration; and (c) community export. Dashed lines indicate extrapolated data.

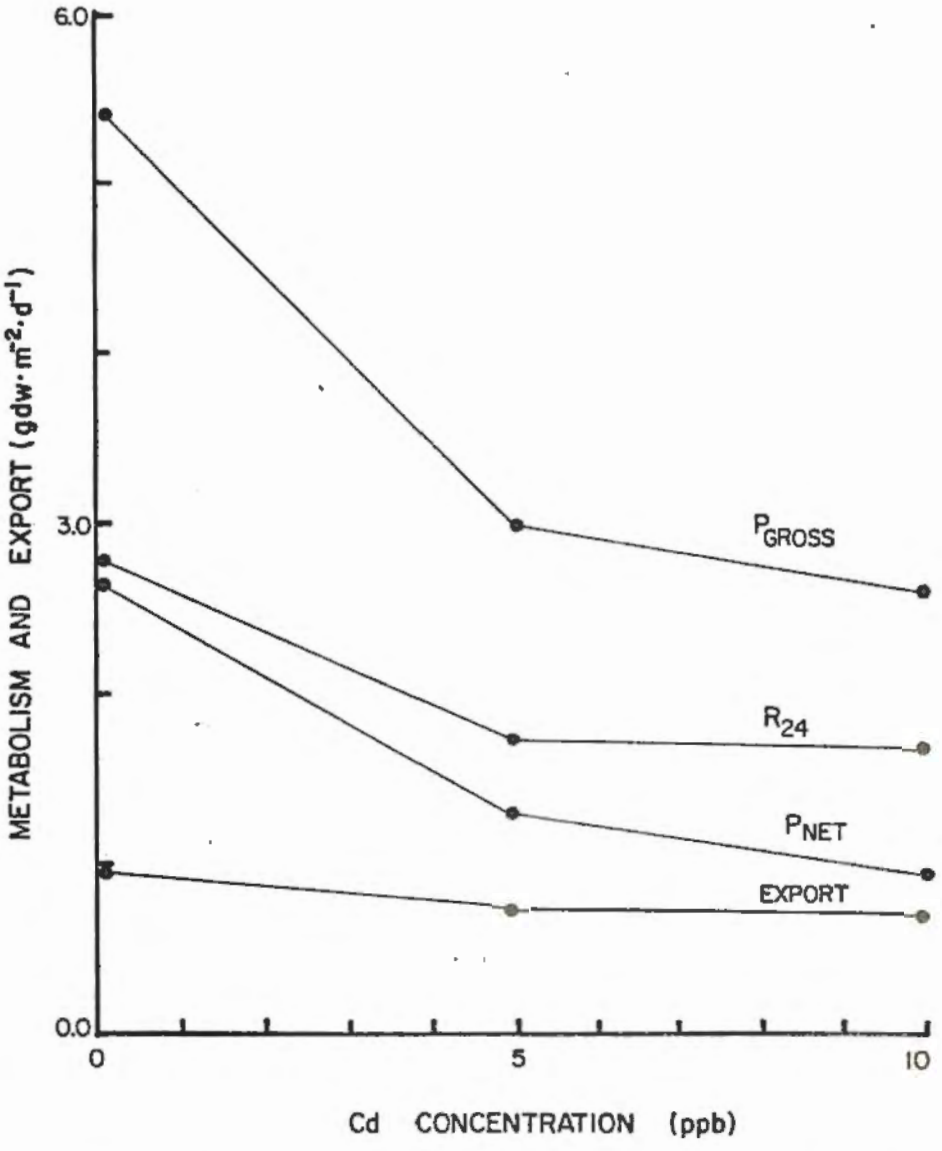

Figure 6.5. Summary graph of system-level parameters measured in artificial streams receiving continuous Cd inputs. Point represent 1-yr averages for two replicate streams at each treatment.

Mosquito fish residing in the stream channels demonstrated the slowest Cd uptake observed, with saturation apparently not reached after 6 mo of uptake. Cadmium concentrations at that time were approximately 2, 24, and 40 μg Cd·g dry weight^{-1} for control, 5, and 10 ppb Cd treatments.

No Cd was found to be associated with the sand sediments in the streams or with the plastic-liner material. Therefore, all Cd losses from the stream water must have been due to biological uptake. Measurements of Cd concentration in unfiltered water samples indicated an average lowering of effective concentration by 0.2 ppb in the 5-ppb treatment and 0.35 ppb in the 10-ppb channels.

STREAM MODEL SIMULATIONS

General Model

An aggregated model of a stream ecosystem was developed for experimentation with toxin and consumer manipulations. Figure 6.6 illustrates the overall model with the inflow and outflow of water carrying nutrients (where N represents nitrogen) and the toxin, Cd, which interact with a complicated biological system. The biological system tested is typical of streams in low-slope areas with moderate to slow current velocities. Primary producers include macrophytes (rooted plants, Q_3) and their associated periphytic algae (Q_2). In this model, consumers are lumped into one unit (Q_4). All unassimalated and dead material is cycled through the detrital-microbial storage (Q_5), which in many stream systems is intimately associated with the periphytic algae. Nitrogen replenishment within the community is entirely from microbial decomposition of detritus.

Figure 6.7 is a diagram of the details of the algal community. Remaining sunlight (J_R) interacts with nitrogen (N) and algal biomass to contribute to gross photosynthesis. A direct enhancement of primary production by Cd was also included as a limiting-factor relationship because of the literature data indicating such an effect (Arndt-Schulz Law). Cadmium is also absorbed from solution in a cycling-receptor module with biomass as the limiting substrate. Cadmium is lost from the algae by depuration and particulate loss to export, consumers, and detritus.

Cadmium toxicity to the algal component is modeled as a direct interactive drain by water Cd concentration on algal biomass. Sunlight acts on algal biomass through photorespiration, which may have been important in the shallow Cd streams.

Macrophyte interactions are summarized in Fig. 6.8. All flows are analogous to the algal flows described for Fig. 6.7 except that no photorespiration mechanism was included in the respiration pathway.

Figure 6.9 illustrates the aggregated consumer community in this model stream ecosystem. Consumer biomass (Q_4) feeds on algae, macrophytes, and detritus-microbes, with some of the material assimilated and some lost directly to detritus. Cadmium is absorbed and lost from this storage by the same mechanisms modeled in the producer units, and Cd toxicity acts directly as a drain on consumer biomass.

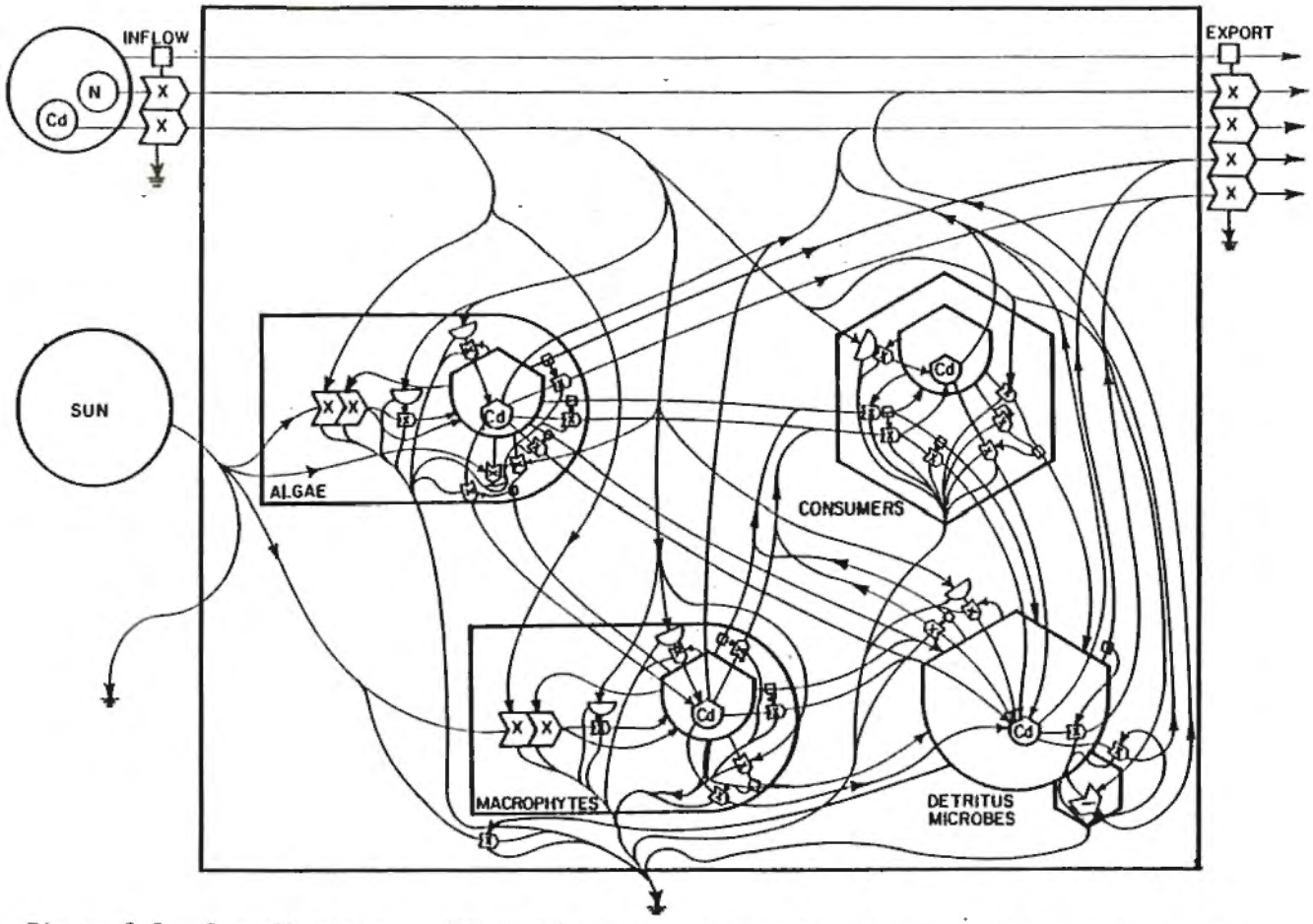

Figure 6.6. Overall system model of Cd streams. Sunlight interacts with dissolved chemicals to maintain complicated biological systems and Cd cycling. Each unit has stimulative and toxic action of Cd (see details in Figs. 6.7–6.10). Computer program and rate constants are listed in Tables B.5–B.7.

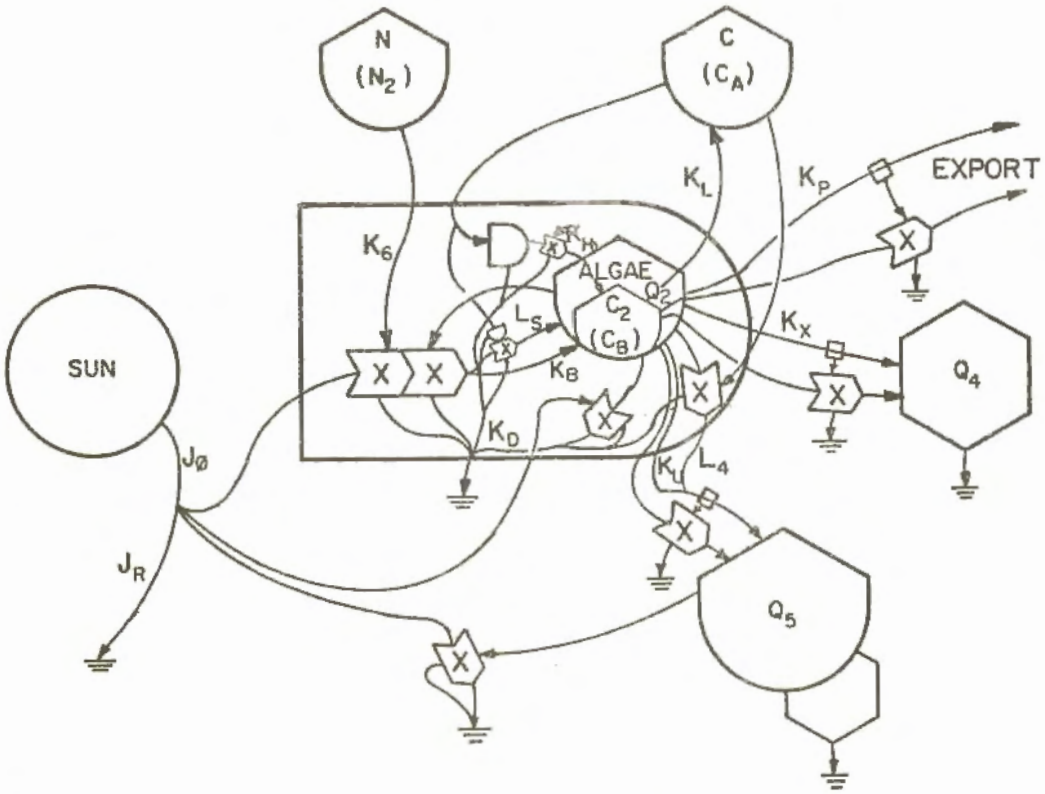

$$\dot{Q}_2 = (K_8 N_2 J_R Q_2)(1+\frac{L_S C_A}{L_U+C_A}) - K_D Q_2 J_R - K_X Q_2 Q_4 - K_P Q_2 - K_u Q_2 - L_4 Q_2 C_Z$$

$$\dot{C}_2 = K_H Q_2 (\frac{C_A}{K_1+C_A}) - K_L C_2 - C_B (K_X Q_2 Q_4) - C_B (K_U Q_2 J_R + L_4 Q_2 C_A) - C_B (K_P Q_2)$$

Figure 6.7. Detail of Cd-stream model showing interactions of the algal component of the periphyton. Points of interest include stimulatory effect of Cd on primary production (L_S) and photorespiration. Computer program and rate constants are listed in Tables B.5–B.7.

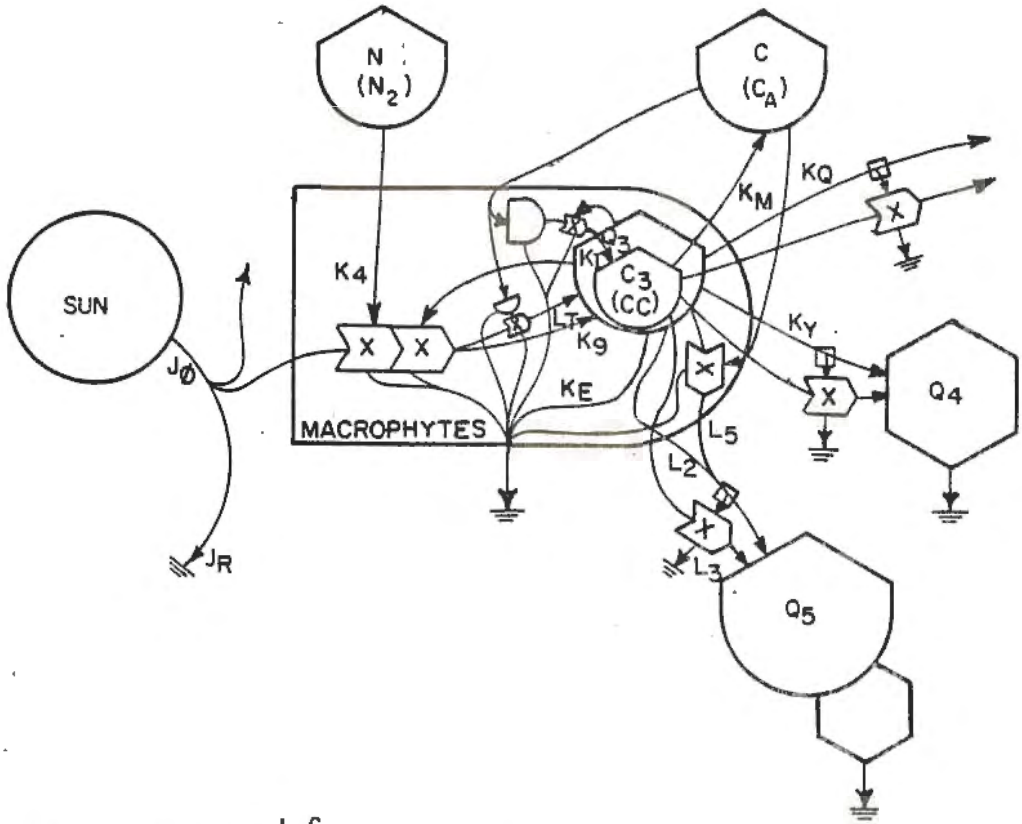

$$\dot{Q}_3 = (K_9 N_2 J_R Q_3)(1 + \frac{L_T C_A}{L_U + C_Z}) - K_Q Q_3 - K_Y Q_3 Q_4 - L_2 Q_3 - L_5 Q_3 C_A - K_E Q_3$$

$$\dot{C}_3 = K_I Q_3 (\frac{C_A}{K_1 + C_A}) - C_C K_Y Q_3 Q_4 - C_C (L_2 Q_3 + L_5 Q_3 C_A) - K_M C_3 - C_C K_Q Q_3$$

Figure 6.8. Detail of the Cd-stream model showing interaction of macrophytic plant community. As with the algae, a stimulatory effect of Cd is included (L_t). Computer program and rate constants are listed in Tables B.5–B.7.

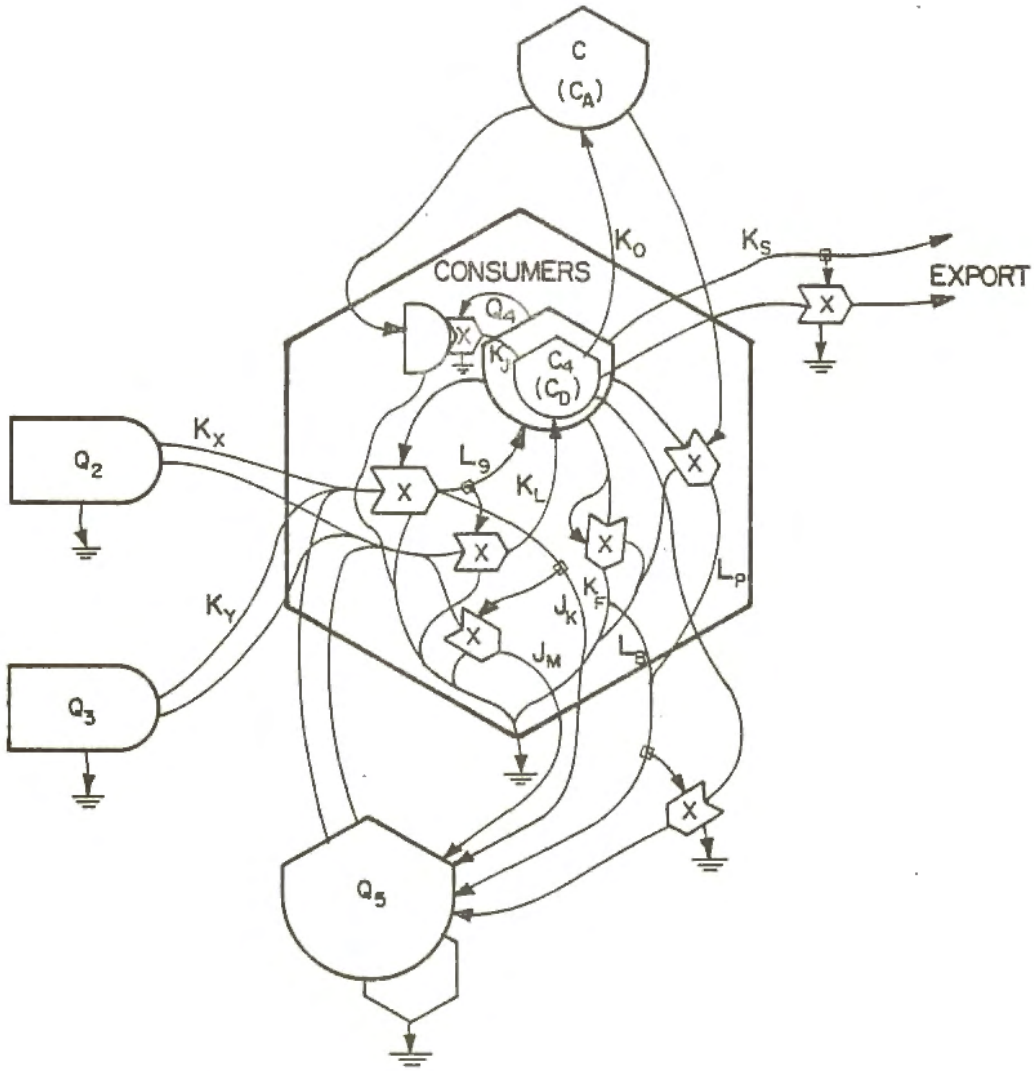

$$\dot{Q}_4 = L_9Q_4(K_XQ_2+K_YQ_3+L_6Q_5)-K_SQ_4-L_BQ_4^2-L_PQ_4C_A-K_FQ_4^2$$

$$\dot{C}_4 = L_9Q_4(K_XC_2+K_YC_3+L_6C_5)+K_JQ_4\left(\frac{C_A}{K_1+C_A}\right)-K_OC_4-C_D(L_BQ_4^2+L_PQ_4C_A)-C_D(K_SQ_4)$$

Figure 6.9. Detail of the Cd-stream model showing the aggregated consumer interactions. Cadmium is taken up through both surface adsorption and feeding. Computer program and rate constants are listed in Tables B.5–B.7.

The last section of this stream model is diagramed in Fig. 6.10. The storage of detritus and associated microbes (bacteria and fungi) is indicated as Q_5, receiving inputs from all of the biological components in the model. Cadmium is taken up and lost as in the other components, but exerts its toxic action as a reduction of nutrient regeneration and metabolism of the microbes. As shown in Fig. 6.7, the storage Q_5 intercepts a portion of the incoming sunlight and therefore, reduces remaining sunlight (J_R) available for photosynthesis.

The model shown in Fig. 6.6 represents a simplification of the actual streams and yet is a very complex nonlinear model. Since the purpose of the model simulations was to provide approximate data for the effects of Cd concentrations not actually studied in the artificial streams to be used in example correlations of embodied energy and toxicity effect; exact fitting of model output to actual data was not attempted. Instead, the model was simplified whenever possible, while retaining both fate and effects of the toxin. Simulations were made using a desk-top microcomputer and BASIC computer language because of the immediate feedback between model and modeler. Slowness of these simulations run at small time-step intervals was a disadvantage and limited the goodness of fit between model results and actual measured data.

A complete list of the model storages, pathways, and parameters is given in Tables B.6 and B.7. A copy of the BASIC computer program used for the simulations reported in this section is given in Table B.5.

Parameterization

Although the model illustrated in Fig. 6.6 is a simplification of the actual stream microcosms, it contains 39 constants that had to be estimated from data collected during the Cd study or from published reports. Many of these constants were not known exactly and in fact many may not have been constant during the 2-yr successional period. A discussion of the basis for the choice of the model parameters is presented below.

Units—

Flows in the model were in the following units: pure energy, Cal (kilogram calories); biomass, grams of dry weight (g dw); nitrogen, mg N; and Cd, µg Cd. Rates are all on a per square meter per day basis ($m^{-2} \cdot d^{-1}$).

Solar Input—

As seen in Fig. 6.6, solar energy is one of the two primary driving forces included in the stream's model. For simplicity on the microcomputer, solar input (JØ) was simulated by a sine function with maximum and minimum values of 6000 and 2720 $Cal \cdot m^{-2} \cdot d^{-1}$, respectively. Actual solar energy at the channels was taken as 70% of these maximum values from averge cloud cover data published for Columbia, South Carolina (NOAA 1976, 1977).

In the channels, remaining solar input (JR) was calculated for use in productivity formulations. JR was equal to JØ minus solar energy absorbed by algae (FA), by macrophytes (FB), and by the detritus-microbes (FC). The constant of photosynthetic efficiency used for algae and macrophytes was 2.8% measured by the author at Silver Springs, Florida (Knight 1980). Using a conversion factor of 4 $Cal \cdot g^{-1}$ for dry weight at 2.8% efficiency, 143

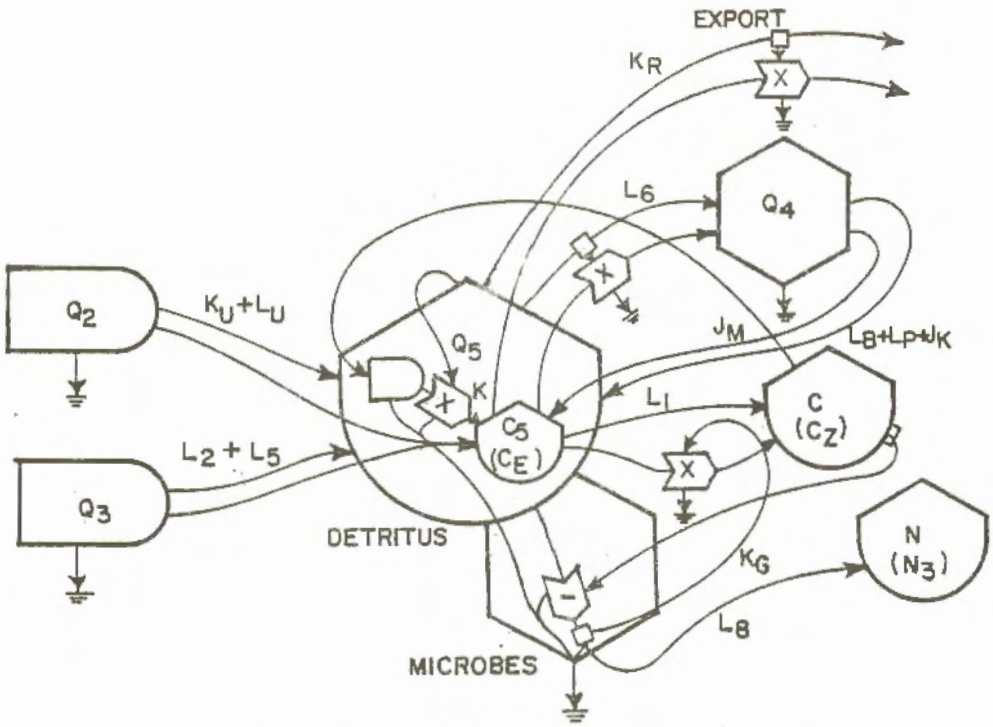

$$\dot{Q}_5 = L_2Q_3+K_UQ_2J_R+L_BQ_4^2+L_4Q_2C_A+L_5Q_3C_A+L_PQ_4C_A-K_GQ_5(1-L_EC_A)-K_RQ_5$$
$$\underbrace{+(K_X-L_9)Q_2Q_4+(K_Y-L_9)Q_3Q_4+(L_6-L_9)Q_5Q_4}_{J_K}-L_6Q_5Q_4$$

$$\dot{C}_5 = C_C(L_2Q_3+L_5Q_3C_A)+C_B(K_UQ_2J_R+L_4Q_2C_A)+K_KQ_5\left(\frac{C_A}{K_1+C_A}\right)+C_D(L_BQ_4^2+L_PQ_4C_A)$$
$$-L_1C_5-C_E(K_RQ_5)-C_E(L_6Q_5Q_4)-C_E(K_GQ_5[1-L_EC_Z])$$
$$\underbrace{+(K_X-L_9)C_BQ_2Q_4+(K_Y-L_9)C_CQ_3Q_4+(L_6-L_9)C_EQ_4Q_5}_{J_M}$$

Figure 6.10. Detail of Cd-stream model showing configuration of detrital-microbial segment of periphyton. Cadmium toxicity is expressed as a negative interaction with nutrient regeneration. Computer program and rate constants are listed in Tables B.5–B.7.

Cal absorbed per gram of dry weight produced was calculated. Thus the constants KA and KB were set equal to 143 $Cal \cdot g^{-1}$.

Water Inflow—

Incoming water flow (JW) was constant and equal to 136,000 $L \cdot d^{-1}$. This water contained N (N1 = 0.015 mg $N \cdot L^{-1}$) and Cd (C1 = variable with 0.023 µg $Cd \cdot L^{-1}$ as the background concentration).

Nitrogen Dynamics—

The total nitrogen concentration measured in the channel input water was 15.8 µg $N \cdot L^{-1}$ while the total phosphorus concentration was measured as 2.9 µg $\cdot L^{-1}$ giving a ratio by atoms of about 13:1. Since the optimal ratio is generally considered to be 16:1, nitrogen may be slightly more limiting and was chosen as the nutrient to monitor in the model. A few calculations show the importance of this nutrient in the streams and consequently in the model simulations. With a water input of 136,800 $L \cdot d^{-1}$ to each channel with 15.8 µg $N \cdot L^{-1}$ and 56 m^2 surface area, we calculate a nitrogen flow of 38.6 mg $N \cdot m^{-2} \cdot d^{-1}$. Actual net productivities measured in the channels during the second year of study were about 2.5 g $dw \cdot m^{-2} \cdot d^{-1}$. This means, if all of the N was taken up in biomass during each 24-hr period, the N content on a dry weight basis could have only been about 1.5%, which is low for algae and plants (Odum 1973). Luxury uptake of N in the dark is known (Ketchum 1954) but algae cannot take up N from extremely dilute water. Therefore, the constants for N uptake, K4 for algae and K6 for macrophytes, were assumed to be 0.5% or 5 mg $N \cdot g\ dw^{-1}$. The importance of nutrient cycling in these channels for maximizing productivity is immediately obvious from the above discussion.

Recycling of N was simplified in the model by the assumption that all N remineralization was from the detrital-microbial storage (Q5):

$$J8 = L8 \cdot FG \tag{6.1}$$

where L8 = K4 above (0.5 mg $N \cdot g\ dw^{-1}$) and FG is the respiration of storage Q5, discussed below.

Overall N flow in the channel water was:

$$F1 = JN + J8 - F4 - F6 \tag{6.2}$$

where JN is the N in input water:

$$JN = N1 \cdot JW \tag{6.3}$$

and N1 is the N content of the inflow. Nitrogen concentration in the stream water is calculated as:

$$N2 = F1/JW. \tag{6.4}$$

Cadmium Dynamics—

The background Cd concentration (C1) was approximately 0.023 µg $Cd \cdot L^{-1}$. For the model simulations this concentration was varied between ambient and 100 µg $Cd \cdot L^{-1}$.

Cadmium inflow (JC) was calculated as:

$$JC = C1 \cdot JW. \tag{6.5}$$

Cadmium uptake by the biota was modeled as a hyperbolic Michaelis-Menton function:

$$FH = \frac{KH \cdot CA \cdot Q2}{K1 + CA} \text{ (algae)} \tag{6.6}$$

$$FI = \frac{KI \cdot CA \cdot Q3}{K1 + CA} \text{ (macrophytes)} \tag{6.7}$$

$$FJ = \frac{KJ \cdot CA \cdot Q4}{K1 + CA} \text{ (consumers)} \tag{6.8}$$

$$FK = \frac{KK \cdot CA \cdot Q5}{K1 + CA.} \text{ (detritus-microbes)} \tag{6.9}$$

This uptake function has been observed for Cd with most biota studied (see Section 4). The half-saturation constant (K1) was set equal to 200 µg $Cd \cdot L^{-1}$ as a rough average of the data shown in Figs. 4.17–4.20.

The Cd content (µg $Cd \cdot m^{-2}$) of each of the four biological storages was included in the model: C2, Cd in algae; C3, Cd in macrophytes; C4, Cd in consumers; and C5, Cd in detritus-microbes.

Loss of Cd from each of these storages was in two forms: 1. dissolved Cd modeled as a simple linear decay; and 2. particulate Cd transport to other storages. For the algae Cd decay was equal to:

$$FL = KL \cdot C2 \tag{6.10}$$

where KL was measured in the streams as 0.065 d^{-1}. For the macrophytes, Cd decay equaled:

$$FM = KM \cdot C3 \tag{6.11}$$

where KM was measured as 0.02 d^{-1} in the artificial streams. For the consumers, Cd decay was modeled as:

$$FO = KO \cdot C4 \tag{6.12}$$

where a value of 0.0055 d^{-1} was used for KO as measured for mosquito fish in the channels. For the detritus-microbes, Cd decay was equal to:

$$J1 = L1 \cdot C5 \tag{6.13}$$

with L1 = KL = 0.065 d^{-1}. Cd was also remineralized in microbial respiration:

$$FT = FG \cdot CE \tag{6.14}$$

where CE was the concentration of Cd in Q5 and was equal to C5/Q5.

Cd loss in particulate form was simply calculated as g $dw \cdot m^{-2} \cdot d^{-1}$ multiplied times the Cd concentration in the storage (µg $Cd \cdot g\ dw^{-1}$).

Overall Cd flow in the channel water was equal to:

$$F2 = JC + FL + FM + FO + FT + J1 - FK - FJ - FH - FI \quad (6.15)$$

and Cd concentration in this stream water was calculated as:

$$CA = \frac{F2}{JW} \quad (6.16)$$

Algae—

The living algal component (Q2) of the periphyton (see Fig. 6.7) was monitored separately because of its importance in the primary energy fixation in the channels. The modeled relationship for gross primary production was:

$$F8 = K8 \cdot N2 \cdot JR \cdot Q2. \quad (6.17)$$

Algal respiration was equal to:

$$FD = KD \cdot Q2 \cdot JR \quad (6.18)$$

where the JR term indicates the possibility of photorespiration in the shallow streams. In addition the algal storage is also drained by consumer feeding:

$$FX = KX \cdot Q2 \cdot Q4 \quad (6.19)$$

by death to detritus:

$$FU = KU \cdot Q2 \quad (6.20)$$

and by export:

$$FP = KP \cdot Q2. \quad (6.21)$$

The effect of Cd was modeled as both stimulatory at low concentrations:

$$J8 = \frac{LS \cdot F8 \cdot CA}{LU + CA} \quad (6.22)$$

and as a toxic drain on biomass:

$$J4 = L4 \cdot Q2 \cdot CA. \quad (6.23)$$

The constants in the above relationships (K8, KD, KX, KU, KP, LS, LU, and L4) were all adjusted by an initial approximation and then simulation runs to fit model output to observed algal biomass patterns.

Macrophytes—

The aquatic macrophyte population (Q3) is illustrated in Fig. 6.8. All flows are analagous to the algal flows except that respiration:

$$FE = KE \cdot Q3 \quad (6.24)$$

had no sunlight component. Table 8.6 lists the details of these flows. Once again the eight constants governing macrophyte dynamics were adjusted by simulations to fit observed biomass changes in the artificial streams.

Consumers—

Details of the consumer component (Q4) of the stream model are shown in Fig. 6.9. Consumers fed on algae:

$$FX = KX \cdot Q2 \cdot Q4 \tag{6.25}$$

on macrophytes:

$$FY = KY \cdot Q3 \cdot Q4 \tag{6.26}$$

and on detritus-microbes:

$$J6 = L6 \cdot Q5 \cdot Q4. \tag{6.27}$$

Assimilation efficiency was assumed to be 30%

$$J9 = L9 \cdot (FX + FY + J6) \tag{6.28}$$

where L9 = 0.3. The remainder of the ingested food was returned to the detritus-microbes:

$$JK = FX + FY + J6 - J9. \tag{6.29}$$

Losses from the consumers were respiration:

$$FF = KF \cdot Q4^2 \tag{6.30}$$

with a square term to indicate predation or crowding effects; death to detritus:

$$JB = LB \cdot Q4 \tag{6.31}$$

and export:

$$FS = KS \cdot Q4. \tag{6.32}$$

Cd toxicity was modeled as an interactive drain:

$$JP = LP \cdot Q4 \cdot CA. \tag{6.33}$$

Once again the constants listed above (KX, KY, L6, KF, LB, KS, and LP) were approximated and then adjusted to give realistic output.

Detritus-Microbes—

The detritus-microbe subsystem (Q5) is illustrated in Fig. 6.10. These two portions of the stream ecosystem comprise the greatest portion of the periphyton >98% by weight (with the remainder composed of living algae).

Detritus and microbes may be conveniently modeled together because of their intimate association.

Inputs to Q5 were mentioned in the preceding paragraphs. The two major drains on Q5 are export:

$$FR = KR \cdot Q5 \tag{6.34}$$

and respiration:

$$FG = KG \cdot Q5 \cdot (1 - LE \cdot CA). \tag{6.35}$$

As seen in equation 6.35, Cd toxicity to the detritus-microbes is a negative interaction with respiration and nutrient remineralization. This formulation is consistent with actual stream data for leaf litter packs (Giesy et al. 1979).

Parameter Approximation—

In order to approximate the unmeasured constants discussed above, a "steady state" period of the artificial streams succession was evaluated. Figure 6.11 illustrates the four biomass storages with inputs and outputs of dry weight for data from September 1976 when little net growth was observed. Biomass values, total net production and respiration, and export values were known. Gross productivity was partitioned between the algae and macrophytes as shown. The partition of respiration was also based on assumptions. Total export at this time was assumed to be twice the measured value or 3 g $dw \cdot m^{-2} \cdot d^{-1}$. This number divided by the total biomass of 210 g $dw \cdot m^{-2}$ gives the export constants of 0.014 d^{-1}. Consumer feeding on algae and macrophytes was assumed to be 0.2%, and 0.08% for detritus-microbes. With 30% assimilation efficiency, the return of ingested material to detritus was calculated as 0.168 g $dw \cdot m^{-2} \cdot d^{-1}$. Cd toxicity was taken as zero for these control stream data. By difference, death to detritus was calculated for each storage. These calculations resulted in a small net loss for Q5 of 0.011 g $dw \cdot m^{-2} \cdot d^{-1}$. The constants calculated by this procedure are also shown in Fig. 6.11. These approximate constants were used in initial simulations but many were varied to give better fit to the actual time-series data from the Cd streams. The final values used in the control model simulation are listed in Table B.7.

Control Simulation

As a baseline for calibration of the stream model, data from the control channels of the Cd streams project were used. This control model was simulated for November 1975 through August 1977. Initial conditions in the model were roughly those in the experimental streams: clean and uncolonized except for the plants and consumers that were added. Model parameters were adjusted as discussed above until simulation results were comparable to the measured data.

Biological Parameters—

Figure 6.12 illustrates a comparison between simulation results and detrital-microbial biomass. Simulated values were in the same range as the

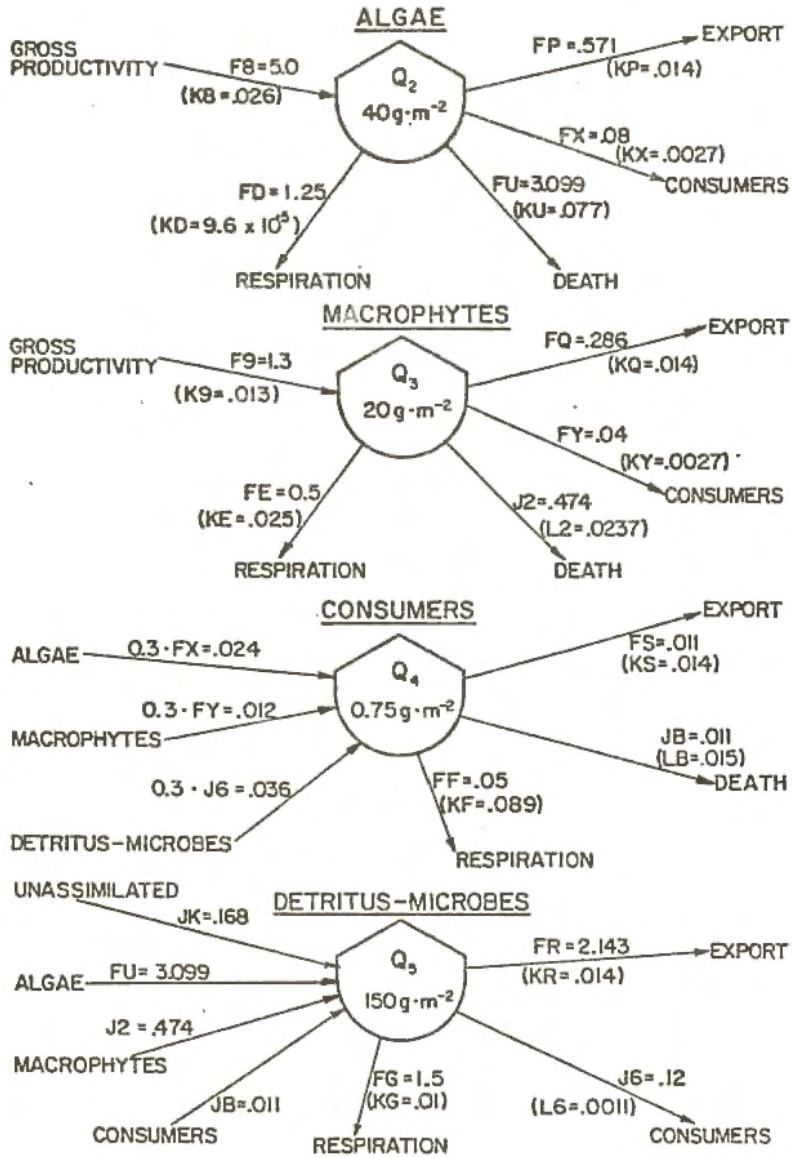

Figure 6.11. Input-output diagram for four biological storages in Cd stream model. Data from September 1976 were used to approximate steady state flows for parameter estimation. Storages are in g dw·m^{-2}; flows are in g dw·m^{-2}·d^{-1}; and constants in parentheses have variable units listed in Table B.7.

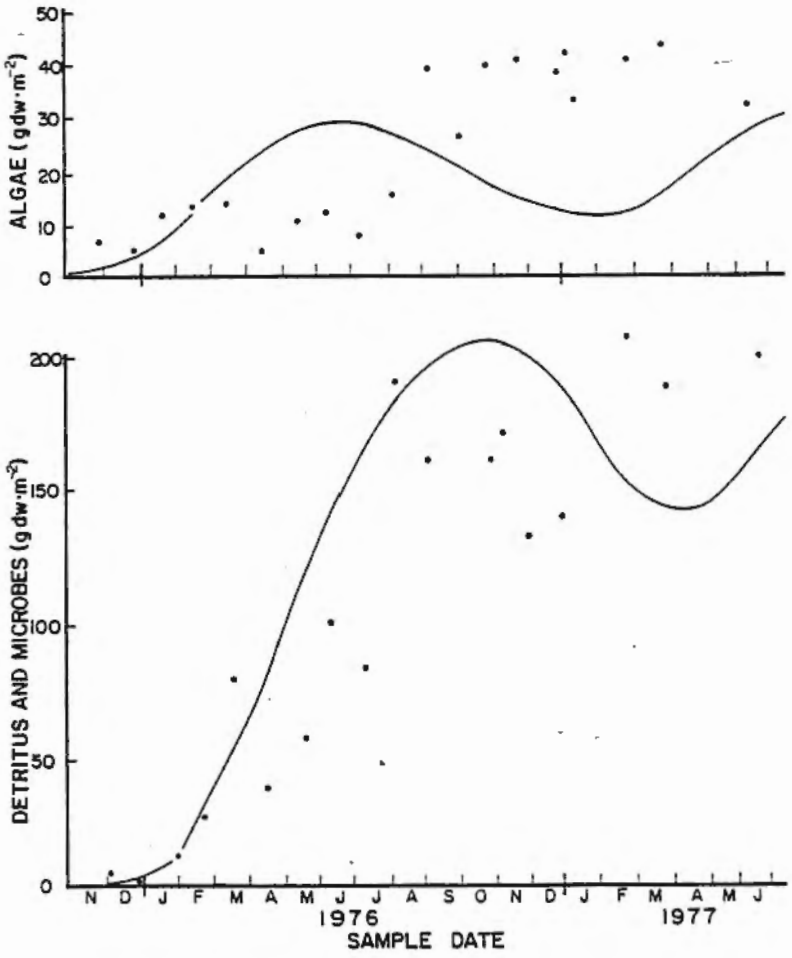

Figure 6.12. Stream model simulation results for algal and detrital-microbial biomasses at control Cd concentration of 0.023 µg $Cd \cdot L^{-1}$. Solid lines are simulation results and dots are measured data from Figs. 6.1 and 6.2.

measured ones, but the timing of peaks and troughs did not overlap. This effect is also seen in Fig. 6.13, which compares simulated output for gross production, system respiration, and export to the measured data. Figure 6.14 compares simulated and actual data for macrophyte and macroinvertebrate biomass. The model was poorest at predicting an increase observed for macrophytic biomass during the second summer.

For all of the above parameters the timing of the model was approximately 1–2 months early. This effect may have been due to the simple sinusoidal solar input used as opposed to the actual stochastic variation in solar input to the streams. A more complex forcing function with this same model could have perhaps provided a better fit between simulated and actual data; however, the model behaved realistically enough for experimentation with Cd toxicity effect.

Cadmium Dynamics—

A measured Cd input concentration of 0.023 ppb (control streams) resulted in concentrations in most biota of about 1 μg Cd·g dw^{-1}. Depuration constants for Cd from the various storages were presented earlier in this section. Uptake rates were also estimated from stream data, and maximum uptake rates were calculated from these values for a half-saturation constant of K1 = 200 ppb Cd. These values were altered slightly to improve the fit of model data to measured concentrations and are reported in Table B.6.

The control simulation run predicted all Cd concentrations to be between 0.2 and 1.0 μg Cd·g dw^{-1} during most of the year. These values were slightly lower than the observed concentrations indicated.

Cadmium Input

Cadmium input in the model was regulated by a series of IF...THEN statements. Cadmium concentration of the input water was set as C1. When time reached 136 days (March 18, 1976), C1 was set equal to ZZ, which was the elevated Cd content of the input water, and when time reached 503 days (March 18, 1977), C1 was set back to the control Cd concentration.

Biological Parameters—

Data from the 5 and 10 ppb Cd streams were used to calibrate the toxicity constants L4, L5, LP, and LE. The constants LS and LT allowed direct stimulatory effect of Cd on primary production as possibly indicated in Figs. 4.7–4.9.

Simulated and measured values for algal and detrital-microbial biomass are presented in Fig. 6.15. The model shows some reduction in algal and detrital biomasses at 5 and 10 ppb Cd but the fit to the actual data was disappointing. The model also gives a reduction in macroinvertebrate and macrophyte biomasses with Cd input (Fig. 6.16).

Figure 6.17 shows actual and simulated values of the system-level parameters at 5 and 10 ppb Cd. The fit between actual and simulated data for these parameters is better because they were of primary consideration in adjustment of toxicity constants.

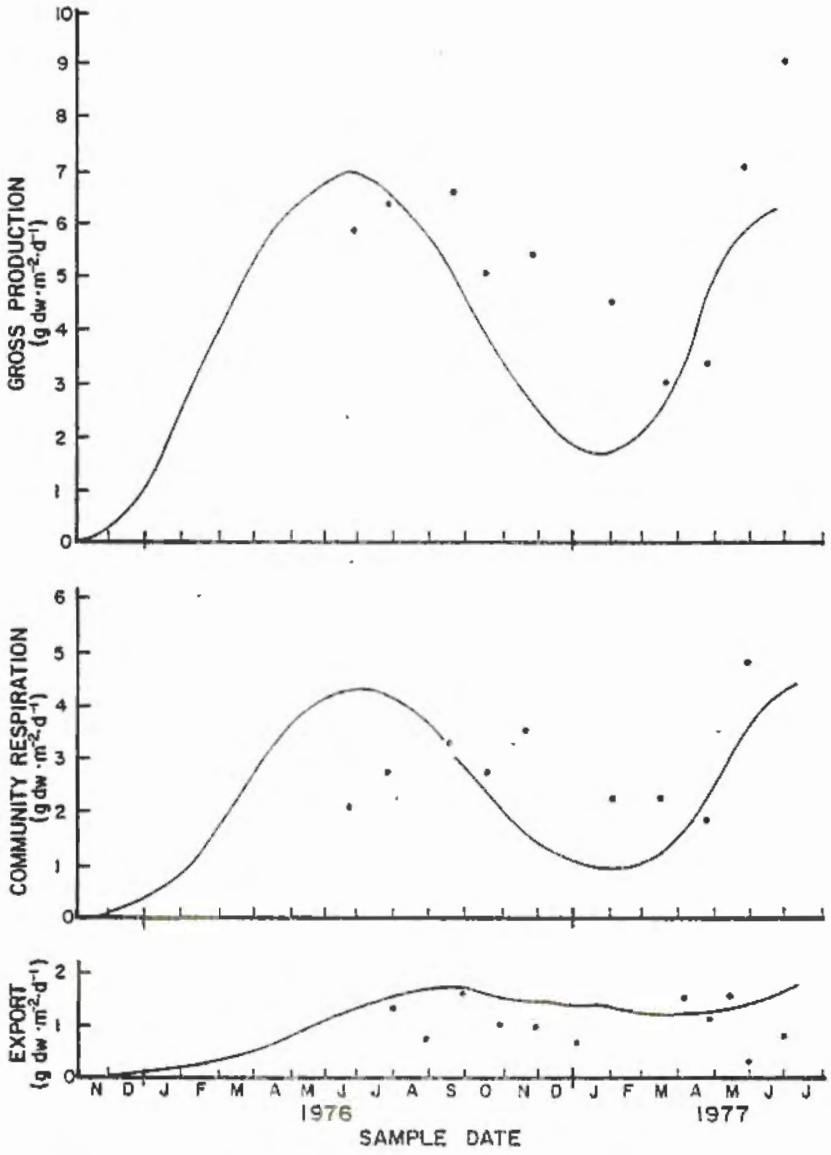

Figure 6.13. Stream model simulation results for gross production, community respiration, and export at control Cd concentration of 0.023 µg $Cd \cdot L^{-1}$. Solid lines are simulation results and dots are measured data from Fig. 6.4.

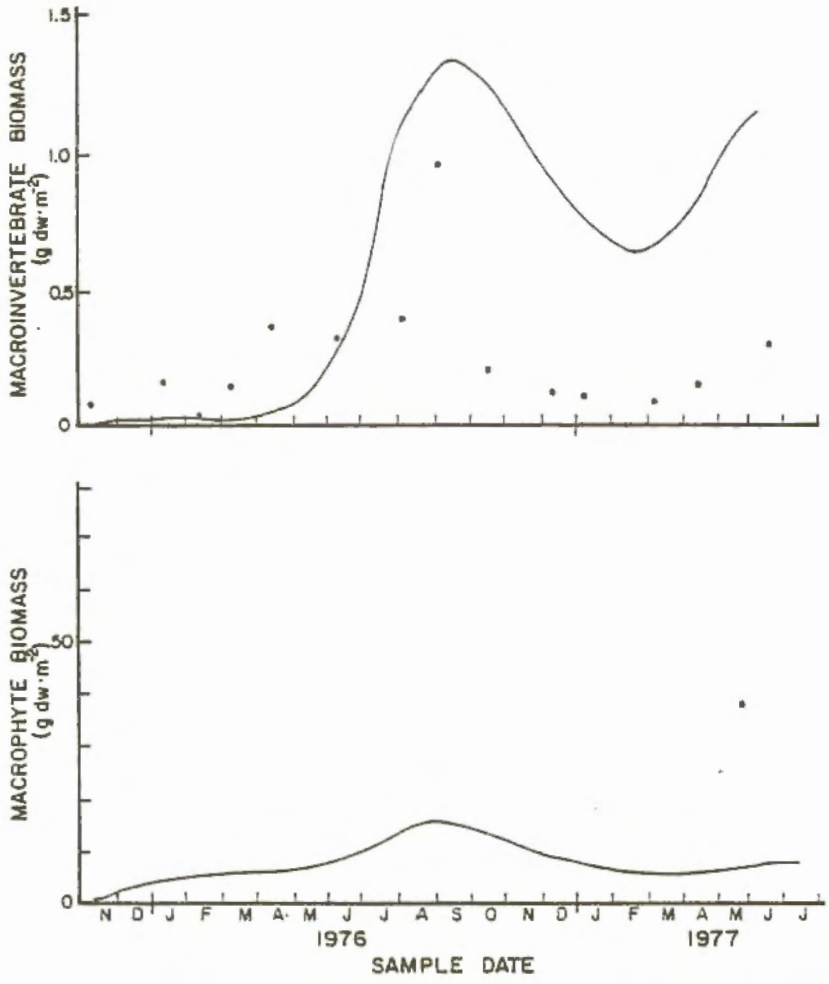

Figure 6.14. Stream model simulation results for macroinvertebrate and macrophyte biomasses at control Cd concentration of 0.023 µg $Cd \cdot L^{-1}$. Solid lines are simulation results and dots are measured data from Fig. 6.3 and the text.

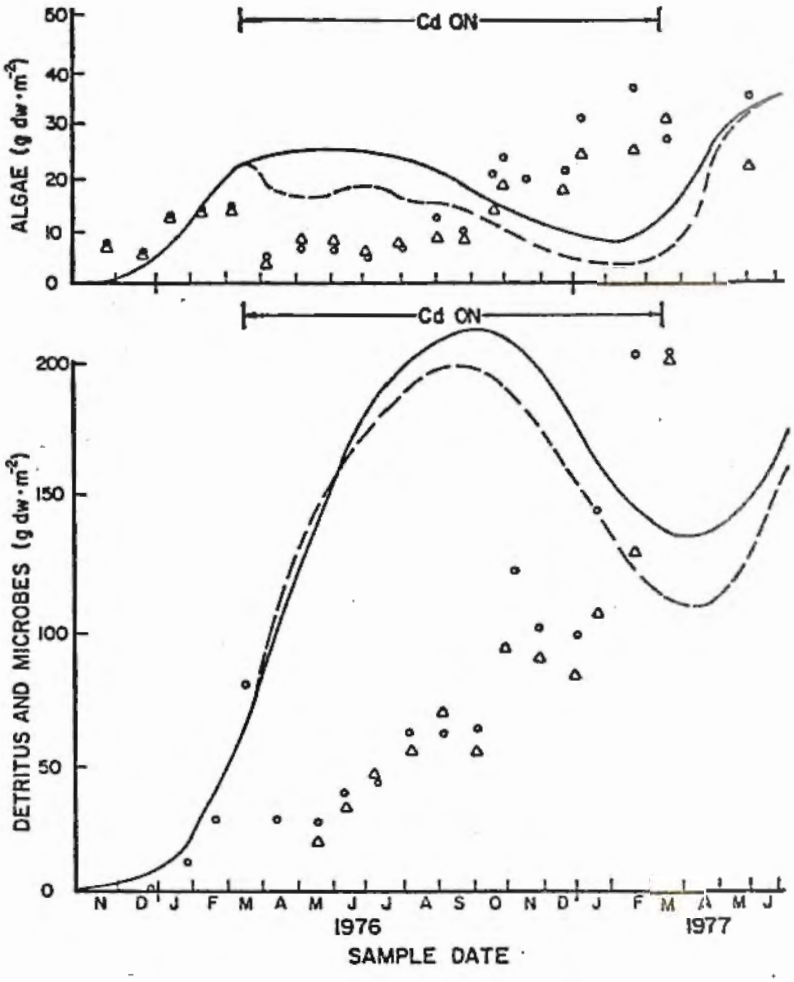

Figure 6.15. Stream model simulation results for algal and detrital-microbial biomasses at 5 and 10 ppb Cd input levels. Solid and dotted lines are simulation results for 5 and 10 ppb Cd, and circles and triangles are measured values for 5 and 10 ppb Cd from Fig. 6.1 and 6.2.

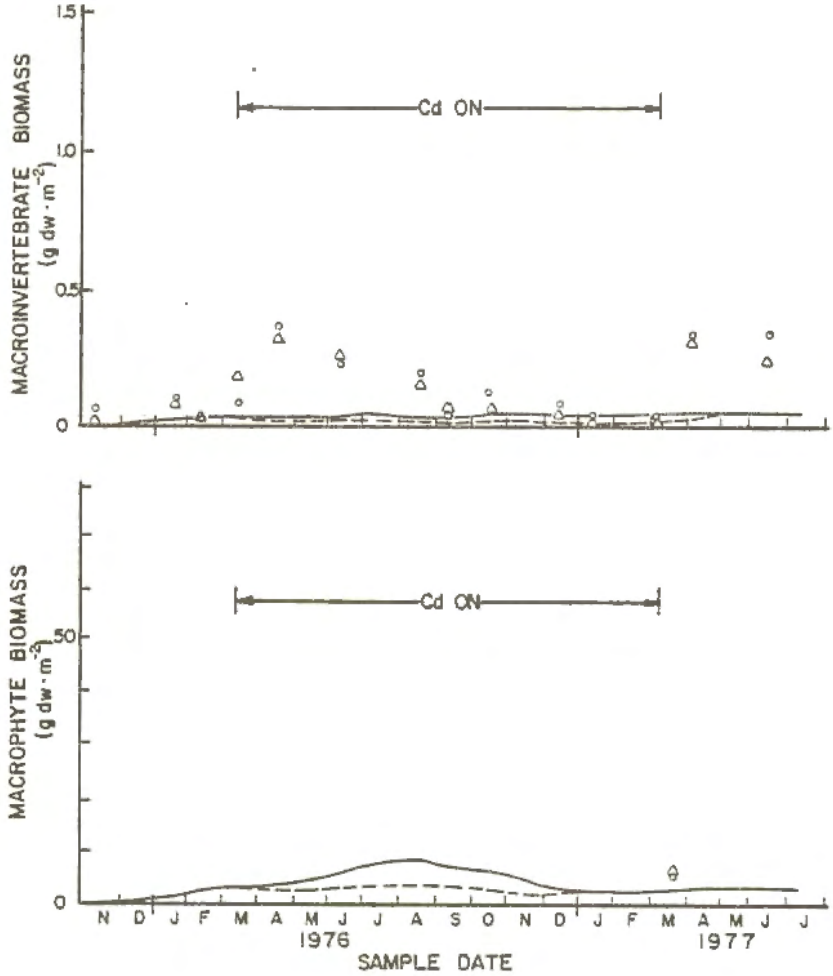

Figure 6.16. Stream model simulation results for macroinvertebrate and macrophyte biomasses at 5 and 10 ppb Cd input levels. Solid and dotted lines are simulation results for 5 and 10 ppb Cd, and circles and triangles are measured values for 5 and 10 ppb Cd from Fig. 6.3 and the text.

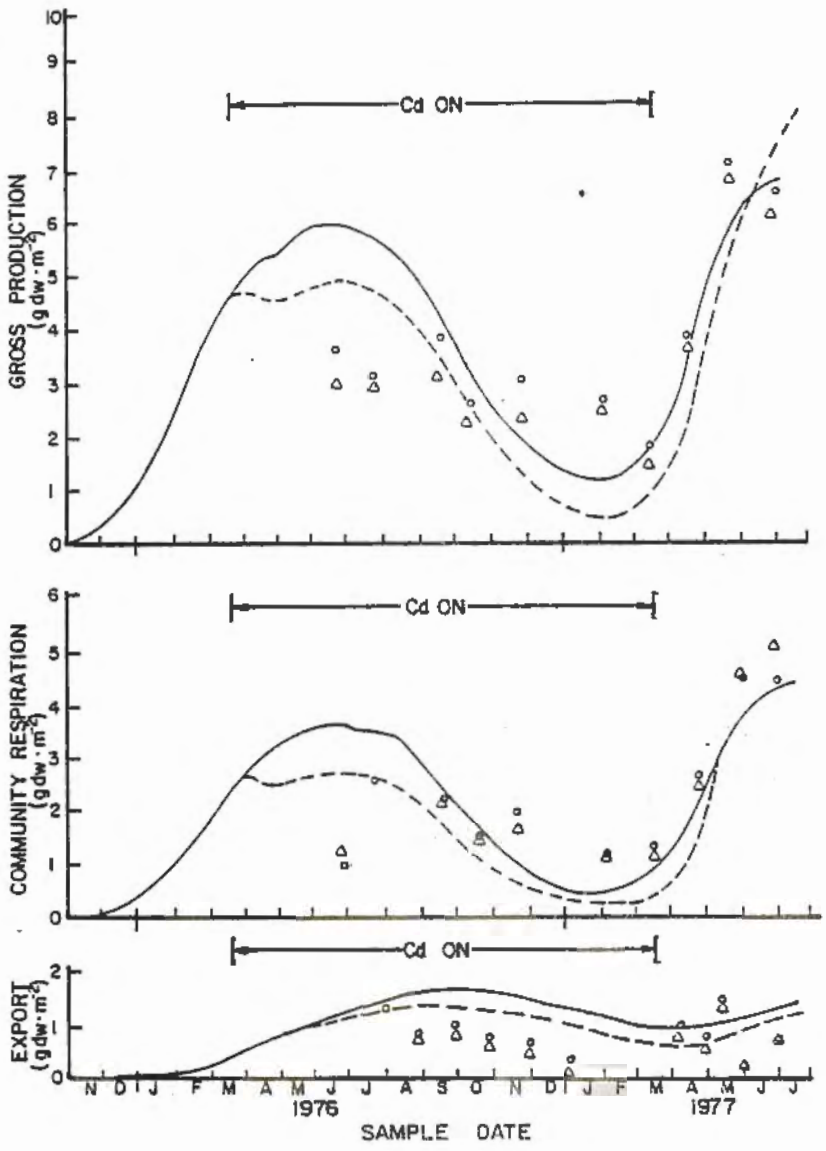

Figure 6.17. Stream model simulation results for gross production, community respiration, and export at 5 and 10 ppb Cd input levels. Solid and dotted lines are simulation results for 5 and 10 ppb Cd, and circles and triangles are measured values for 5 and 10 ppb Cd from Fig. 6.4.

Cadmium Dynamics—

The dynamics of Cd concentration in the various biological storages was monitored in the model simulated for comparison to the actual measured data. Steady state concentrations of Cd in the biota at a water concentration of 5 ppb Cd were: algae, 35; macrophytes, 50; consumers, 33; and detritus-microbes, 30 μg Cd·g dw^{-1}. For the 10 ppb Cd water input concentration, biotic Cd concentrations were: algae, 60; macrophytes, 90; consumers, 40; and detritus-microbes, 58 μg Cd·g dw^{-1}. These compare favorably with the values presented earlier in this section.

The stream model provides a convenient means of summarization of the fate of Cd in the aquatic ecosystem because all flows of the metal are accounted for. Figure 6.18 illustrates the major Cd flows and storages predicted by the model at the three Cd concentrations actually tested during steady state conditions (averaged over a 1-yr period). All flows are in μg $Cd \cdot m^{-2} \cdot d^{-1}$ and storages are in μg $Cd \cdot m^{-2}$. The model predicted an average lowering of water Cd concentration of 0.1 ppb in the 5 ppb Cd channels, and 0.2 ppb in the 10 ppb Cd channels. These values were slightly smaller than the measured values of 0.2 and 0.3 ppb Cd. Data in Fig. 6.18 indicate that only 0.4% of the Cd output from the channels was in particulate form. Also, the model indicated that Cd uptake and depuration by biota was about 3% of the dissolved Cd flow through.

Model Experimentation

The calibrated streams model presented above allows experimentation with exogenous and internal controls other than those actually tested in South Carolina. Of particular interest to this report are the effects of other Cd toxicity functions on stream system dynamics, and prediction of toxin effect over a range of Cd concentrations outside the ones actually studied.

Toxicity Functions—

Particular attention was directed toward the occurrence of stimulatory effects at low Cd concentrations. The stream model as presented in Fig. 6.6 indicates a direct stimulatory (limiting factor) role in primary production. A question to be answered is whether the model will predict the Arndt-Schultz effect independently of the built-in stimulation.

The model was simulated for a series of Cd concentrations ranging from background to 5 ppb Cd with the stimulatory constants LS and LT equal to zero. No stimulation of productivity was found. This may be due to the simplicity of the model in terms of population growth characteristics or simply a prediction that no stimulation would have been observed in these systems. However, for the example correlation of embodied energy and energy effect in the next section, the stimulatory effect was added to the model with LS and LT equal to 0.025.

Cd Toxicity—

The predicted response of system-level parameters to a wide range of Cd concentrations is presented in Fig. 6.19. The data from the three concentrations actually studied are shown for comparison. As presented in Figs. 6.6–6.10, the stream model predicts maximum enhancement of stream metabolism

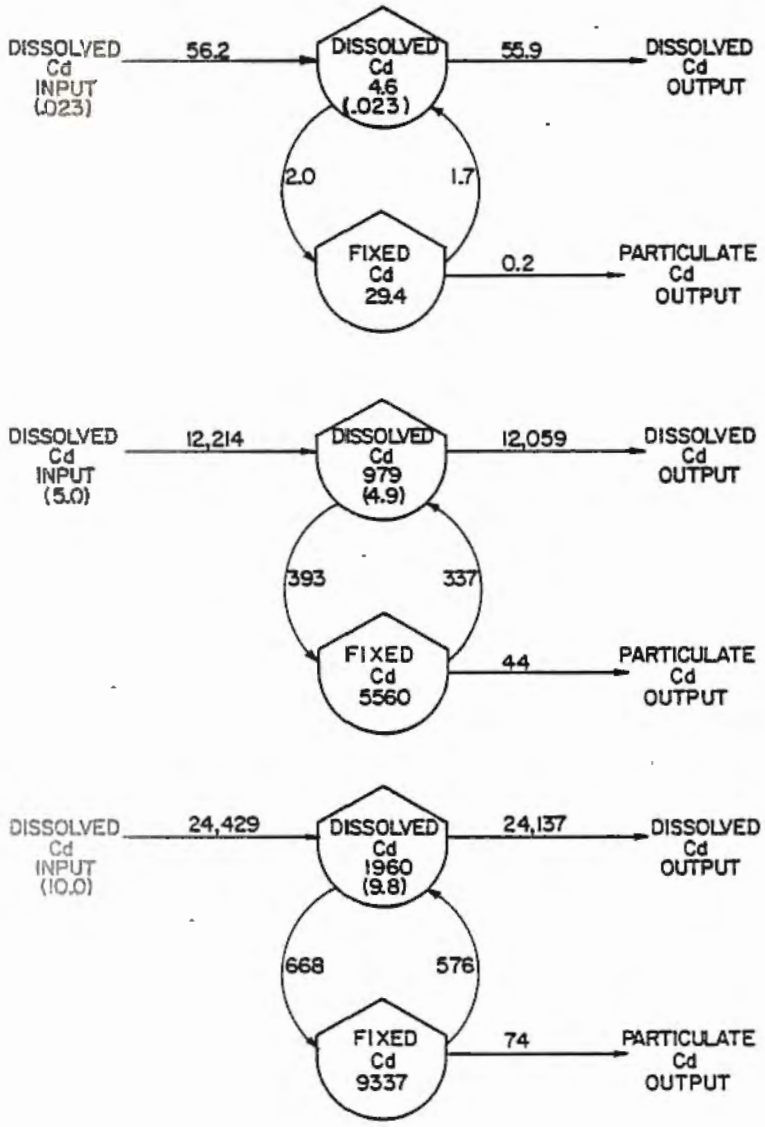

Figure 6.18. Overview of Cd fate in artificial streams from model output. Values are averages over a 1-yr period. Storages are in μg $Cd \cdot m^{-2}$, flows are in μg $Cd \cdot m^{-2} d^{-1}$, and concentrations (in parentheses) are in μg $Cd \cdot L^{-1}$.

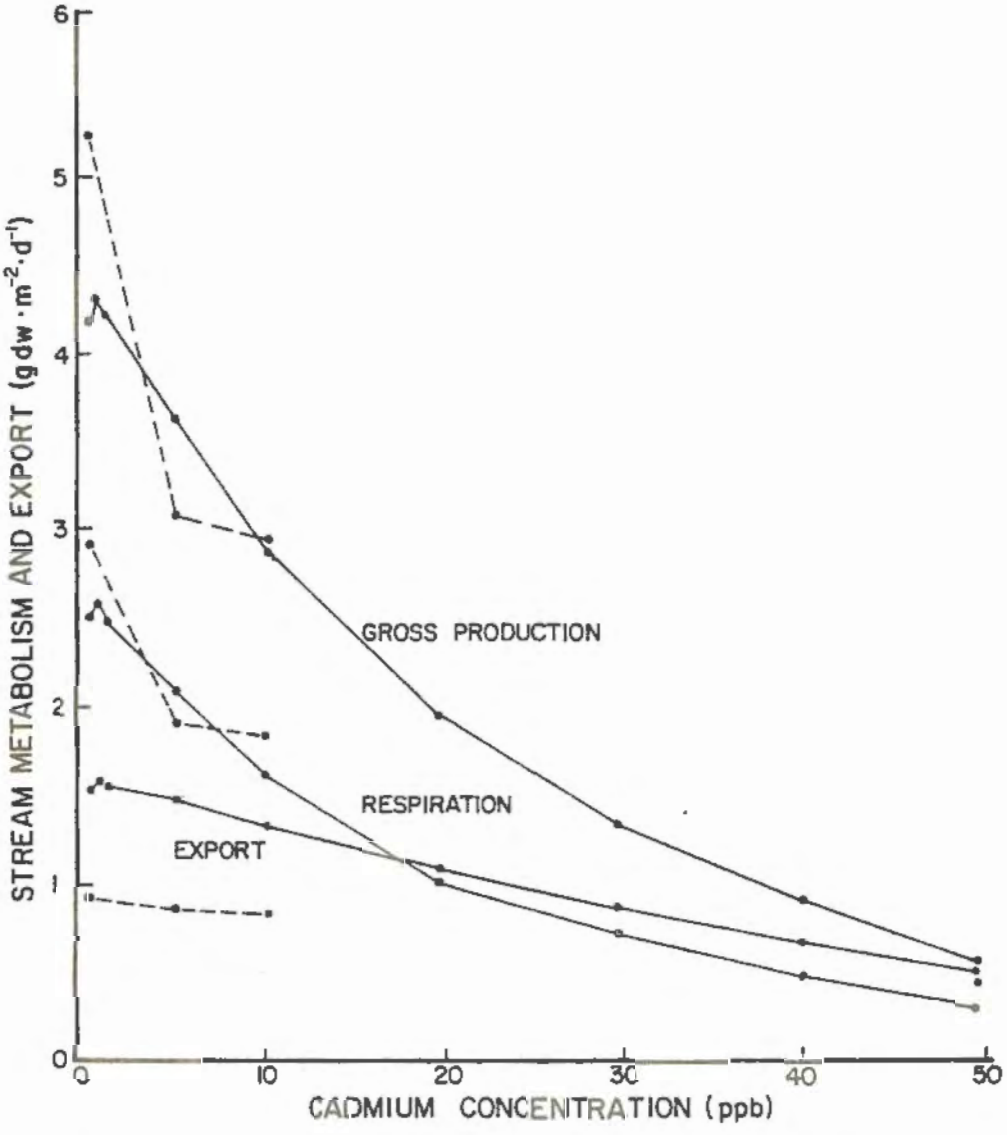

Figure 6.19. Average gross productivity, respiration, and export values during 1 yr of continuous Cd input predicted by stream model for Cd concentrations up to 50 ppb. measured data from Cd streams are indicated by dashed lines for comparison.

at a Cd concentration of 0.5 ppb. These predicted data may now be used for illustration in the calculation of energy effect of Cd in the next section.

EMBODIED ENERGY AND CONTROL

Quality Factors

The calibrated Cd-streams model facilitates calculation of quality factors for analysis of the amplifier effect by toxins on system energy flow.

The entire energy income of the Cd streams must be known in order to calculate ratios of energy transformation (quality factors). If we consider the situation in natural streams, we can appreciate the effect of energy concentration in the maintenance of a stream. Not only is energy received directly from the sun, but energy is also concentrated from indirect sources such as runoff from the watershed, which creates the stream flow and structure. In the Cd streams this flow and structure were added to the incoming sunlight from human energies and fossil fuel work. These additional energies can only be estimated, and although errors in their calculation may affect the magnitude of the numbers reported, the qualitative results remain the same.

The average yearly solar energy used in the model was 3052 S.E. $Cal \cdot m^{-2} \cdot d^{-1}$. The total structure of the streams including plastic, sand, concrete blocks, and labor cost approximately 6×10^{-4} $\$ \cdot m^{-2} \cdot d^{-1}$. This expenditure probably represents the minimum possible energy cost of this structure. Using the 1972 energy-to-dollar ratio of 43.2×10^{6} S.E. $Cal \cdot \$^{-1}$ from Odum et al. (1980), this expenditure is equivalent to 2.79×10^{4} S.E. $Cal \cdot m^{-2} \cdot d^{-1}$ for the channel area. The other major energy input is the water flow in the streams. This flow may be approximately evaluated by the free energy change for the essential nutrient, nitrogen. Using the concentration change measured in the control channels (10.4 ppb–3.6 ppb N) and the equation for Gibb's free energy:

$$\Delta G = nRT \ln \frac{C_2}{C_1} \qquad (6.36)$$

where ΔG is the change in Gibb's free energy; n is the number of moles of reactants; R is the universal gas constant = 1.99×10^{-3} $Cal \cdot {}^{\circ}K^{-1} \cdot mol^{-1}$; T is the absolute temperature in °K and C_1 and C_2 are the concentrations of nitrogen before and after the free-energy change; a decrease in free energy along the reach of the streams of 0.045 $Cal \cdot g\,N^{-1}$ was calculated, which is equivalent to 1.15×10^{-3} $Cal \cdot m^{-2} \cdot d^{-1}$. Using the quality factor for chemical potential of dissolved solids in stream flow of 1.17×10^{6} S.E. $Cal \cdot Cal^{-1}$ given by Wang et al. (1980), an energy contribution from stream flow of 1346 S.E. $Cal \cdot m^{-2} \cdot d^{-1}$ was calculated.

The total energy contribution to the streams is the sum of the three factors listed above in equivalent energy quality units and is equal to 32,298 S.E. Cal·m^{-2}·d^{-1}. Energy transformation ratios have been calculated using yearly averages from the stream model and the total energy input given above. A conversion factor of 4 Cal·g dry $weight^{-1}$ was used to convert the biomass units to energy units. These values are listed in Table 6.1.

Energy Quality–Energy Effect Correlation

The Cd-streams model was simulated at a series of Cd concentrations from background (0.023 ppb) to 100 ppb Cd. Yearly averages of gross productivity, respiration, export, algae, macrophytes, consumers, and detritus-microbes were calculated for analysis of the effect of Cd on components of varying energy quality. The effect of Cd on a given energy flow or storage, relative to the control case, was converted from actual energy to embodied energy using the values in Table 6.1. This effect could be either positive or negative at different Cd concentrations.

Cadmium transformation ratio was calculated for the different concentrations simulated in the stream model. As a baseline, the transformation ratio of pure Cd calculated for the industrial process in Section 4 (4.6×10^7 S.E. Cal·g Cd^{-1}) was used. Using the solubility of $CdCl_2$ in water (1400 g $CdCl_2 \cdot L^{-1}$) from Hammons et al. (1978), a water concentration of 8.6×10^8 ppb Cd (saturated) was assumed to have a transformation ratio equal to pure Cd. The lowest concentration of Cd normally found in water is approximately 0.02 ppb, and the free energy change between these two Cd concentrations was calculated using equation 6.36 as 0.13 Cal·g Cd^{-1}. Dividing this value into 4.6×10^7 S.E. Cal·g Cd^{-1} gives the transformation ratio of pure Cd on a Cal per Cal basis of 3.5×10^8 S.E. Cal·Cal^{-1}.

In order to calculate the transformation ratio of Cd at any other water Cd concentration, the free energy change between the saturated solution and the given concentration must be calculated. For example, at 10 ppb Cd, the free energy change is $\Delta G = -0.097$ Cal·g Cd^{-1}. This value is multiplied by 3.5×10^8 S.E. Cal·Cal^{-1} to give the change in transformation ratio going from the saturated Cd solution to a less concentrated one. For 10 ppb Cd this change equals -3.4×10^7 S.E. Cal·g Cd^{-1}. This value is subtracted from 4.6×10^7 S.E. Cal·g Cd^{-1} to give the transformation ratio of Cd at 10 ppb, or

$$TR_{Cd,\ 10\ ppb} = 1.2 \times 10^7 \text{ S.E. Cal·g } Cd^{-1}.$$

These calculations of embodied energy of Cd were combined with calculations of energy effect from data predicted by the stream model. Figure 6.20 presents the correlation diagrams for the system-level parameters and for the biological storages. All of the parameters except the macrophyte storage showed first a positive, then a negative, and finally zero correlation between these two parameters. Positive correlations between Cd transformation ratio and energy effect were generally found at concentrations below 0.1 ppb Cd. Figure 6.20 also indicates that as a biological control-

TABLE 6.1. ENERGY TRANSFORMATION RATIOS FOR MAJOR STORAGES AND FLOWS IN CD-STREAMS MODEL. ENERGY VALUES ARE DERIVED FROM DRY WEIGHT VALUES USING THE FACTOR 4 CAL = 1 G DRY WEIGHT. TOTAL ENERGY INPUT TO STREAMS TAKEN AS 32,298 S.E. CAL·M^{-2}·D^{-1} AND GROWTH TIMES OF STORAGES TAKEN FROM MODEL SIMULATION DATA. ALL DATA USED ARE FROM CONTROL STREAM SIMULATION (0.023 PPB CD)

Flow or Storage	Average Value	Actual Energy Cal·m^{-2}·d^{-1}	Energy Transformation Ratio S.E. Cal·Cal^{-1}
Gross production	4.21 g d.w.·m^{-2}·d^{-1}	16.8	1923
Community respiration	2.51 g d.w.·m^{-2}·d^{-1}	10.0	3217
Export	1.52 g d.w.·m^{-2}·d^{-1}	6.1	5312
Algae (Q_2)	21.4 g d.w.·m^{-2}	2.1[a]	15,093
Macrophytes (Q_3)	8.06 g d.w.·m^{-2}	0.161[b]	2.0×10^5
Consumers (Q_4)	0.70 g d.w.·m^{-2}	0.014[b]	2.3×10^6
Detritus-Microbes (Q_5)	159.0 g d.w.·m^{-2}	3.18[b]	10,157

[a]Charge-up time to steady state biomass was estimated as 40 days.
[b]Charge-up time to steady state biomass was estimated as 200 days.

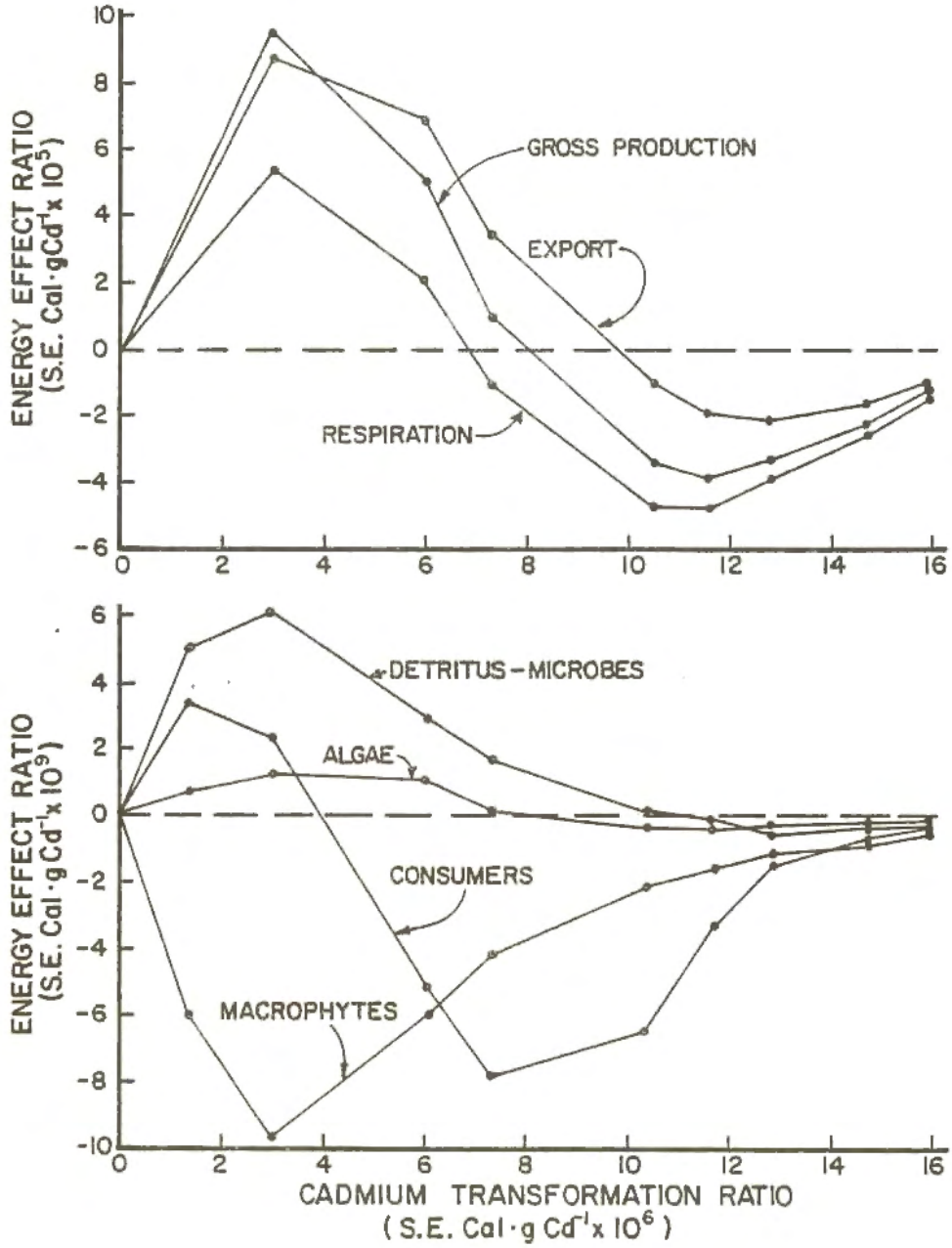

Figure 6.20. Predicted correlation between Cd transformation ratio and Cd energy effect ratio for system-level parameters and for storages. Values are calculated from 1-yr averages of simulation data from Cd-streams model.

ler, Cd has little marginal effect above a transformation ratio of 16×10^6 S.E. Cal·g Cd^{-1} (100 ppb Cd).

The actual values of the two parameters in Fig. 6.20 show an order-of-magnitude comparison between energy effect and transformation ratio of a controller like Cd. Given the assumptions upon which these calculations were made, this result is encouraging. Notice that the storages have a much higher energy effect than the system parameters. The significance of this finding may be that selection is taking place for maximizing metabolism rather than storage as discussed in Section 4.

The results presented in Fig. 6.20 are model predictions and, therefore, only as accurate as the model is an accurate description of the real Cd streams. A second qualifier of this simulation data (and the actual data, too) is that the streams were still in a successional state during the period of Cd inputs.

Actual stream systems that are capable of steady state growth populations may have much tighter correlations between the transformation ratio of Cd (its cost to the system) and the energy effect of Cd (its ability to control the system). If these correlations are found to be consistent in other systems and with other controllers, embodied energy of a controller may be calculated from its effect and vice versa. Widely different studies of toxicity effect could be compared using embodied energy values. Studies of several seemingly unique toxins may be comparable if their embodied energy content is known. The idea of toxin effect being a direct function of energy cost may allow a needed synthesis of information in dealing with the modern world's increasing toxic wastes. The recognition of the stimulatory role of naturally occurring chemicals in biological systems greatly broadens our theoretical understanding of the world's processes and allows a more finely tuned control of our life-support systems.

LITERATURE CITED

Abell, G. 1964. Exploration of the universe. Holt, Reinhart & Winston, New York. 656 pp.

American Public Health Association. 1975. Standard methods for the examination of water and wastewater, 14th ed. American Public Health Association, Washington, D.C. 1193 pp.

Atlan, H. 1968. Application of information theory to the study of the stimulating effects of ionizing radiation, thermal energy, and other environmental factors. J. Theoret. Biol. 21:45–70.

Battelle Columbus Laboratories. 1975. Energy use patterns in metallurgical and nonmetallic mineral processing. (Phase 4—energy data and flow sheets, high-priority committees). U.S. Bur. Mines OFR 80-75, NTIS PB 245759/AS. 192 pp.

Benoit, D. A., E. N. Leonard, G. M. Christensen, and J. T. Fiandt. 1976. Toxic effects of cadmium on three generations of brook trout (Salvelinus fontinalis). Trans. Am. Fish Soc. 4:550–60.

Bingham, F. T., A. L. Page, R. J. Mahler, and T. J. Ganje. 1976. Yield and cadmium accumulation of forage species in relation to cadmium content of sludge-amended soil. J. Environ. Qual. 5:57–60.

Brkovic-Popovic, I., and M. Popovic. 1977. Effects of heavy metals on survival and respiration rates of tubificid worms: Pt. 2 - Effects on respiration rate. Environ. Pollut. 13:93–8.

Bureau of Mines. 1980. Mineral commodity summaries. U.S. Bur. Mines. 191 pp.

Cammarota, V. A. 1978. Zinc. Mineral commodity profiles MCP-12. U.S. Bur. Mines. 25 pp.

Cammarota, V. A., and J. M. Lucas. 1977. Zinc. U.S. Bur. Mines Minerals Year Book, vol. 1. 34 pp.

Castellan, G. W. 1964. Physical chemistry. Addison-Wesley Co., Reading, Mass. 717 pp.

Cearley, J. E., and R. L. Coleman. 1973. Cadmium toxicity and accumulation in southern naiad. Bull. Environ. Contam. Toxicol. 9:100.

Cearley, J. E., and R. L. Coleman. 1974. Cadmium toxicity and bioconcentration in largemouth bass and bluegill. Bull. Environ. Contam. Toxicol. 11:146–51.

Copeland, B. J., and W. R. Duffer. 1964. Use of a clear plastic dome to measure gaseous diffusion rates in natural waters. Limnol. Oceanogr. 9:494–99.

Doyle, J. J., R. T. Marshall, and P. Fander. 1975. Effects of cadmium on the growth and uptake of cadmium by microorganisms. Appl. Microbiol. 29:562–64.

Gardiner, J. 1974. The chemistry of cadmium in natural water, II. The adsorption of cadmium on river muds and naturally occurring solids. Water Res. 8:157–64.

Giesy, J. P. 1978. Cadmium inhibition of leaf decomposition in an aquatic microcosm. Chemosphere 6:467–75.

Giesy, J. P., G. J. Leversee, and D. R. Williams. 1977. Effects of naturally occurring aquatic organic fractions on cadmium toxicity to Simocephalus serrulatus (Daphnidae) and Gambusia affinis (Poeciliidae). Water Res. 11:1013–20.

Giesy, J. P., H. J. Kania, J. W. Bowling, R. L. Knight, S. Mashburn, and S. Clarkin. 1979. Fate and biological effects of cadmium introduced into channel microcosms. EPA-600/3-79-039. 156 pp.

Gloyna, E. F., and J. D. Ledbetter. 1969. Principles of radiological health. Marcel Dekker, Inc., New York. 473 pp.

Hammons, A. S., J. E. Huff, H. M. Braunstein, J. S. Drury, C. R. Shriner, E. B. Lewis, B. L. Whitfield, and L. E. Towill. 1978. Reviews of the environmental effects of pollutants: IV - Cadmium. ORNL/EIS-106. EPA-600/1-78-026. 251 pp.

Hart, B. A., and P. W. Cook. 1975. The effect of cadmium on freshwater phytoplankton. Water Resour. Res. Center Completion Report. University of Vermont, Burlington.

Hiatt, V., and J. E. Huff. 1975. The environmental impact of cadmium: An overview. Int. J. Environ. Stud. 7:277–85.

John, M. K., and C. J. van Laerhoven. 1976. Differential effects of cadmium on lettuce varieties. Environ. Pollut. 10:163–72.

Judson, S. 1968. Erosion of the land or what's happening to our continents? Am. Sci. 56:356–74.

Kania, H. J., and R. F. Beyers. 1974. NTA and mercury in artificial stream systems. EPA-660/3-73-025. 25 pp.

Kania, H. J., R. L. Knight, and R. J. Beyers. 1976. Fate and biological effects of mercury introduced into artificial streams. EPA-600/3-76-060. 128 pp.

Katagiri, K. J. 1975. The effects of cadmium on Anacystis nidulans. Master's thesis, University of Vermont, Burlington.

Kerfoot, W. B., and S. A. Jacobs. 1976. Cadmium accrual in combined wastewater treatment—aquacultural system. Environ. Sci. Technol. 10:662—67.

Ketchum, B. H. 1954. Mineral nutrition of phytoplankton. Ann. Review Plant Physiology 5:55—74.

Klass, E., D. W. Rowe, and E. J. Massaro 1974. The effect of cadmium on population growth of the green algae Scenedesmus quadricauda. Bull. Environ. Contam. Toxicol. 12:442—45.

Knauer, G. A., and J. H. Martin. 1973. Seasonal variations of cadmium, copper, manganese, lead, and zinc in water and phytoplankton in Monterey Bay, California. Limnol. Oceanogr. 18:597—604.

Kneip, T. J., K. Buehler, and H. L. Hirshfield. 1974. Cadmium in an aquatic ecosystem: Distribution and effects. Interim Progess Report, N.Y. Med. Center Inst. Environ. Med. 85 pp.

Knight, R. L. 1980. Energy basis of control in aquatic ecosystems. Ph.D. dissertation, University of Florida. 198 pp.

Kumada, H., S. Kimura, M. Yokote and Y. Matida. 1973. Acute and chronic toxicity, uptake, and retension of cadmium in freshwater organisms. Bull. Freshwater Fish Res. Lab. Tokyo 22:157—65.

Lamanna, C., and M. F. Mallette. 1953. Basic bacteriology. Williams & Wilkins, Co., Baltimore.

Lotka, A. J. 1922. Contributions to the energetics of evolution. Proc. Natl. Acad. Sci. 8:147—51.

Lucas, J. M. 1979. Cadmium. Mineral commodity profiles. U.S. Bur. Mines. 13 pp.

McKellar, H. N. 1975. Metabolism and models of estuarine bay ecosystems affected by a coastal power plant. Ph.D. dissertation, University of Florida, Gainesville. 270 pp.

National Oceanographic and Atmospheric Administration. 1976. Climatological data: National summary, vol. 27. Ashville, N.C.

National Oceanographic and Atmospheric Administration. 1977. Climatological data: National summary, vol. 28. Ashville, N.C.

Odum, E. P. 1973. Fundamentals of ecology, 3rd Ed. W. B. Saunders, Philadelphia. 574 pp.

Odum, E. P., J. T. Finn, and E. H. Franz. 1979. Perturbation theory and the subsidy-stress gradient. BioScience 29:349–52.

Odum, H. T. 1956. Primary production in flowing waters. Limnol. Oceanogr. 1:102–16.

Odum, H. T. 1968. Work circuits and system stress. Pages 81–138 in Y. Young (ed.), Primary production and mineral cycling in natural ecosystems. University of Maine Press, Orono.

Odum, H. T. 1971. Environment, power, and society. Wiley-Interscience, New York. 331 pp.

Odum, H. T. 1978. Energy analysis, energy quality, and environment. Pages 55–78 in M. W. Gilliland (ed.), Energy analysis: A new public policy tool. Westview Press, Boulder, Colo.

Odum, H. T. 1979. Energy quality control of ecosystem design. Pages 221–35 in R. F. Dame (ed.), Marsh-estuarine systems simulation. University of South Carolina Press, Columbia.

Odum, H. T., and R. F. Pigeon (eds.). 1970. A tropical rain forest. U.S. Atomic Energy Commission, NTIS, TID-24270(PRNC-138), Springfield, Va.

Odum, H. T., and R. C. Pinkerton. 1955. Time's speed regulator: The optimum efficiency for maximum power output in physical and biological systems. Am. Sci. 43:331–43.

Odum, H. T., and E. C. Odum. 1980. Energy basis of New Zealand and the use of embodied energy for evaluating benefits of international trade. Pages 106–67 in Proceedings of Energy Modeling Symposium, Ministry of Energy and Victoria University of Wellington, Tech. Publ. No. 7, Wellington, N.Z. November 1979.

Odum, H. T., M. J. Lavine, F. C. Wang, M. A. Miller, J. F. Alexander, and T. Butler. 1980. A manual for using energy analysis for power plant siting. Final Report to the Nuclear Regulatory Commission, Center for Wetlands, University of Florida, Gainesville.

Page, A. L., F. T. Bingham, and C. Nelson. 1972. Cadmium absorption and growth of various plant species as influenced by solution cadmium concentration. J. Environ. Qual. 1:288–91.

Petrick, A., H. J. Bennett, K. E. Starch, and R. C. Weisner. 1979. The economics of by-product metals - Pt. 2. U.S. Bur. Mines Info. Cir. 8570. 10–14 pp.

Pickering, Q. H., and M. H. Gast. 1972. Acute and chronic toxicity of cadmium to the fathead minnow (Pimephales promelas). J. Fish. Res. Board Can. 29:1099–106.

Ravera, O., R. Gommes, and H. Muntau. 1974. Cadmium distribution in aquatic environment and its effects on aquatic organisms. Pages 317–30 in European colloquim problems of the contamination of man and his environment by mercury and cadmium. Commission of European Communities Conference, Luxenbourg, 3–5 July 1973.

Rzewuska, E., and A. Wernikowska-Ukleja. 1974. Research on the influence of heavy metals on the development of Scenedesmus quadricauda (Turp.) Breb. Pt. 1. Mercury. Pol. Arch. Hydrobiol. 21:109–17.

Sellars, W. D. 1965. Physical climatology. University of Chicago Press, Chicago. 272 pp.

Spehar, F. L., E. N. Leonard, and D. L. DeFoe. 1978. Chronic effects of cadmium and zinc mixtures on flagfish (Jordanella floridae). Trans. Am. Fish. Soc. 107:354–60.

Thorp, J. H., J. P. Giesy, and S. A. Wineriter. 1979. Effects of chronic cadmium exposure on crayfish survival, growth, and tolerance to elevated temperatures. Arch. Environ. Contam. Toxicol. 8:449–56.

Turner, M. A. 1973. Effect of cadmium treatment on cadmium and zinc uptake by selected vegetable species. J. Environ. Qual. 2:118–19.

Vlasov, K. A. 1966. Geochemistry of rare elements, Vol. 1; Cadmium. Israel Program for Scientific Translations, Jerusalem. 397–436.

Wallace, A., E. M. Romney, G. V. Alexander, S. M. Sonfi, and P. M. Patel. 1977. Some interactions in plants among cadmium, other heavy metals, and chelating agents. Agron. J. 69:18–20.

Wang, F. C., H. T. Odum, and P. C. Kangas. 1980. Energy analysis for environmental impact assessment. J. Water Res. Plan. Manage. Division ASCE 106:451–66.

Wedepohl, K. H. 1970. Handbook of geochemistry, Vol. 2; Cadmium. Springer-Verlag, New York.

Williams, D. R., and J. P. Giesy. 1978. Relative importance of food and water sources to cadmium uptake by Gambusia affinis (Poeciliidae). Environ. Res. 16:326–32.

Woodwell, G. M. 1967. Radiation and the patterns of nature. Science 156:461–70.

APPENDIX A

DIURNAL OXYGEN CURVES

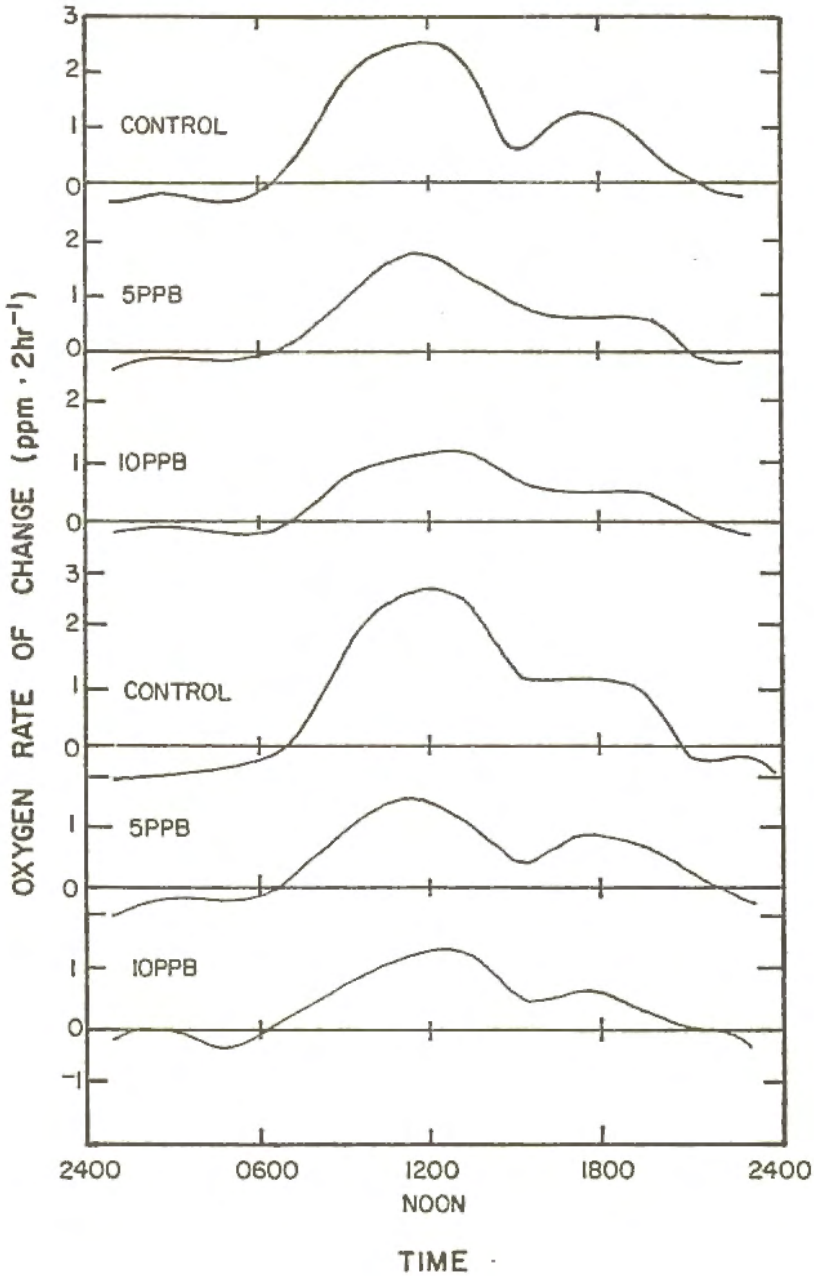

Figure A.1. Diurnal oxygen change curves from June 30, 1976, for six experimental streams receiving Cd inputs.

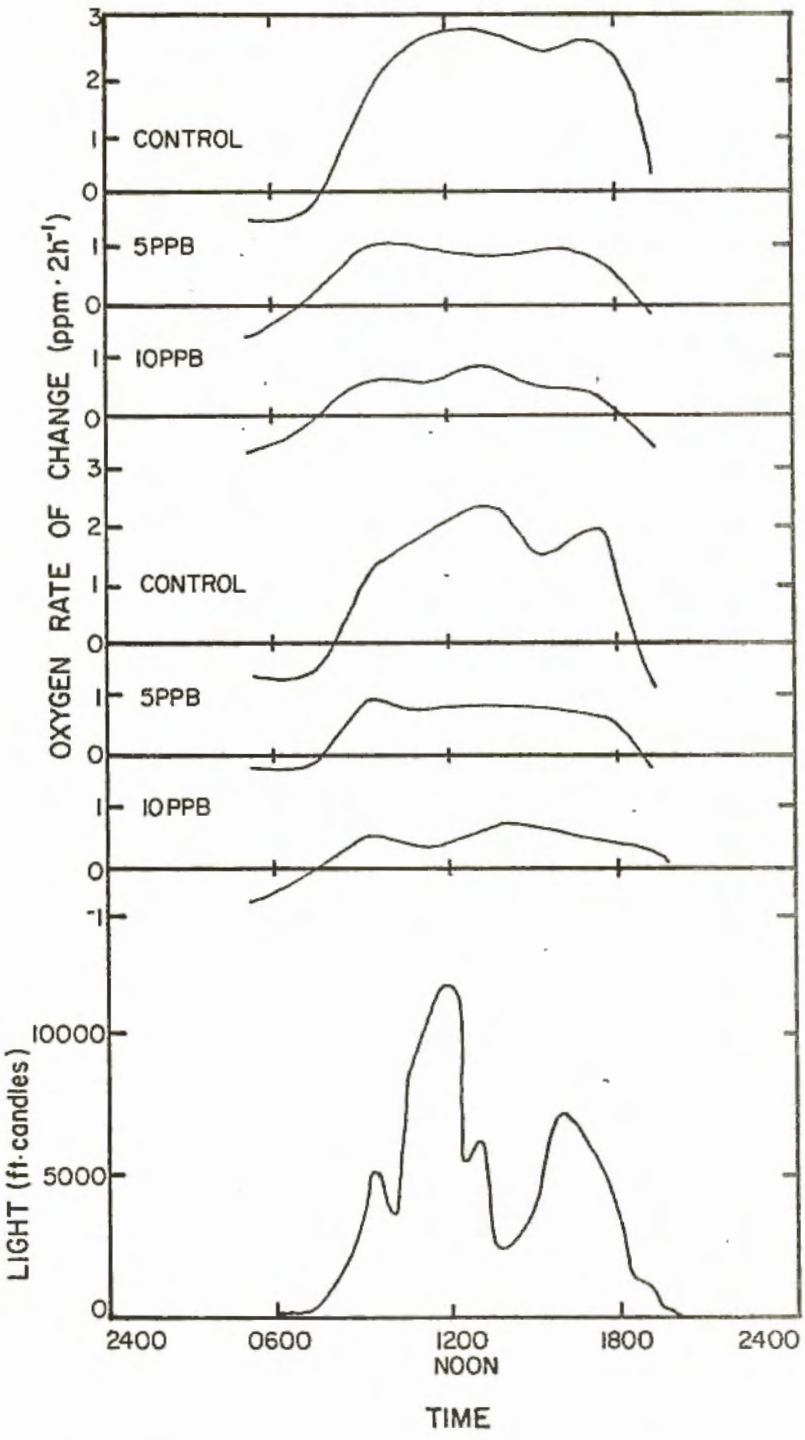

Figure A.2. Diurnal oxygen change curves from July 28, 1976, for six experimental streams receiving Cd inputs.

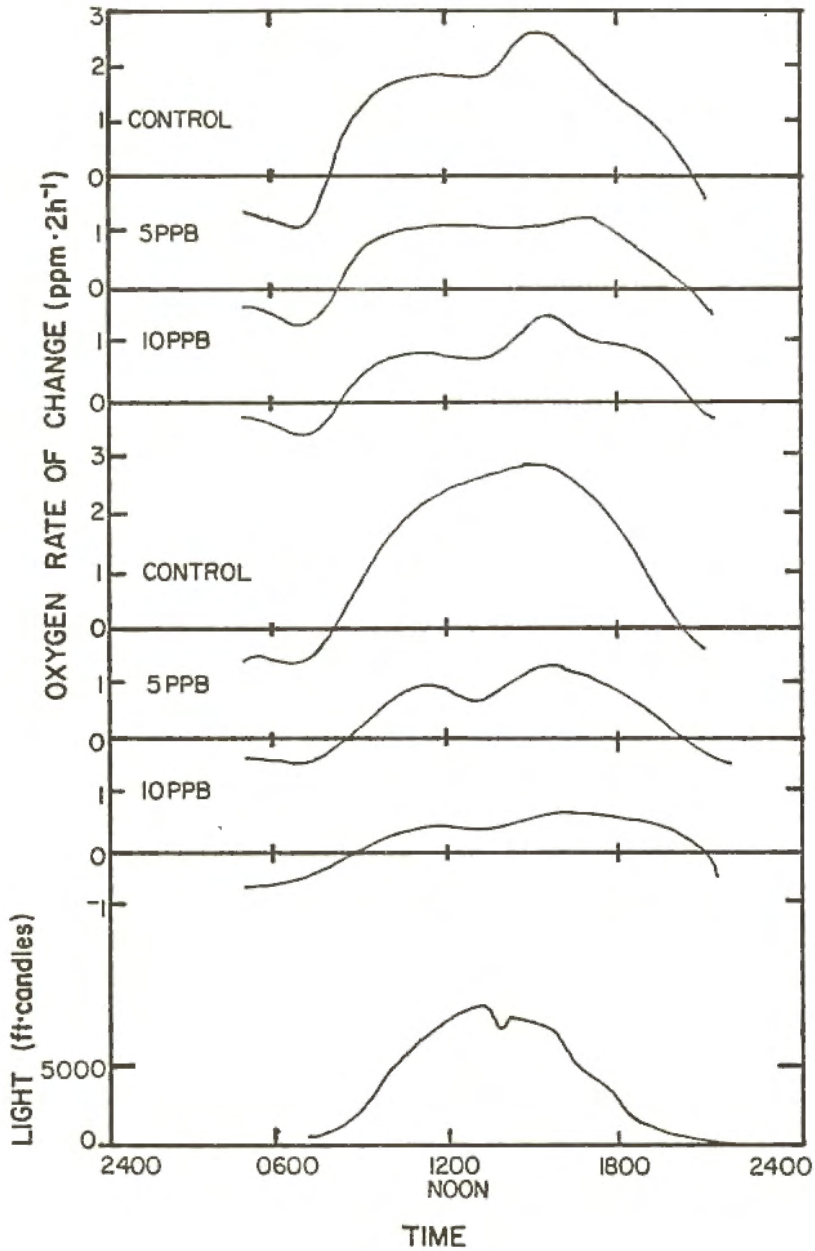

Figure A.3. Diurnal oxygen change curves from September 23, 1976, for six experimental streams receiving Cd inputs.

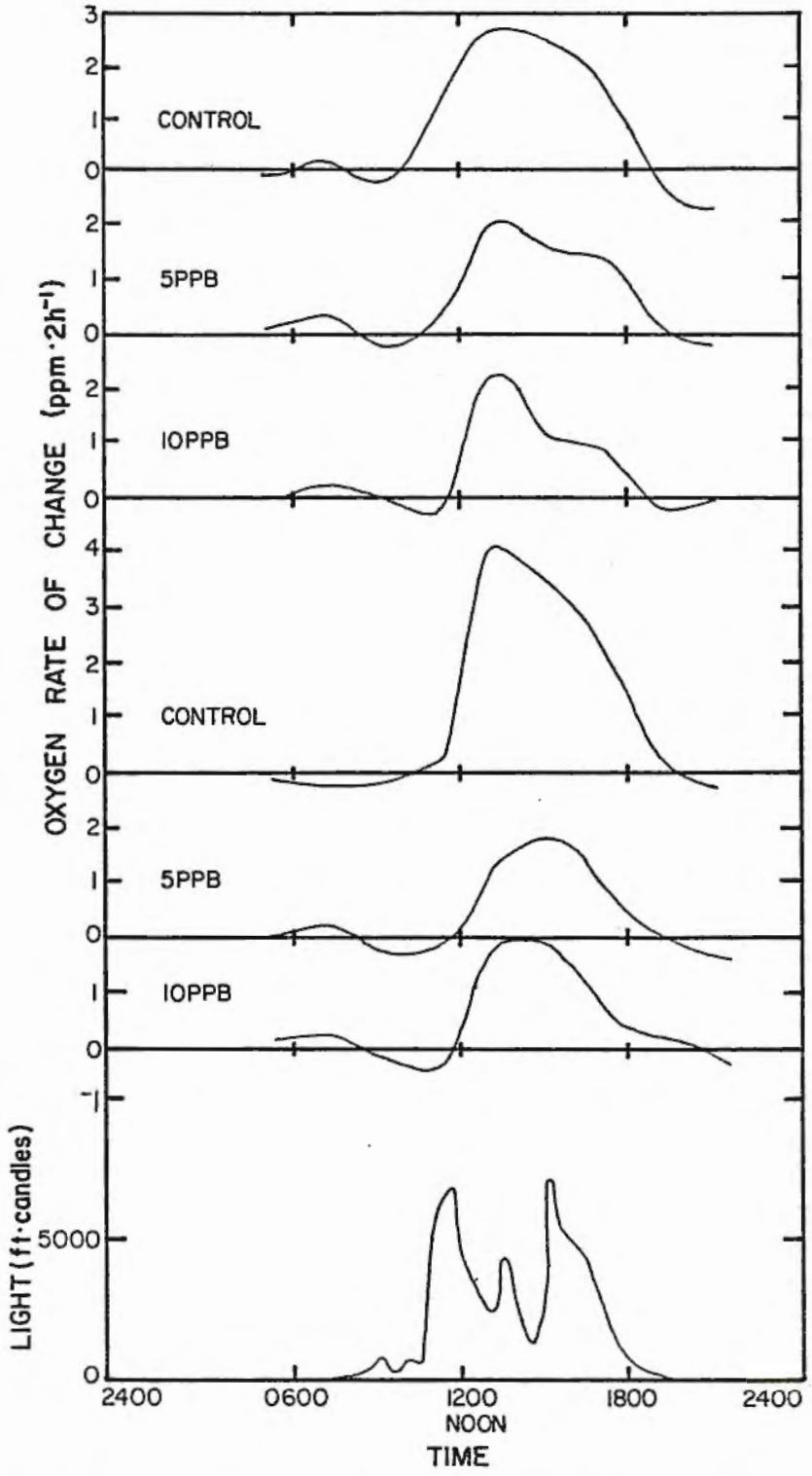

Figure A.4. Diurnal oxygen change curves from October 20, 1976, for six experimental streams receiving Cd inputs.

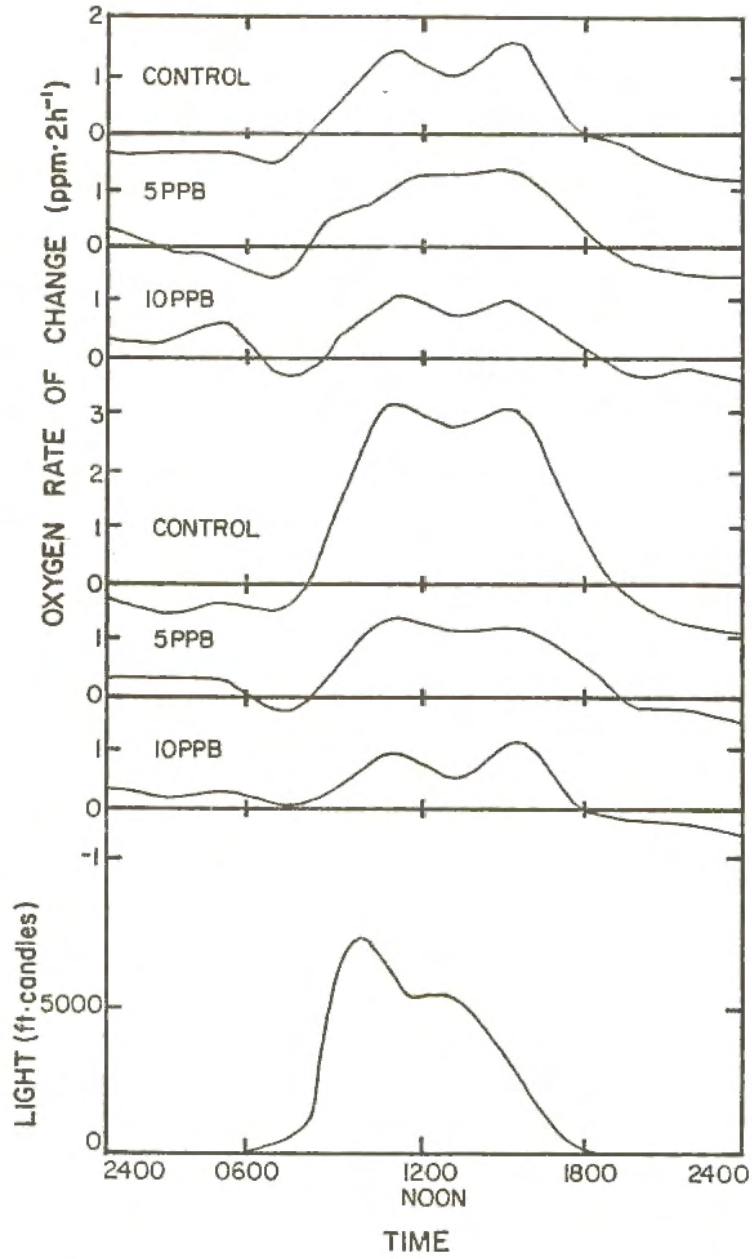

Figure A.5. Diurnal oxygen change curves from November 24, 1976, for six experimental streams receiving Cd inputs.

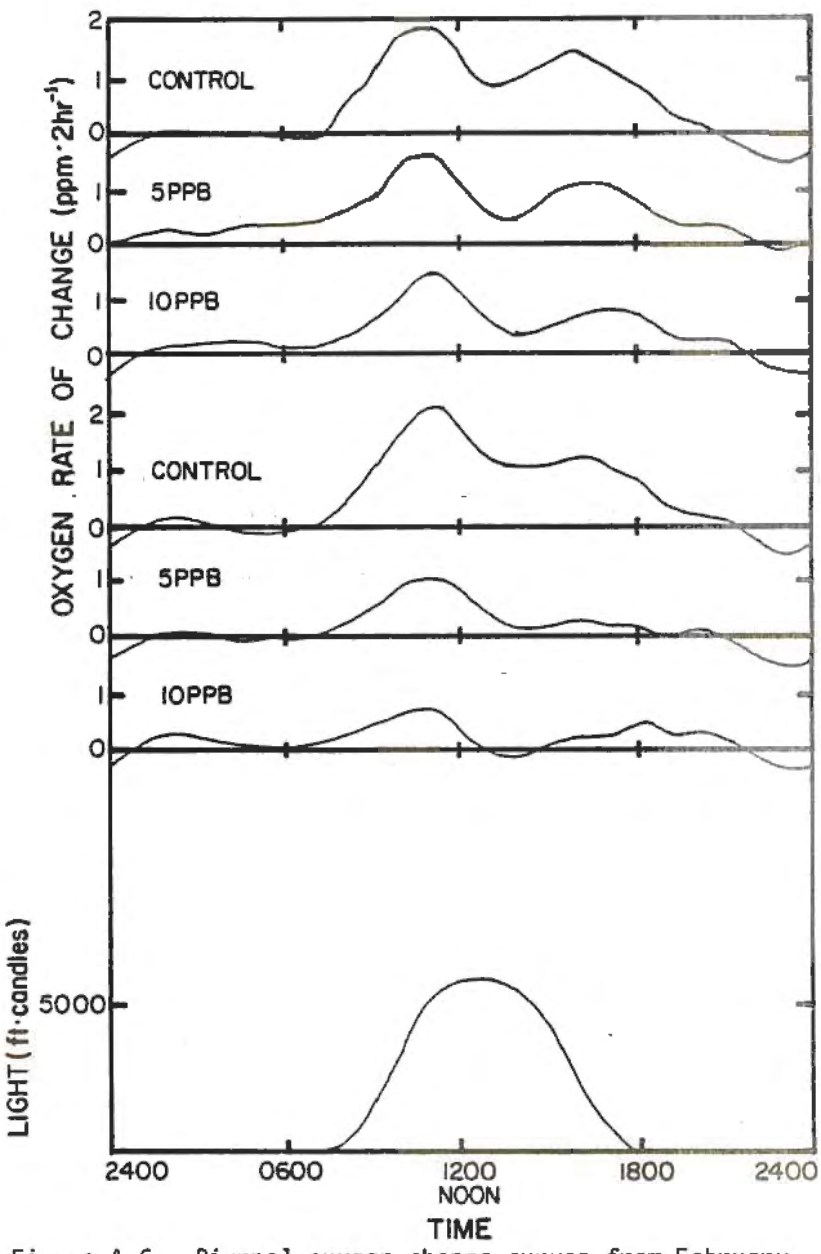

Figure A.6. Diurnal oxygen change curves from February 9, 1977, for six experimental streams receiving Cd inputs.

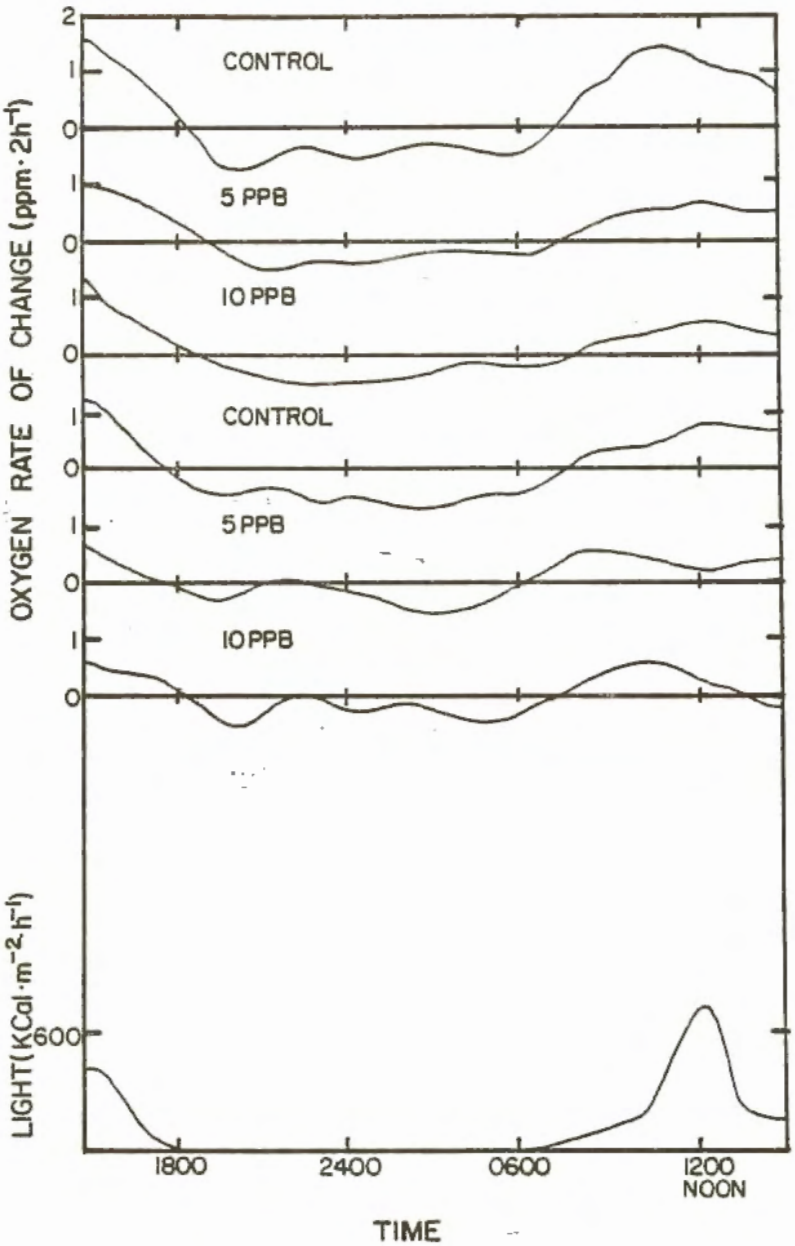

Figure A.7. Diurnal oxygen change curves from March 16–17, 1977, for six experimental streams receiving Cd inputs.

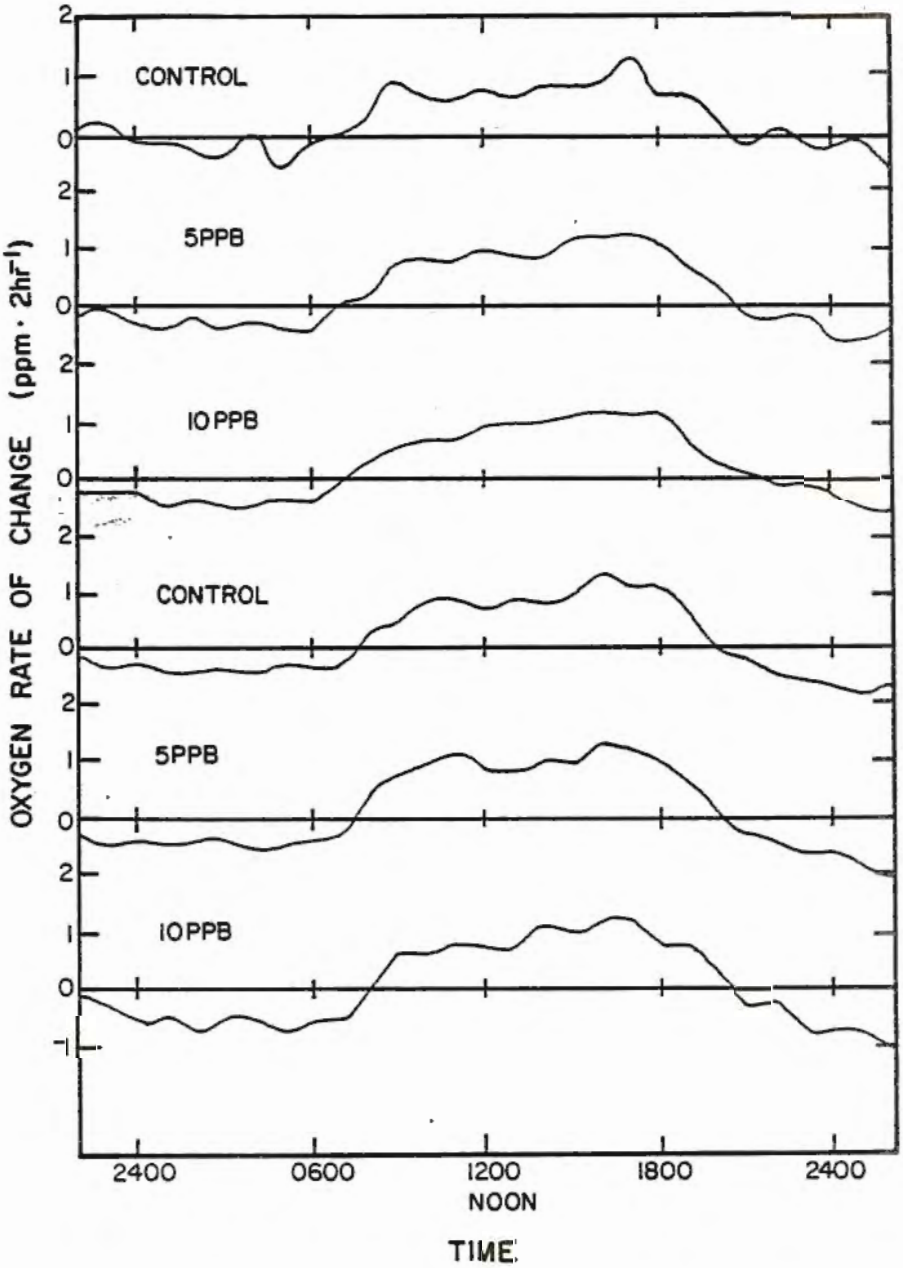

Figure A.8. Diurnal oxygen change curves from April 29, 1977, for six experimental streams previously receiving Cd inputs.

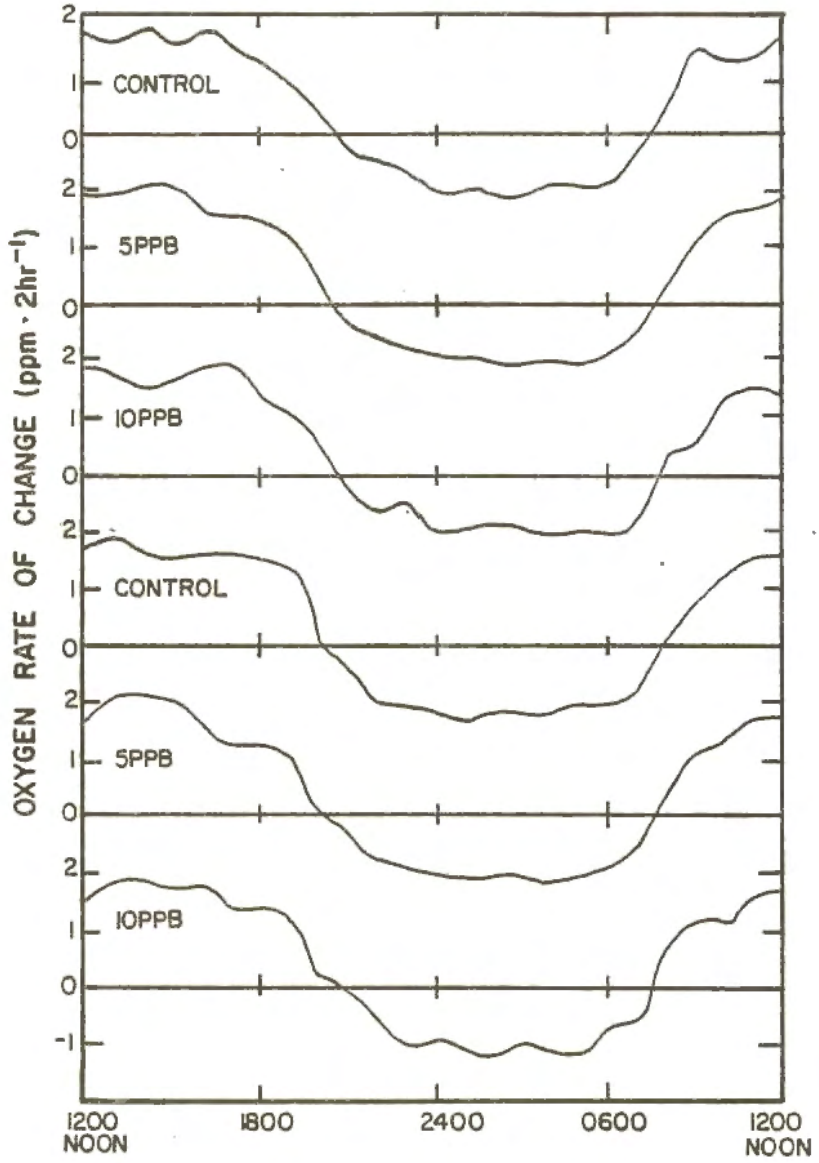

Figure A.9. Diurnal oxygen change curves from May 31—June 1, 1977, for six experimental streams previously receiving Cd inputs.

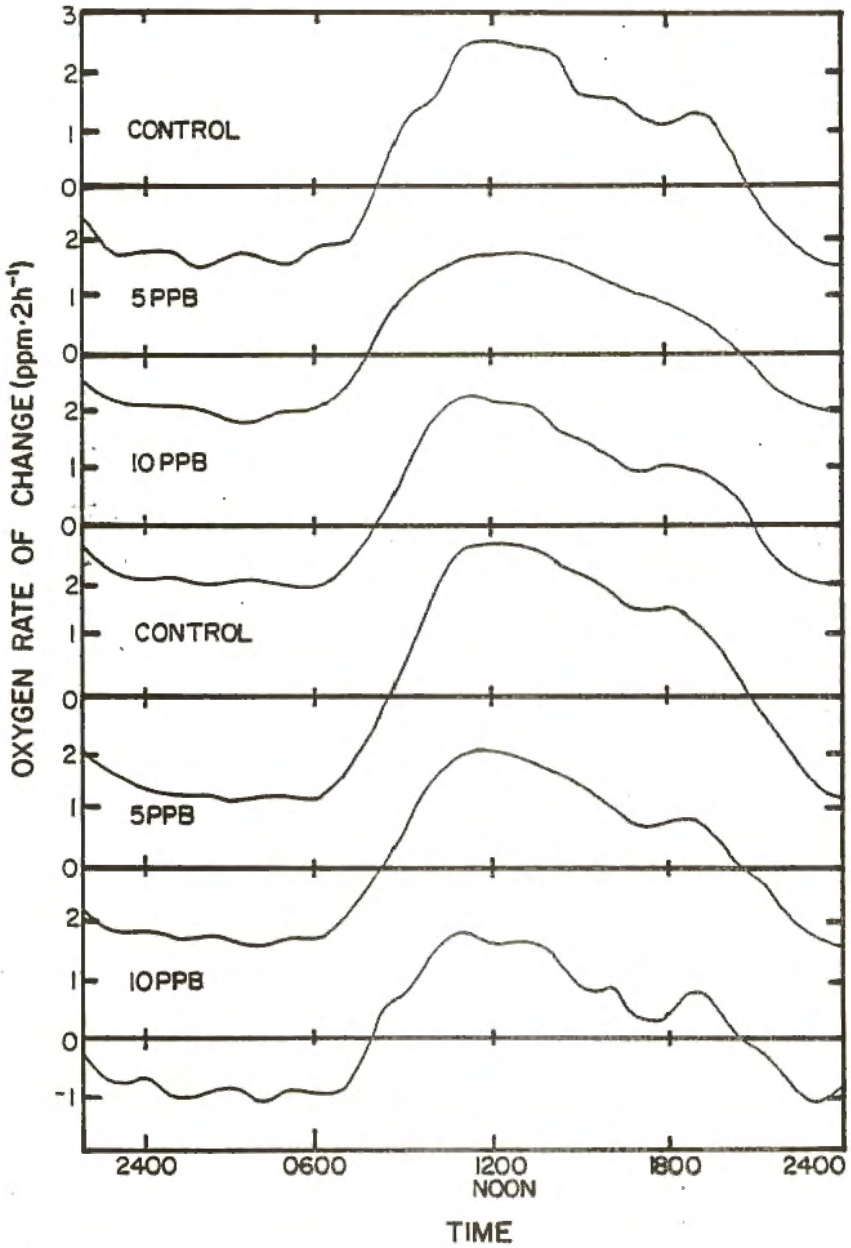

Figure A.10. Diurnal oxygen change curves from July 6, 1977, for six experimental streams previously receiving Cd inputs.

APPENDIX B

COMPUTER PROGRAMS

TABLE B.1. COMPUTER MODEL IN BASIC USED TO SIMULATE MINIMODEL ILLUSTRATED IN FIG. 4.14

```
10 PLOT 29,18
20 PLOT 12
30 J=1
40 DT=1/J
50 ND=25
60 S=10
70 Q=1000
80 TX=.1
90 K1=.001
100 K2=1E-5
110 K3=.05
200 T=0
210 I=0
220 P=K1*Q*S
230 R=K2*Q*Q
240 JX=K3*Q*TX
250 Q=Q+DT*(P-R-JX)
260 IF Q<0 THEN Q=0
270 I=I+1
280 IF I=J GOTO 300
290 GOTO 220
300 T=T+1
310 IF T=ND GOTO 850
315 GOTO 210
320 PLOT 29,18
330 PLOT 29,22
340 PLOT 2,T,Q/15,255
350 PLOT 29,18
360 PLOT 2,T,P,255
370 PLOT 29,17
380 PLOT 2,T,JX,255
800 GOTO 210
850 PLOT 29,18
860 PLOT 2,TX*10,Q/10,255
864 PRINT TX,Q,P,R,JX
870 TX=TX+.5
880 IF TX>10 GOTO 999
890 GOTO 200
999 PLOT 29,18
1000 END
```

TABLE B.2. COMPUTER MODEL IN BASIC USED TO SIMULATE MINIMODEL ILLUSTRATED IN FIG. 4.15

```
10 PLOT 29,18
20 PLOT 12
30 J=1
40 DT=1/J
50 ND=50
55 TX=.1
60 J0=4000
62 JR=2000
64 JX=2000
70 Q=1000
90 K1=5.52E-5
100 K2=1E-5
110 K3=.011
112 K4=2
200 T=0
208 S=0
210 I=0
212 JR=J0-JX
214 IF JR<0 THEN JR=0
220 P=K1*JR*TX*EXP(-K4*TX)*Q
230 R=K2*Q*Q
240 JX=K3*JR*TX*EXP(-K4*TX)*Q
250 Q=Q+DT*(P-R)
260 IF Q<0 THEN Q=0
270 I=I+1
280 IF I=J GOTO 300
290 GOTO 220
300 T=T+1
310 IF T=ND GOTO 850
311 S=S+.2
312 IF S<1 GOTO 210
315 PLOT 8
316 PRINT T,Q,P,R,JX
320 PLOT 29,18
330 PLOT 29,22
340 PLOT 2,T,Q/15,255
350 PLOT 29,18
800 GOTO 208
850 PLOT 29,18
860 PLOT 2,TX*10,Q/10,255
864 PRINT TX,Q,P,R,JX
870 TX=TX+.5
880 IF TX>10 GOTO 999
890 GOTO 60
999 PLOT 29,18
1000 END
```

TABLE B.3. COMPUTER MODEL IN BASIC USED TO SIMULATE MINIMODEL ILLUSTRATED IN FIG. 4.16

```
10 PLOT 29,18
20 PLOT 12
25 PLOT 2,253,0,0,242,0,191,159,191,159,0,0,0,255
30 J=1
40 DT=1/J
50 ND=50
55 TX=.01
70 Q=50
75 N=20
80 N0=2
85 K1=1E-2
87 K2=5E-3
89 K3=5E-6
91 K4=1E-4
93 K5=.1
95 K6=4.9E-6
97 K7=.05
98 K8=K3/K1
200 T=0
208 S=0
210 I=0
220 P=K1*Q*N
222 R=K2*Q*Q
224 N1=K3*Q*N
226 N2=K8*(J1+R)
228 N3=K5*N
230 J1=K7*Q*TX
250 Q=Q+DT*(P-R-J1)
252 N=N+DT*(N0+N2-N1-N3)
260 IF Q<0 THEN Q=0
262 IF N<0 THEN N=0
270 I=I+1
280 IF I=J GOTO 300
290 GOTO 220
300 T=T+1
310 IF T=ND GOTO 850
311 S=S+.2
312 IF S<1 GOTO 210
314 PLOT 8
315 PRINT T,Q,N,P,R
320 PLOT 29,18
330 PLOT 29,22
340 PLOT 2,T,Q,255
350 PLOT 29,18
800 GOTO 208
850 PLOT 29,18
860 PLOT 2,TX*10,P*10,255
864 PRINT TX,Q,N,P,R
870 TX=TX+.5
880 IF TX>10 GOTO 999
890 GOTO 70
999 PLOT 29,18
1000 END
```

TABLE B.4. COMPUTER MODEL IN BASIC USED TO SIMULATE MINIMODEL ILLUSTRATED IN FIG. 4.21

```
10 J=3
20 DT=1/J
30 C0=.0001
40 T=0
50 ND=10
60 J0=4000
70 JR=3000
80 B=20
90 R=1E-4
100 AT=3*B/R
110 N=1
120 C1=20
130 KZ=100
140 AS=KZ*C1
150 A=AT-AS
160 K1=3.33E-3
170 K2=3.0E-5
180 K4=3.33E-5
190 K5=.05
200 K6=.03
210 K7=.005
220 K8=.005
230 K9=.03
240 KA=.07
250 KB=.01
260 KC=.01
270 KF=1
280 KG=3/R
290 KE=3/R
300 I=0
310 F1=K1*B*JR
320 F2=K2*B*JR
330 F4=K4*B*JR
340 F5=K5*B
350 F6=K6*B
360 F9=K9*A*C0
370 F7=KZ*F9
380 F8=KZ*F9
390 F3=3*(F2-F5)/R
400 FA=KA*C1
410 FB=KZ*FA
420 FC=KZ*FA
430 FD=(F7-F8)+(FB-FC)
440 FE=KE*(A/AT)*F6
450 FF=KF*C*F6
460 FG=KG*(AS/AT)*F6
470 K5=.08
480 JR=J0-F1
490 B=B+DT*(F2-F5-F6)
500 C1=C1+DT*(F9-FA-FF)
510 A=A+DT*(FC-F7-FE+F3)
520 AS=AS+DT*(F8-FB-FG)
530 AT=AS+A
540 C=C1/B
550 IF B<0 THEN B=0
560 IF C1<0 THEN C1=0
570 IF A<0 THEN A=0
580 IF AS<0 THEN AS=0
590 IF AT<0 THEN AT=0
600 I=I+1
610 IF I=J GOTO 630
620 GOTO 310
630 T=T+1
640 IF T=ND GOTO 660
650 GOTO 300
660 PLOT 29,18
670 PLOT 2,C0*100,C/10,255
680 PLOT 29,18
690 PLOT 11
700 PRINT C0,C
710 C0=C0+.005
720 IF C0=1 GOTO 999
730 GOTO 40
999 PLOT 29,18
1000 END
```

TABLE B.5. COMPUTER MODEL IN BASIC USED TO SIMULATE CD-STREAMS. THIS MODEL IS ILLUSTRATED IN FIGS. 6.6–6.10

```
1 CLEAR (500)
10 PLOT 29,18
20 PLOT 12
30 PLOT 2,253,0,0,242,0,191,159,191,159,0,0,0,255
31 GOSUB 2000
32 PLOT 4
35 V=3
40 J=1
50 DT=V/J
55 NT=DT
60 ND=600
70 S=300
75 T1=0
76 T2=0
77 T3=0
78 NZ=0
79 BZ=0
80 T4=0
102 J0=3442
104 JR=3000
106 JW=2442.86
108 N1=.015
109 ZZ=.023
110 C1=.023
112 Q2=.1
114 Q3=1
116 Q4=.1
118 Q5=.1
120 N2=.015
124 C2=Q2
126 C3=Q3
128 C4=Q4
130 C5=Q5
132 CA=.023
134 CB=1
136 CC=1
138 CD=1
140 CE=1
141 CZ=.023
142 F1=36.64
144 F2=56.2
152 FI=.049
154 FJ=.018
156 FK=.036
158 FL=.061
160 FM=.0036
164 FO=.4
174 FX=.0001
175 FE=.003
```

TABLE B.5. (CONTINUED)

```
176 FD=.125
177 J4=0
178 J5=0
180 JP=0
202 K1=200
204 K2=.136
210 K4=5
214 K6=5
216 K8=.009
218 K9=.0024
220 KA=143
222 KB=143
224 KC=.003
226 KD=6E-5
228 KE=.018
230 KF=.03
232 KG=.00012
234 KH=180
236 KI=100
238 KJ=8
240 KK=80
242 KL=.045
244 KM=.02
248 KO=.0055
250 KP=.008
252 KQ=KP
254 KR=KP
256 KS=KP
260 KU=.06
266 KX=.0027
268 KY=.0015
272 L1=.065
274 L2=.02
278 L4=.003
280 L5=.0015
282 L6=.0007
286 L8=K6
288 L9=.3
289 LP=.008
290 LA=.136
291 LB=.015
293 LE=.01
299 LS=.025
301 LT=.025
302 LU=.2
308 T=0
310 I=0
320 J0=(4360+1640*SIN(((6.28)/365)*(S-80)))*.7
332 JN=N1*JW
334 JC=C1*JW
336 F8=K8*N2*JR*Q2
338 F9=K9*N2*JR*Q3
339 FD=KD*Q2*JR
341 FE=KE*Q3
```

TABLE 8.5. (CONTINUED)

```
342 F4=K4*(F9-FE)
343 IF F4<0 THEN F4=0
350 F6=K6*(F8-FD)
351 IF F6<0 THEN F6=0
356 FA=KA*F8
358 FB=KB*F9
360 FC=KC*Q5*JR
366 FF=KF*Q4*Q4
368 FG=KG*Q5*(1-LE*CA)
377 IF FG<0 THEN FG=0
386 FP=KP*Q2
388 FQ=KQ*Q3
390 FR=KR*Q5
392 FS=KS*Q4
393 F3=FP+FQ+FR+FS
394 FT=FG*CE
396 FU=KU*Q2
398 FV=CB*(FU+J4)
400 FW=CB*FX
402 FX=KX*Q2*Q4
404 FY=KY*Q3*Q4
406 FZ=CC*FY
410 J2=L2*Q3
412 J3=CC*(J2+J5)
414 J4=L4*Q2*CA
416 J5=L5*Q3*CA
418 J6=L6*Q5*Q4
420 J7=CE*J6
422 J8=L8*FG
424 J9=L9*(FX+FY+J6)
428 JB=LB*Q4
432 JD=CD*(JB+JP)
434 JF=FP*CB
436 JG=FQ*CC
438 JH=FR*CE
440 JI=FS*CD
441 JJ=JF+JG+JH+JI
442 JK=FX+FY+J6-J9
443 JL=L9*(FW+FZ+J7)
444 JM=FW+FZ+J7-JL
445 JR=J0-FA-FB-FC
446 IF JR<0 THEN JR=0
448 JP=LP*Q4*CA
450 JS=LS*CA*F8/(LU+CA)
452 JT=LT*CA*F9/(LU+CA)
458 GP=F8+JS+F9+JT
460 RT=FD+FE+FF+FG
500 Q2=Q2+DT*(F8+JS-FD-FX-FP-FU-  4)
510 Q3=Q3+DT*(F9+JT-FQ-FY-J2-FE-  5)
520 Q4=Q4+DT*(J9-FS-JB-FF-JP)
530 Q5=Q5+DT*(J2+FU+JB+JK-FR-FG+  2+J5+J4-J6)
531 IF Q2<0 THEN Q2=0.01
532 IF Q3<0 THEN Q3=0.01
533 IF Q4<0 THEN Q4=0.01
```

TABLE B.5. (CONTINUED)

```
534 IF Q5<0 THEN Q5=0.01
541 AZ=(CA/(K1+CA))
542 N2=F1/JW
543 FH=KH*AZ*Q2
545 FI=KI*AZ*Q3
546 CA=F2/JW
547 FJ=KJ*AZ*Q4
549 FK=KK*AZ*Q5
550 CB=C2/Q2
551 FL=KL*C2
552 CC=C3/Q3
553 FM=KM*C3
554 CD=C4/Q4
555 FO=KO*C4
556 CE=C5/Q5
557 J1=L1*C5
558 F1=JN+J8-F4-F6
559 F2=JC+FL+FM+FO+FT+J1-FK-FJ-FH-FI
562 IF F1<0 THEN F1=0
566 IF F2<0 THEN F2=0
570 C2=C2+NT*(FH-FL-FW-FV-JF)
572 C3=C3+NT*(FI-FZ-J3-FM-JG)
574 C4=C4+NT*(JL+FJ-FO-JD-JI)
576 C5=C5+NT*(J3+FV+FK+JD+JM-J1-JH-J7-FT)
577 IF C5<0 THEN C5=0.01
581 IF C2<0 THEN C2=0.01
582 IF C3<0 THEN C3=0.01
583 IF C4<0 THEN C4=0.01
584 IF T<138 OR T>503 THEN GOTO 610
585 NZ=NZ+1
590 T1=GP+T1
595 T2=RT+T2
600 T3=F3+T3
605 T4=J0+T4
610 I=I+1
620 IF I=J GOTO 640
630 GOTO 320
640 T=T+V
650 S=S+V
652 IF T>138 THEN C1=ZZ
653 IF T>503 THEN C1=.023
660 IF T>ND GOTO 805
698 PLOT 29,18
715 TG=T/5
719 PLOT 8
720 PLOT 29,18
740 PLOT 2,TG,75+J0/150,255
750 PLOT 29,22
755 PLOT 2,TG,2*Q2,255
760 PLOT 29,17
765 PLOT 2,TG,Q3,255
770 PLOT 29,20
775 PLOT 2,TG,Q5/2,255
782 PLOT 29,18
```

.. TABLE B.5. (CONTINUED)

```
785 PLOT 2,TG,Q4*10,255
786 BZ=BZ+1
787 IF BZ<6 THEN GOTO 800
788 Q=(J0/150)+30 : F=1 : GOSUB 5000
791 GOSUB 3060
799 PRINT P$ : P$=A$ : BZ=0
800 GOTO 310
805 A1=T1/NZ
810 A2=T2/NZ
815 A3=T3/NZ
820 A4=T4/NZ
990 PRINT A1,A2,A3,A4
995 PLOT 5
999 PLOT 29,18
1000 END
2000 REM
2010 FOR I=1 TO 8 : A$=A$+"          :" : NEXT
2020 FOR I=1 TO 8 : A1$=A1$+"----------!" : NEXT
2030 F$="1234567890"
2040 RETURN
3000 REM BIOMASSPLOT SUBROUTINE
3010 Q=Q2*0.6 : F=2 : GOSUB 5000
3012 Q=Q3*0.6 : F=3 : GOSUB 5000
3014 Q=Q4*30 : F=4 : GOSUB 5000
3016 Q=Q5/3.33 : F=5 : GOSUB 5000
3018 RETURN
3030 REM SYSTEM PARAMETER PLOT SUBROUTINE
3032 Q=GP*6 : F=6 : GOSUB 5000
3034 Q=RT*6 : F=7 : GOSUB 5000
3036 Q=F3*6 : F=8 : GOSUB 5000
3038 RETURN
3060 REM CDCONC PLOT SUBROUTINE
3062 Q=CB/2 : F=2 : GOSUB 5000
3064 Q=CC/2 : F=3 : GOSUB 5000
3066 Q=CD : F=4 : GOSUB 5000
3068 Q=CE : F=5 : GOSUB 5000
3070 RETURN
5000 REM PLOTTING ROUTINE FOR PRINTER
5010 Q=INT(Q)
5020 IF Q<2 THEN Q=2
5030 IF Q>80 THEN Q=80
5040 Z$=MID$(F$,F,1)
5050 P$=LEFT$(P$,Q-1)+Z$+RIGHT$(P$,80-Q)
5060 RETURN
```

TABLE 8.6. LIST OF PARAMETERS WITH DESCRIPTIONS AND EQUATIONS FOR CD-STREAMS MODEL ILLUSTRATED IN FIGS. 6.6–6.10

Model Parameter	Description	Equation
N	Dissolved nitrogen in periphyton layer	N = N+DT*(J8-F5-F4-F6)
C	Dissolved Cd in periphyton layer	C = C+DT*(FL+FM+FO+FT+J1-JZ-FK-FJ-FH-FI)
Q2	Algal biomass	Q2 = Q2+DT*(F8+JS-FD-FX-FP-FU-J4)
Q3	Macrophytic biomass	Q3 = Q3+DT*(F9+JT-FQ-FY-J2-FE-J5)
Q4	Consumer biomass	Q4 = Q4+DT*(J9-FS-JB-FF-JP)
Q5	Detrital-microbial biomass	Q5 = Q5+DT*(J2+FU+JB+JK-FR-FG+J4+JP+J5-J6)
C2	Bound Cd in algae	C2 = C2+DT*(FH-FL-FW-FV-JF)
C3	Bound Cd in macrophytes	C3 = C3+DT*(FI-FZ-J3-FM-JG)
C4	Bound Cd in consumers	C4 = C4+DT*(JL+FJ-FO-JD-JI)
C5	Bound Cd in detritus-microbes	C5 = C5+DT*(J3+FV+FK-J1-JH-J7-FT+JD+JM)
N2	Dissolved nitrogen concentration in stream	$\frac{F1}{JW}$
CA	Dissolved Cd concentration in stream	$\frac{F2}{JW}$

TABLE B.6. (CONTINUED)

Model Parameter	Description	Equation
N1	Dissolved nitrogen concentration in inflow water	Constant, 15 μg $N \cdot L^{-1}$
C1	Dissolved Cd concentration in inflow water	Variable
CB	Cd concentration in algae	$\frac{C2}{Q2}$
CC	Cd concentration in macrophytes	$\frac{C3}{Q3}$
CD	Cd concentration in consumers	$\frac{C4}{Q4}$
CE	Cd concentration in detritus and microbes	$\frac{C5}{Q5}$
JØ	Solar energy flux	Sine function, 365 days; maximum value = 6000 $Cal \cdot m^{-2} \cdot d^{-1}$ minimum value = 2720 JØ = 0.7·TOTAL
JR	Remaining solar flux (albedo)	JØ-FA-FB-FC
JW	Water input	Constant, 2443 $L \cdot m^{-2} \cdot d^{-1}$
JN	Dissolved nitrogen input	N1·JW
JC	Cd input	C1·JW
F1	Nitrogen flow	JN+J8-F4-F6

TABLE B.6. (CONTINUED)

Model Parameter	Description	Equation
F2	Cd flow	JC+FL+FM+FO+FT+J1-FK-FJ-FH-FI
F3	Total dry matter export	FP+FQ+FR+FS
F4	Nitrogen uptake by macrophytes	K4·(F9-FE)
F6	Nitrogen uptake by algae	K6·(F8-FD)
F8	Gross production by algae	K8·N2·JR·Q2
F9	Gross production by macrophytes	K9·N2·JR·Q3
FA	Light absorption by algae	KA·F8
FB	Light absorption by macrophytes	KB·F9
FC	Light absorption by detritus and microbes	KC·Q5·JR
FD	Algal respiration	KD·Q2·JR
FE	Macrophyte respiration	KE·Q3
FF	Consumer respiration	KF·Q4·Q4
FG	Microbial respiration	KG·Q5·(1-LE·CA)
FH	Algal Cd uptake	$KH\cdot\left(\frac{CA}{K1+CA}\right)\cdot Q2$

TABLE B.6. (CONTINUED)

Model Parameter	Description	Equation
FI	Macrophytic Cd uptake	$KI \cdot (\frac{CA}{K1+CA}) \cdot Q3$
FJ	Consumer Cd uptake	$KJ \cdot (\frac{CA}{K1+CA}) \cdot Q4$
FK	Detrital-microbial Cd uptake	$KK \cdot (\frac{CA}{K1+CA}) \cdot Q5$
FL	Algal Cd decay	KL·C2
FM	Macrophytic Cd decay	KM·C3
FO	Consumer Cd decay	KO·C4
FP	Algal export	KP·Q2
FQ	Macrophyte export	KQ·Q3
FR	Detrital-microbial export	KR·Q5
FS	Consumer export	KS·Q4
FT	Cd release in microbial respiration	FG·CE
FU	Algal loss to detritus	KU·Q2
FV	Particulate Cd loss from algae to detritus	CB(FU+J4)
FW	Particulate Cd loss from algae to consumers	CB·FX

TABLE B.6. (CONTINUED)

Model Parameter	Description	Equation
FX	Algal consumption by consumers	KX·Q2·Q4
FY	Macrophyte consumption by consumers	KY·Q3·Q4
FZ	Particulate Cd loss from macrophytes to consumers	CC·FY
J1	Detrital-microbial Cd decay	L1·C5
J2	Macrophytic loss to detritus	L2·Q3
J3	Particulate Cd loss from macrophytes to detritus	CC(J2+J5)
J4	Cd toxicity to algae	L4·Q2·CA
J5	Cd toxicity to macrophytes	L5·Q3·CA
J6	Detrital-microbial consumption by consumers	L6·Q5·Q4
J7	Particulate Cd loss from detritus-microbes to consumers	CE·J6
J8	Nitrogen remineralization from microbial respiration	L8·FG
J9	Total assimilation by consumers	L9·(FX+FY+J6)
JB	Consumer loss to detritus	LB·Q4

TABLE B.6. (CONTINUED)

Model Parameter	Description	Equation
JD	Particulate Cd loss from consumers to detritus	CD(JB+JP)
JF	Particulate Cd loss from algae to export	FP*CB
JG	Particulate Cd loss from macrophytes to export	FQ*CC
JH	Particulate Cd loss from detritus-microbes to export	FR*CE
JI	Particulate Cd loss from consumers to export	FS*CD
JJ	Total particulate Cd flow in export	JF+JG+JH+JI
JK	Loss of unassimilated food by consumers to detritus	FX+FY+J6-J9
JL	Assimilation of particulate Cd by consumers	L9*(FW+FZ+J7)
JM	Loss of unassimilated particulate Cd from consumers to detritus	FW+FZ+J7-JL
JP	Cd toxicity to consumers	LP*Q4*CA
JS	Cd stimulation of algal production	$\frac{LS*CA*F8}{LU+CA}$

TABLE B.6. (CONTINUED)

Model Parameter	Description	Equation
JT	Cd stimulation of macrophytes	$\frac{LT \cdot CA \cdot F9}{LU+CA}$
GP	Total gross production	F8+F9+JS+JT
RT	Community respiration	FD+FE+FF+FG

TABLE B.7. LIST OF INITIAL CONDITIONS AND TRANSFER COEFFICIENTS USED IN SIMULATION OF CD-STREAMS MODEL ILLUSTRATED IN FIGS. 6.6–6.10

Initial Conditions

Q2	0.1 $g \cdot m^{-2}$	CA	0.023 $\mu g\ Cd \cdot L^{-1}$
Q3	1.0 $g \cdot m^{-2}$	C1	0.023–100.0 $\mu g\ Cd \cdot L^{-1}$
Q4	0.1 $g \cdot m^{-2}$	CB	1.0 $\mu g\ Cd \cdot g^{-1}$
Q5	0.1 $g \cdot m^{-2}$	CC	1.0 $\mu g\ Cd \cdot g^{-1}$
C2	0.1 $\mu g\ Cd \cdot m^{-2}$	CD	1.0 $\mu g\ Cd \cdot g^{-1}$
C3	1.0 $\mu g\ Cd \cdot m^{-2}$	CE	1.0 $\mu g\ Cd \cdot g^{-1}$
C4	0.1 $\mu g\ Cd \cdot m^{-2}$	JØ	3442 $Cal \cdot m^{-2} \cdot d^{-1}$
C5	0.1 $\mu g\ Cd \cdot m^{-2}$	JR	3000 $Cal \cdot m^{-2} \cdot d^{-1}$
N2	0.015 $mg\ N \cdot L^{-1}$	JW	2443 $L \cdot m^{-2} \cdot d^{-1}$
N1	0.015 $mg\ N \cdot L^{-1}$		

Transfer Coefficients

K1	200 $\mu g\ Cd \cdot L^{-1}$	KP	0.008 d^{-1}
K4	5 $mg\ N \cdot g^{-1}$	KQ	0.008 d^{-1}
K6	5 $mg\ N \cdot g^{-1}$	KR	0.008 d^{-1}
K8	0.009 $L \cdot m^{2} \cdot Cal^{-1} \cdot mg\ N^{-1}$	KS	0.008 d^{-1}
K9	0.0024 $L \cdot m^{2} \cdot Cal^{-1} \cdot mg\ N^{-1}$	KU	0.06 d^{-1}
KA	143 $Cal \cdot g^{-1}$	KX	0.0027 $m^{2} \cdot d^{-1} \cdot g^{-1}$
KB	143 $Cal \cdot g^{-1}$	KY	0.0015 $m^{2} \cdot d^{-1} \cdot g^{-1}$
KC	0.003 $m^{2} \cdot g^{-1}$	L1	0.065 d^{-1}
KD	$6 \times 10^{-5}\ m^{2} \cdot Cal^{-1}$	L2	0.02 d^{-1}
KE	0.018 d^{-1}	L4	0.003 $L \cdot d^{-1} \cdot \mu g\ Cd^{-1}$
KF	0.03 d^{-1}	L5	0.0015 $L \cdot d^{-1} \cdot \mu g\ Cd^{-1}$
KG	0.00012 d^{-1}	L6	0.0007 $m^{2} \cdot d^{-1} \cdot g^{-1}$
KH	180 $\mu g\ Cd \cdot g^{-1} \cdot d^{-1}$	L8	5 $mg\ N \cdot g^{-1}$
KI	100 $\mu g\ Cd \cdot g^{-1} \cdot d^{-1}$	L9	0.3
KJ	8 $\mu g\ Cd \cdot g^{-1} \cdot d^{-1}$	LP	0.008 $L \cdot d^{-1} \cdot \mu g\ Cd^{-1}$
KK	80 $\mu g\ Cd \cdot g^{-1} \cdot d^{-1}$	LB	0.015 d^{-1}
KL	0.045 d^{-1}	LE	0.01 $L \cdot \mu g\ Cd^{-1}$
KM	0.02 d^{-1}	LS	0.025
KO	0.0055 d^{-1}	LT	0.025
		LU	0.2 $\mu g\ Cd \cdot L^{-1}$